THE UNIVERSITY of ADELAIDE

Earth observation remote sensing of spatial and temporal relationships between rivers and receiving coastal waters

Thesis submitted for the degree of

Doctor of Philosophy

Hannah Caitlin Claire Auricht

School of Biological Sciences

The University of Adelaide

December 2022

Thesis declaration

I certify that this work contains no material which has been accepted for the award of any other degree or diploma in my name, in any university or other tertiary institution and, to the best of my knowledge and belief, contains no material previously published or written by another person, except where due reference has been made in the text. In addition, I certify that no part of this work will, in the future, be used in a submission in my name, for any other degree or diploma in any university or other tertiary institution without the prior approval of the University of Adelaide and where applicable, any partner institution responsible for the joint-award of this degree.

I acknowledge that copyright of published works contained within this thesis resides with the copyright holder(s) of those works.

I also give permission for the digital version of my thesis to be made available on the web, via the University's digital research repository, the Library Search and also through web search engines, unless permission has been granted by the University to restrict access for a period of time.

I acknowledge the support I have received for my research through the provision of an Australian Government Research Training Program Scholarship.

Hannah Auricht

21/11/2022

Acknowledgements

Prior to writing this acknowledgements section, I discovered a page in my notebook entitled "What kind of researcher do I want to be?" I explored this question ~halfway through candidature in an attempt to recall why I chose to pursue a PhD, during a time when it couldn't feel less important (during a global pandemic). I listed qualities I would like to further develop; kindness, passion, fearlessness, grace and integrity. I now realise that all the qualities I value and want to have as a researcher, are actually just the characteristics and personal qualities I have observed in my supervisors, peers, friends and family. I acknowledge some of these people here.

First and foremost, thank you to my primary supervisor, Dr Ken Clarke for several years of guidance, unwavering support and mentorship. I am deeply grateful for your supervision and friendship through this process. My sincere thanks to my co-supervisors Dr Luke Mosley and Professor Megan Lewis for all of your supportive efforts both in the past and ongoing. Each of my supervisors are exemplary. Ken, Luke and Megan have been patient, wise and encouraging. They are wonderful supervisors who have never failed to remind me of the importance of science and research when I had doubts, especially if these doubts were about my own work.

I also want to express thanks and acknowledge the positive environment in which I conducted my studies and those who listened to my worries and frustrations, helped me solve my problems and offered reassurance, encouragement and opportunities to escape the confines of my mind and office desk. For that I thank both past and present members of the Spatial Sciences Group, URAF team and broader network of the School of Biological Sciences. I treasure our unique, welcoming and accepting community and I already miss all our tea breaks.

Lastly, I feel the most important people to acknowledge are the people who form the most invulnerable layer of my support network; my partner, friends and family. I feel

incredibly fortunate, every day, because of your collective care for and belief in me. Thank you for helping me to navigate through these recent challenging years.

Publications arising from this thesis

Peer reviewed journal articles:

Auricht, H., Clarke, K.D., Lewis, M.M., & Mosley, L.M. (2018). Have droughts and increased water extraction from the Murray River (Australia) reduced coastal ocean productivity? *Marine and Freshwater Research, 69*, 343-356.

Auricht, H., Mosley, L., Lewis, M., & Clarke, K. (2022). Mapping the long-term influence of river discharge on coastal ocean chlorophyll-a. *Remote Sensing in Ecology and Conservation,* 8, 629-643.

Articles written for publication:

Auricht, H., Mosley, L., Lewis, M., & Clarke, K. (2022). Changing influence of river discharge on coastal ocean chlorophyll-a and turbidity.

Conference Presentations:

Auricht, H., Mosley, L., Lewis, M., & Clarke, K. (2018). Have droughts and increased water extraction from the Murray River (Australia) reduced coastal ocean productivity? In, *55th Annual Australian Marine Science Association Conference, Canyons to Coast 2018*. Adelaide, Australia

“The more clearly we can focus our attention on the wonders and realities of the universe about us, the less taste we shall have for destruction.”

- Rachel Carson

Abstract

River discharge can have a significant and profound influence on coastal ocean water quality and productivity and therefore the global biogeochemical cycle. However, there is little acknowledgement or understanding of the influence of river discharge on coastal ocean productivity or water quality at local and regional scales. To a greater extent, there is a paucity of knowledge on the global scale influence of river discharge on global productivity (as indicated by chlorophyll-a concentrations), though there have been previous attempts to estimate the global change in chl-a of the open oceans at decadal time scales. Here, the influence of river discharge is assessed from local and regional to global scales via analysis of river discharge time series and remotely sensed MODIS satellite imagery products. In the first research chapter (Chapter 2) these products are applied to investigate how a lack of river discharge from Australia's Murray River (due to a drought period) and a flooding event affected the water quality and productivity of the adjacent coastal ocean waters. Findings indicate that Murray River discharge can stimulate productivity of the Southern Ocean coastal waters, up to 60 km from the river mouth. This effect was reduced to background seasonal levels during the a prolonged drought. The following chapter (Chapter 3) investigates the long-term influence of river discharge on coastal ocean chlorophyll-*a* to objectively identify where river discharge has influence under a broad range of flow conditions for 11 global rivers. This is done with a non-parametric spatiotemporal correlation analysis. The method is found to be more effective on rivers which do not have strong seasonal patterns, such as the Rhone (of France) and Murray (of Australia) rivers in temperate latitudes. The final research chapter (Chapter 4) uses the method developed in Chapter 3 to extract time series data from areas identified as influenced by river discharge, to then investigate the presence, absence and direction of trend. This is done to investigate whether the magnitude and scale of influence of river discharge may be changing over time. Some trends are detected contrary to that of previous research. A number of recommendations for future research are identified and proposed. This research is important to understand the current and

potential future impacts of river management on coastal ocean environments, and to enable more accurate and rigorous estimation of regional and global scale trends in ocean productivity and biogeochemistry. Future research is imperative in understanding the role and influence of river discharge and river and coastal management on coastal ocean productivity and water quality in the future, at local to global spatial scales.

Table of Contents

Thesis declaration II

Acknowledgements IV

Publications arising from this thesis VII

Abstract XI

List of Figures XVIII

List of Tables XXII

Chapter 1 1

1.1 Introduction 3

1.1.1 Significance of regulated river discharge on coastal ecology and productivity 4

1.1.2 Declining river flow 5

1.1.3 Indirect drivers of river flow reductions 7

1.1.4 Traditional techniques for monitoring river plumes 8

1.1.5 Remote sensing water quality 9

1.1.6 Previous global scale ocean colour research 18

1.1.7 Summary of knowledge gaps 20

1.2 Aims and objectives of the research 21

1.3 Thesis structure 23

1.4 References 24

Chapter 2 35

Abstract 40

2.1 Introduction 41

2.2 Materials and Methods 45

2.2.1 Study area 45
2.2.2 Hydrological and water-quality data 45
2.2.3 MODIS-Aqua satellite image products 48
2.2.4 Image analysis 49
2.2.5 Extrapolation to historical flow dataset 50
2.3 Results 51
2.3.1 River discharge and nutrient loads 51
2.3.2 Near-shore temporal patterns in water quality and primary productivity 51
2.3.3 Offshore temporal patterns in water quality and primary productivity ... 58
2.3.4 Hindcast mean chl-a and POC concentrations 60
2.4 Discussion 62
2.5 Conclusions 66
2.6 References 68
Appendix A 75
A.1 Nutrient loading interpolations 75
A.2 Coastal Ocean in situ water quality 76
A.3 Relationships at incremental distances from Murray Mouth 77
Chapter 3 79
Abstract 83
3.1 Introduction 83
3.2 Methods 85
3.2.1 Ocean colour products 85
3.2.2 River flow data and Selection 86
3.2.3 Spatiotemporal correlation analysis 89

3.3 Results and Discussion 91
3.3.1 Clear patterns of influence in temperate regions 91
3.3.2 Patterns of influence in tropical and subtropical regions 95
3.3.3 Complex coastal regions with unclear responses to river discharge 101
3.3.4 Limitations 104
3.4 Conclusions 105
3.5 References 106
Appendix B 116
B.1 Additional river discharge station information 116
B.2 Residual analyses 117
B.3 Chl-*a* observation maps 120
Chapter 4 123
Abstract 127
4.1 Introduction 128
4.2 Methods 131
4.2.1 River discharge data and regions of river discharge influence (RoRIs) 131
4.2.2 MODIS ocean colour products 131
4.2.3 Extracting time series for trend analysis 133
4.2.4 Trend tests and overall correlation 135
4.3 Results 136
4.3.1 Murray River 136
4.3.2 Mississippi River 137
4.3.3 Amazon River 137
4.3.4 Mekong, Parana and Rhone rivers 138

4.4 Discussion 146

4.5 Conclusion 151

4.6 References 152

Appendix C 158

C.1 Additional statistical information and results from Mann-Kendall trend test on river discharge, chl-*a*, and turbidity 158

Chapter 5 161

5.1 Key findings 163

5.1.1 Local to regional scale stimulative effects of river discharge on coastal water quality. 163

5.1.2 Image based ocean colour analysis can be used to effectively identify regions of river discharge influence. 164

5.1.3 Development of a more objective, repeatable method of identifying coastal waters influenced by river discharge. 166

5.2 Significance and broader implications 166

5.3 Limitations and general recommendations 168

5.3.1 Awareness of general limitations in monitoring change in natural environments 168

5.3.2 Refining methodology and testing alternative approaches 169

5.4 Recommendations for future research 172

5.4.1 Using spatiotemporal analysis to explore effects of other broad scale phenomena 172

5.4.2 A necessity for further in situ coastal water quality monitoring alongside remote sensing methodologies 173

5.4.3 Sensor development, increased sampling and advancement of optical algorithms 174

5.5 References 177

List of Figures

Figure 2.1: Study area showing location and extent of Australia's Murray–Darling Basin 44

Figure 2.2: Murray River flow time series, total nitrogen and total phosphorous loadings 47

Figure 2.3: Example of MODIS–Aqua (monthly composite) satellite imagery products 53

Figure 2.4: Temporal profiles for (a) mean chlorophyll-*a* (chl-*a*) concentration and (b) mean particulate organic carbon (POC) within an 8-km radial zone of the marine waters beyond the Murray River Mouth 55

Figure 2.5: Relationship between (a) mean chlorophyll-*a* (chl-a) and (b) mean particulate organic carbon (POC) concentration with mean daily river (barrage) outflow 56

Figure 2.6: Temporal profiles for (a) the mean particulate inorganic carbon (PIC) concentration and (b) mean sea-surface temperature (SST) within an 8-km radial zone of the marine waters beyond the Murray River Mouth 57

Figure 2.7: Continuous in situ transect data for salinity taken on 25 February 2011 during a high-flow event. 58

Figure 2.8: Hovmöller distance–time plots, showing the mean chlorophyll-a (chl-*a*) concentration (mg m^{-3}) 59

Figure 2.9: Hovmöller distance–time plots showing mean particulate organic carbon (POC) concentration (mg m^{-3}) 60

Figure 2.10: (a) Hindcast prediction of chlorophyll-a (chl-*a*) concentration in 8-km radial zone of Murray Mouth 61

Figure 3.1: Map of flow stations for rivers investigated in this paper 88

Figure 3.2: Flow chart summarising the overall process for the spatiotemporal correlation analysis. 90

Figure 3.3: Maps of river discharge influence based on Spearman correlation analysis on remotely sensed MODIS chl-a concentrations and corresponding river flow time series and chl-a concentrations at pixel (with location on top right of time series plot) for the a) Murray River on the coastal waters in the Southern Ocean of South Australia, b) Rhone River in the Gulf of Lion, France, c) Amazon River on the mid-Atlantic Ocean and along the northeastern coast of South America and d) Parana River on the Southern Atlantic Ocean.....94
Figure 3.4: Maps of river discharge influence based on Spearman correlation analysis on remotely sensed MODIS chl-a concentrations and corresponding river flow time series and chl-a concentrations at pixel (with location on top right of time series plot) for the (a) Mekong River on the South China Sea, (b) Mississippi River on the northern Gulf of Mexico, (c) the Niger River on the coastal waters in the Gulf of Guinea and (d) the Pearl River in the Gulf of Mexico. 100
Figure 3.5: Maps of river discharge influence based on Spearman correlation analysis on remotely sensed MODIS chl-a concentrations and corresponding river flow time series and chl-a concentrations at pixel (with location on top right of time series plot) for the (a) St. Lawrence River draining to the Gulf of St. Lawrence, (b) the Thames River draining to the North Sea and (c) Columbia River on the Pacific Ocean. 103
Figure 4.1: Lengths of available historical river discharge data used in this paper compared to MODIS Aqua data product availability.....134
Figure 4.2: The spatial extent of the Murray region of river discharge influence (RoRI), where $r_s > 0.3$ is shown in a). The results of Hamed and Rao modified Mann-Kendall trend tests on b) Murray River discharge, c) sum of chl-*a* concentrations per month within Murray RoRI d) sum of Rrs645 (turbidity) concentrations per month within the Murray RoRI, and Spearman rank correlation (r_s) between e) river discharge and chl-*a* concentration, f) river discharge and turbidity, and g) turbidity and chl-*a* over the MODIS time period.....139
Figure 4.3: The spatial extent of the Mississippi region of river discharge influence (RoRI), where $r_s > 0.3$ is shown in a). The results of Hamed and Rao modified Mann-

Kendall trend tests on b) Mississippi River discharge, c) sum of chl-*a* concentrations per month within Mississippi RoRI d) sum of Rrs645 (turbidity) concentrations per month within the Mississippi RoRI, and Spearman rank correlation (r_s) between e) river discharge and chl-*a* concentration, f) river discharge and turbidity, and g) turbidity and chl-*a* over the MODIS time period. 140
Figure 4.4: The spatial extent of the Amazon region of river discharge influence (RoRI), where $r_s > 0.3$ is shown in a). The results of Hamed and Rao modified Mann-Kendall trend tests on b) Amazon River discharge, c) sum of chl-*a* concentrations per month within Amazon RoRI d) sum of Rrs645 (turbidity) concentrations per month within the Amazon RoRI, and Spearman rank correlation (r_s) between e) river discharge and chl-*a* concentration, f) river discharge and turbidity, and g) turbidity and chl-*a* over the MODIS time period..... 141
Figure 4.5: The spatial extent of the Mekong region of river discharge influence (RoRI), where $r_s > 0.3$ is shown in a). The results of Hamed and Rao modified Mann-Kendall trend tests on b) Mekong River discharge, c) sum of chl-*a* concentrations per month within Mekong RoRI d) sum of Rrs645 (turbidity) concentrations per month within the Mekong RoRI, and Spearman rank correlation (r_s) between e) river discharge and chl-*a* concentration, f) river discharge and turbidity, and g) turbidity and chl-*a* over the MODIS time period..... 142
Figure 4.6: The spatial extent of the Rhone region of river discharge influence (RoRI), where $r_s > 0.3$ is shown in a). The results of Hamed and Rao modified Mann-Kendall trend tests on b) Rhone River discharge, c) sum of chl-*a* concentrations per month within Rhone RoRI d) sum of Rrs645 (turbidity) concentrations per month within the Rhone RoRI, and Spearman rank correlation (r_s) between e) river discharge and chl-*a* concentration, f) river discharge and turbidity, and g) turbidity and chl-*a* over the MODIS time period..... 143
Figure 4.7: The spatial extent of the Parana region of river discharge influence (RoRI), where $r_s > 0.3$ is shown in a). The results of Hamed and Rao modified Mann-Kendall trend tests on b) Parana River discharge, c) sum of chl-*a* concentrations per month

within Parana RoRI d) sum of Rrs645 (turbidity) concentrations per month within the Parana RoRI. Spearman rank correlation (r_s) between e) river discharge and chl-*a* concentration, f) river discharge and turbidity, and g) turbidity and chl-*a* over the MODIS time period..... 144

List of Tables

Table 1.1: Satellite sensors capable of and used for ocean colour measurements. 12

Table 3.1: River flow data used in this study. 87

Table 4.1: Region of river discharge influence (RoRI) for the study rivers where correlation between river discharge and chl-*a* concentration is >= 0.3..... 135

Table 4.2: Trend directions from Hamed and Rao modified Mann-Kendall trend tests on monthly river discharge data, chl-*a* concentrations in coastal areas 136

Chapter 1

Introduction

1.1 Introduction

In many regions of the world freshwater discharge has a profound influence on coastal ocean productivity and water quality (e.g. Phillips *et al.* 2017; Shi *et al.* 2019; Swieca *et al.* 2020). River discharge can alleviate nutrient limitations for phytoplankton and other marine life and have a bottom-up, stimulating and supportive effect on trophic webs, with positive consequences for the local environment and industries (Bellier *et al.* 2007; Drinkwater and Frank 1994; Fernández-Nóvoa *et al.* 2019; Gillanders and Kingsford 2002; Gong *et al.* 2006; Grimes and Kingsford 1996; Lazure *et al.* 2009; Planque *et al.* 2007). Some authors suggest riverine discharge plumes are generally among the most productive places in the sea (Grimes and Kingsford 1996). This suggests river discharge plays a strong ecological role in supporting a variety of life in marine environments.

River discharge can have a range of important consequences on coastal water environments and species. Freshwater from rivers supplies sediments, dissolved and undissolved nutrients and materials to coastal waters, which may otherwise be nutrient limited. River discharge can increase the turbidity, nutrient concentration of receiving coastal waters and reduce light penetration depth (Baird *et al.* 2021). Furthermore, the physical force of water flowing into ocean regions can also change coastal circulation dynamics (Babin *et al.* 2012). These contributions and influences can often cause significant changes in phytoplankton and productivity in these locations, affecting several marine ecosystem processes. For example, the Bay of Biscay on the north coast of Spain and west coast of France, is considered highly productive (Fernández-Nóvoa *et al.* 2019). Phytoplankton biomass and primary production in this region is influenced not only by convective upwelling, but also river discharge from the Loire and Gironde river plumes (Álvarez-Romero *et al.* 2011). Several studies have shown these particular plumes are the preferred spawning area of anchovy and sardines (Bellier *et al.* 2007; Fernández-Nóvoa *et al.* 2019), and that the region is characterised by high socio-economic importance due to activities including tourism, shellfish farming and other fisheries (Lazure *et al.* 2009). Similarly, Phillips *et al.* (2018) found that seabirds *Ardenna grisea* and *Uria aalge* selectively occupy and track Columbia River plume

waters off the south western coast of Washington, USA, especially in plume boundary waters. This was found to be due to aggregation of zooplankton which attract prey fishes in river plume waters. Apex predators and marine mammals can be signs of healthy and productive ecosystems (Block *et al.* 2011; Colombelli-Négrel 2015). Thus, river discharge can have surprising and important influences on coastal ecosystem ecology and marine food-web dynamics.

1.1.1 Significance of regulated river discharge on coastal ecology and productivity

The stimulative services of coastally-discharging rivers are often only acknowledged in hindsight, following extensive river damming and regulations, when the positive interactions between rivers and coastal environments have been drastically modified or lost. Several historical examples demonstrate the consequences of reductions and alterations to natural river flow on primary productivity of coastal environments and therefore, local fish stocks, environments and industries. A well-known example is the case of the Aswan Dam. The high nutrient levels and large quantities of organic matter delivered to the Mediterranean Sea by the influx of Nile flood waters encouraged intense phytoplankton blooms in the coastal region. (Drinkwater and Frank 1994). These blooms maintained the site of significant reproduction events and nurseries of sardines and prawns, supporting major fisheries. During the construction of Aswan Dam, completed in 1969, flow decreased by 40 km^3 $year^{-1}$ (Grimes and Kingsford 1996) causing decline in primary productivity off the delta. This had consequences for Egyptian fisheries and catches in the Mediterranean Sea decreased from ~37,800 t in 1962 to ~7,140 t in 1976 (Bebars and Lasserre 1983). Following this fisheries collapse, discharge rates from the dam were increased and the stocks of the sardine fishery recovered to approximately one third of their pre-dam levels (Grimes and Kingsford 1996; Smetacek 1986).

In addition, construction of China's Three Gorges Dam (completed in 2006) caused decline in primary productivity in the East China Sea by ~86% (between 1998 and 2003), as freshwater and nutrient loads from the river became drastically reduced (Chai *et al.* 2009; Gong *et al.* 2006). This is believed to have ultimately caused the decline of fishery

catches in the region (Gong *et al.* 2006). Similar phenomena occurred after significant volumes of water were diverted from the Colorado River for agriculture, reducing discharge into the Gulf of California. The population of the totoaba (*Totoaba macdonaldi*), the largest sciaenid fish in the world and endemic to the Gulf of California, declined such that it was declared 'vulnerable' under the US Endangered Species Act 1973 (Barrera-Guevara 1990; Cisneros-Mata *et al.* 1995). It has been illegal to catch this species since 1979. Although it could not be confirmed, it was suspected that the significant decrease in freshwater discharge from the Colorado River altered the state of spawning and nursery habitat in the vicinity of the delta (Rowell *et al.* 2008).

These cases demonstrate the ecological and anthropogenic significance of river discharge to coastal waters, and how historical reduction or loss of flows to marine environments can have extreme consequences. River discharge is often thought of as a local scale influencer on phytoplankton biomass and primary productivity, but the influence of river discharge can, as these examples show, surpass the spatial and temporal extents of the river plumes themselves. Increasing modification of natural river flow is therefore of great concern, not only at local scales, but at broader, global scales as well.

1.1.2 Declining river flow

At continental and global scales, irrigation extractions and water reservoir management affect the timing and the volume of freshwater discharge which reaches the oceans. In fact, a global scale study of the world's largest river systems suggested that, by 2005, over half of the world's river systems were already regulated by dams (Nilsson *et al.* 2005). Of these, more than 45,000 were above 15 m high and were collectively capable of holding back about 15% of the total annual river runoff globally (Gornitz 2000). More recent research shows a continuation of the boom in dam construction during the last century. This includes the findings of Grill *et al.* (2019), who suggest that only ~23% of rivers longer than 1000 km remain free-flowing and uninterrupted to the oceans. In most circumstances, river regulations have occurred as a result of increasing demand from agriculture, demand for renewable energy or other economic activities (Nilsson *et al.*

2005; Zarfl *et al.* 2015), and are typically implemented without consideration for the potential effects on marine environments, though they regulate and significantly reduce river flow and the delivery of freshwater constituents to the sea. Biemans *et al.* (2011) studied the effects of global irrigation and reservoirs on river discharge for the period between 1981 and 2000. Their results reported that irrigation lowers global river discharge by 5% between May and August (northern hemisphere summer irrigation season), which is partly offset between October and March, when discharge increases by approximately 2% as extra water is released from reservoirs. Averaged over a year, extraction of irrigation water from rivers (including extraction from water reservoirs) appears to decrease global river discharge by 2.1% or 930 km^3 (Biemans *et al.* 2011). Although this may seem a relatively small decrease, its consequences are more severe in some regions and river basins than in others. In some instances, river flows have ceased entirely for a number of years (e.g. the Murray River, Australia) (CSIRO 2008; Mosley *et al.* 2013), thus the supply of dissolved (e.g. nutrients) and suspended materials to the ocean is lost for prolonged periods. The effects of these changes on marine species can be profound, but in many regions how species may respond is unclear.

To further complicate the situation, Akbarzadeh *et al.* (2019) conducted a global scale study investigating riverine fluxes of nitrogen, nutrient silicon, phosphorus and organic carbon due to damming. Results indicated that since the start of the current century, approximately 7.2% of nitrogen loading to river networks was lost due principally due to dams. The authors also suggested this would increase to 15% by 2030 due to global acceleration of hydro-electric dam construction. The research also suggested that because of nitrogen fixation in reservoirs, damming increases the nitrogen:phosphorus ratio of river discharge and thus reduces nitrogen limitation of primary productivity in receiving marine environments. This creates an interesting dichotomy, highlighting a paucity of knowledge on whether higher nutrient concentrations and loadings of river discharge could offset reduced river discharge volumes in the future.

1.1.3 Indirect drivers of river flow reductions

In addition to the more direct impacts of water extraction for consumptive purposes, such as irrigation and damming, climate change is also altering magnitude and variability of river flow and discharge. These changes presently affect the frequency and length of extreme low flow periods in many rivers, and will likely continue into the future. For example, Morrison *et al.* (2002) created a flow model to predict future changes in flow due to climate change in the Fraser River. This study indicated that trends in both flow and river water temperature closely match the 1961-1990 historical trends which suggests the observed changes at this time may already be related to climate change. More recent research by Milly and Dunne (2020) showed that Colorado River flow is decreasing due to meteorological drought and warming. The authors estimated that mean annual discharge has been decreasing by 9.3% per degree Celsius of warming. The main driver of this decrease is the loss of snow in the upper Colorado River basin, which increases solar radiation and evapotranspiration. These observations led many authors to believe that length and frequency of extreme low flow periods will increase in many rivers in the future (Nilsson *et al.* 2005; Nohara *et al.* 2006; Shi *et al.* 2019; Stahl *et al.* 2010).

Current climate projections estimate an increase in seasonality of river discharge where discharge will increase in high flow periods and decrease in low flow periods, for about one third of the global land surface area for 2071 - 2100 relative to 1971 - 2000 (van Vliet *et al.* 2013). It is also predicted that for high northern latitude areas and in the tropical region, annual river discharge will increase, while in mid-northern latitude regions (US, central America, southern and central Europe, southeast Asia) and the southern latitudes (southern parts of South America, Africa and Australia), mean annual river discharge will decrease (van Vliet *et al.* 2013). Similarly, Milly *et al.* (2005) predicted, by the year 2050, an increase of 10–40% in runoff in eastern equatorial Africa, the La Plata Basin and high latitude North America and Eurasia, and a decrease of 10–30% in runoff in sub-Saharan Africa, southern Australia, southern Europe, the Middle East and mid-latitude western North America.

The effects of anthropogenic interference, climate change, regulation and management of the world's river systems currently effects and will continue to affect coastal ocean environments receiving (or no longer receiving) environmental flows. In those areas of declining river flow the state of coastal ocean environments is likely to continue to change. The compounding effect of ongoing long-term decreases in phytoplankton biomass and productivity could have unprecedented negative effects on marine ecosystems and species. However, more research is needed on how coastal marine environments respond to prolonged low and zero flows, as well as varying volumes and flow concentrations, now and in the future. Fortunately, there are new datasets and ways in which changes to coastal productivity can be estimated as a response to reduced flows across the globe.

1.1.4 Traditional techniques for monitoring river plumes

Historically, changes in ocean productivity in response to changes in river flows have most often been monitored and studied by way of *in situ* ship-borne sampling or data collection from moored instruments. While this has increased the understanding of river plumes and productivity, these methods are spatially and temporally limited. Additionally, ship-borne sampling is heavily dependent on weather conditions and is typically expensive, not to mention that *in situ* sampling in estuaries and coastal regions which receive river discharge is often biased towards high flow conditions, limiting the knowledge and understanding of the system under low or no flow events.

However, it is not only possible, but also more time and cost effective to estimate changes in ocean productivity from remotely sensed ocean colour. Suspended particulate matter, microscopic organisms and coloured dissolved organic matter in water columns influence and contribute to ocean colour. Phytoplankton (the largest contributor to changes in ocean colour) are detectable because they contain the pigment chlorophyll-*a* (henceforth, chl-*a*) which is also the main pigment responsible for photosynthesis. All of these components absorb, reflect, scatter and backscatter light and energy at several wavelengths of the electromagnetic spectrum. This reflected energy (reflectance) can be

measured by remote dsensors aboard platforms such as satellites. These can image the whole of the Earth at regular and frequent intervals. This technology makes it possible to estimate the concentrations and distributions of a variety of water constituents over global spatial and temporal scales from ocean colour imagery products.

1.1.5 Remote sensing water quality

1.1.5.1 Ocean colour sensors and satellite platforms

A number of sensors specifically designed to detect ocean colour have been mounted on Earth orbiting satellites. These sensors vary in design purpose, affecting their revisit time, spectral and spatial resolution. The Coastal Zone Colour Scanner (CZCS) was the first satellite mounted sensor to monitor ocean colour specifically, and its mission was a first feasibility study to determine whether chl-*a* concentrations could be reliably estimated from a satellite based sensor (Bierman 2010; Gordon 1980; Hovis *et al.* 1980). It experienced a number of technical difficulties throughout its relatively brief lifetime, launched in November 1978 and operational until it was retired in 1986 (refer Table 1.1). Despite these challenges, the research arising from the CZCS identified the necessary requirements for validation, calibration, atmospheric correction, bio-optical algorithms, data processing and data access for future ocean colour missions (Barale and Schlittenhardt 1993; Bierman 2010). The development and launch of the CZCS was therefore considered successful.

NASA planned a second mission specifically for monitoring of ocean colour and primary productivity and to gain broader understanding of the global biogeochemical cycle. The Sea-viewing Wide Field-of-view Sensor (SeaWiFS) was launched for this purpose, operating from September 1997 until December 2010 (refer Table 1.1). It had some improvements on CZCS. For instance, SeaWiFS recorded in eight bands compared to CZCS's six. Later, in 2002, the Medium Resolution Imaging Spectroradiometer (MERIS) was launched on board the ENVISAT satellite and was operated by the European Space Agency (ESA) in collaboration with NASA (ESA 2006). The technical specifications of MERIS were further developed than those of the CZCS and SeaWiFS, respectively. MERIS orbited and imaged the Earth every three days and recorded in 15 spectral bands

and was operational until 2012. Both MERIS and the Moderate Resolution Imaging Spectroradiometer (MODIS) built on experience derived from the earlier sensors. However, MODIS has a shorter revisit period (higher temporal resolution) than MERIS. MODIS also records in 36 spectral bands (refer Table 1.1) across the visible to thermal electromagnetic spectrum and its ocean colour bands (in the visible spectrum) are narrower than that of SeaWiFS and CZCS. This aids atmospheric correction (a process which removes absorption and scattering effects from sensor recordings due to the atmosphere). In addition, MODIS also has more rigorous signal-to-noise specifications to reduce sensor-based errors than the aforementioned sensors (Esaias *et al.* 1998).

Other sensors, some of which have been in orbit for longer periods than MERIS and MODIS, include NASA's Landsat 5 and 7 Thematic Mapper (TM) and Enhanced Thematic Mapper (ETM+). These satellite based sensors have also been used in some ocean colour research (e.g. Barnes *et al.* 2014; Ekstrand 1992; Hu 2009), and a key benefit of Landsat is its high spatial resolution of approximately 30 metres. However, Landsat platforms and sensors were designed primarily for land based applications, thus their products are less suitable than those of other sensors developed for the purpose of ocean colour monitoring. In more recent years, instruments on board Copernicus Sentinel-3A and Sentinel 3B (including the ocean and land colour instrument (OLCI) and the Sea and Land Surface Temperature Instrument (SLSTR)) have been used in several assessments of water quality of inland lakes and relatively shallow estuarine and coastal areas (Liu *et al.* 2021; Lyu *et al.* 2020; Soomets *et al.* 2020; Urquhart and Schaeffer 2020) as well as for phytoplankton bloom detection (Polikarpov *et al.* 2021). The two Sentinel-3 satellites have sun-synchronous orbits which enable daily revisit time for SLSTR and less than two day revisit time for OLCI at the equator (ESA 2022). The core focus of Sentinel-3's OLCI is continuity of the Envisat MERIS capability, but with a number of improvements (EUMETSAT 2018). The Sentinel-3 products have relatively high spatial resolution of ~300 m and moderate spectral resolution (21 bands) (refer Table 1.1) and the sensors are therefore quite powerful in their monitoring capabilities.

Although there are more recently developed sensors in orbit today, NASA's MODIS is arguably the most successful ocean colour sensor launched to date. MODIS operates on board two satellites, Terra and Aqua. Terra was launched in 1999, while Aqua was launched in 2002. Both sensors are operational today and have exceeded their designed life expectancy, although Terra began to drift in 2020 (Thome 2022). Terra is also affected by calibration issues which affect ocean colour estimates (Bierman 2010) MODIS therefore provides the longest temporal record among the satellite based sensors designed for ocean colour applications. Estimating ocean colour and water quality from MODIS provides a powerful source of data as it allows worldwide coverage of marine components, measured consistently at regular intervals, and is a useful method for monitoring ocean state (Devlin *et al.* 2015). This provides the basis for the justification of using MODIS data throughout this thesis.

Table 1.1: Satellite sensors capable of and used for ocean colour measurements.

Sensor(s)	**Satellite platform**	**Operation**	**Number of bands**	**Spatial resolution (m)**	**Revisit frequency of satellite platform**
MODIS Aqua	Aqua	2002 - present	36	250, 500, 1000	Daily
Thematic Mapper (TM) and Enhanced Thematic Mapper (ETM+)	Landsat -5 and Landsat -7	1984 - 2017	7	30	8 days
SeaWIFS	SeaStar	1997 - 2010	8	1100	Daily
CZCS	Nimbus 7	1978 - 1986	6	825	6 days
MERIS	Envisat	2002 - 2012	15	300	3 days
Global Imager (GLI)	ADEOS II	2002 - 2003	36	250, 1000	4 days
Ocean and Land Colour Instrument (OLCI)	Copernicus Sentinel-3	2016 - present	21	300	Daily
Hyperion	Earth-Observing 1 (EO-1)	2000 - 2017	220	30	16 days

1.1.5.2 Standard ocean colour algorithms

Detecting changes in water quality with remote sensing techniques relies on the development of both sensors and ocean colour algorithms applied to satellite imagery. As several factors can influence ocean colour, marine waters have been segregated into two distinct classes, Case 1 and Case 2, to distinguish between the primary causes of ocean colour (Bierman 2010). Case 1 waters are characterised as those which are predominantly clear, but are affected principally by phytoplankton. Case 2 waters are coastal and estuarine waters where other constituents affect ocean colour, i.e. not just phytoplankton and related particles, but also other substances such as inorganic particles in suspension and chromophoric dissolved organic matter (CDOM) which vary independently of phytoplankton (IOCCG 2000). This makes Case 2 waters more optically complex than Case 1 waters, and the algorithms needed to assess ocean colour components in either case, different (IOCCG 2000).

1.1.5.2.1 Chlorophyll-*a*

The standard chl-*a* product distributed by NASA's Goddard Space Flight Centre is an estimate in units of mg m^{-3} (equivalent to µg L^{-1}) arising from the OC3M algorithm, which is based on the SeaWiFS OC4v4 algorithm (O'Reilly *et al.* 2000). These algorithms were developed for application in Case 1 waters. The *in situ* dataset used to calibrate and develop the OC3M algorithm consists of 2,853 observations from a range of marine environments with varying optical properties and is the largest dataset ever configured for algorithm refinement (O'Reilly *et al.* 2000). This empirical algorithm is a three-band operational algorithm and uses the maximum blue/green band ratio (Pereira and Garcia 2018). It has been thoroughly reviewed in its effectiveness to accurately estimate chl-*a* concentrations in marine waters (Bierman 2010; Blondeau-Patissier *et al.* 2014). In many studies where OC3M algorithm estimates were compared against *in situ* data of the same area, OC3M performed consistently well and was often most accurate when compared to other algorithms predicting chl-*a* and field sampled data (Bierman 2010; Tilstone *et al.* 2013; Chaves *et al.* in press).

The relationship between chl-*a* concentration and remote sensing reflectance (Rrs) follows the equation:

$$Chlor_a = 10 \wedge (a_0 + a_1 R_{3M} + a_2 R_{3M}^2 + a_3 R_{3M}^3 + a_4 R_{3M}^4)$$

Where $$R_{3M} = log_{10}\left[R_{550}^{443} + R_{550}^{490}\right]$$

The argument of the logarithm is a representation of the maximum of the ratios of remote sensing reflectance at 443 nm (SeaWiFS Band 9) to 550 nm (SeaWiFS Band 12) and 490 nm (SeaWiFS Band 10) to 550 nm (SeaWiFS Band 12) (O'Reilly *et al.* 2000; Bierman 2010).

A number of other ocean colour chl-*a* algorithms have been developed in recent decades. Some of these are described as "semi-*a*nalytical" and rely on physical modelling of in-water radiative transfer processes (inherent optical properties (IOP) of backscattering and absorption) alongside aspects of the model expressed by empirical relationships (CRCSI 2021; Tong *et al.* 2022). A benefit of these algorithms is they enable users to estimate a number of water quality properties from a single water leaving radiance spectrum. The Garver-Siegal-Maritorena (GSM01) algorithm was developed for Case 1 waters and relates the normalised water-leaving radiance (L_{wn}) to IOP of backscatter and absorption and their components (Garver and Siegel 1997; Maritorena *et al.* 2002). Subsequent inversion of the model allows users to determine chl-*a* absorption and therefore, phytoplankton biomass (Maritorena *et al.* 2002; Pereira and Garcia 2018). There have also been several algorithms adjusted to increase accuracy at local and regional scales in particular locations (e.g. Ab Lah *et al.* 2014; Chen and Quan 2013; Tong *et al.* 2022).

The optical complexity of Case 2, turbid and coastal waters means that applying Case 1 algorithms is generally regarded to be unreliable in measuring coastal water quality among the remote sensing community (Acker *et al.* 2005; CRCSI 2021; Darecki *et al.* 2003; IOCCG 2000; Kampel *et al.* 2007). Previous research proposed that algorithms could be selected based on relative contributions of three major absorbing substances in

Case 2 waters (CDOM, phytoplankton and detrital material) and how they modify the spectral signature of a water body (IOCCG 2000). This suggests up to 9 optical classes of water bodies can be established, with only one fitting the Case 1 definition (Darecki *et al.* 2003) and demonstrates the challenges of identifying a generally applicable algorithm which can be applied to satellite imagery across any water body. Some Case 2 algorithms have consequently incorporated red and NIR bands into algorithms to account for other coloured and suspended matter in water columns (Gitelson *et al.* 2009; Ruddick *et al.* 2001).

There has been substantial effort to improve the standard algorithms for estimating a number of optical properties in Case 2 coastal ocean environments, including those affected by river plumes (Ab Lah *et al.* 2014; Babin *et al.* 2012; Chen and Quan 2013). However, there is evidence that algorithms developed for Case 1 waters can be usefully applied to study Case 2 waters. For example, Tilstone *et al.* (2013) found the OC3M algorithm performed better in coastal Case 2 waters of the eastern Arabian Sea when compared to GSM and GIOP chl-*a* algorithms. The OC3M estimations were found to be within 11% of *in situ* measurements of chl-*a*, compared 24% and 55% for the GSM and GIOP algorithms, respectively. Interestingly, the eastern Arabian Sea's water quality is affected by river runoff from a number of rivers (Rivers Perivar, Mahi, Narmada, Indus and Hab) as well as winter convection and monsoonal upwelling. The relatively good performance of the standard OC3M algorithm in these complex waters indicate that Case 1 algorithms can still be useful in Case 2 waters. Similarly, application of semi-analytical algorithms (GSM and Carder algorithms) in the La Plata basin were not found to be significantly more accurate than empirical OC4v4 models (Garcia *et al.* 2006). This region also receives river discharge from the Parana and Uruguay rivers. These studies demonstrate that there is no single, best, standard algorithm for use in Case 2 waters for estimating chl-*a* concentrations and phytoplankton biomass.

1.1.5.2.2 Other useful ocean colour products

A number of algorithms have been designed to detect and estimate concentrations of coloured dissolved organic materials (CDOM), turbidity, particulate organic carbon (POC) and particulate inorganic carbon (PIC) from satellite imagery. These have also been developed and validated to varying degrees in a variety of locations. In addition to the standard OC3M and GSM ocean chl-*a* MODIS products, POC estimates from MODIS ocean colour imagery is also distributed by NASA. POC is produced by phytoplankton during photosynthesis. Oceanic POC particles consist of autotrophic and heterotrophic microorganisms and biologically derived detrital particles suspended in seawater (Stramska 2009). In addition to phytoplankton (where biomass is indicated by chl-*a* concentration), POC is a crucial part of the ocean's "biological pump" (Stramska 2009; Stramski *et al.* 2008). Estimates of POC are calculated from an empirical relationship between *in situ* measurements of POC and blue-to-green band remote sensing reflectance. The algorithm to calculate POC for MODIS imagery is a power-law relationship based on a ratio of remote sensing reflectance (Rrs) at Rrs 443 (Band 9) and Rrs 547 (Band 12) and POC:

$$poc = a \times \left(\frac{Rrs(443)}{Rrs(547)}\right)^{b}$$

Where a = 203.2 and b = -1.034.

Coccolithophores produce POC via removal of carbon for photosynthesis and supply waters with carbon via calcification and production of PIC. PIC estimates are calculated using a semi-analytical reflectance model which calculates normalised water leaving reflectance from a backscattering coefficient, a diffuse attenuation coefficient and a term for backscattering due to coccolithophores (Mitchell *et al.* 2017). These are also used in chl-*a* concentration estimations meaning that between a particular range of PIC (0–3.3 mmol m−3) and chl-a (0–10 mg m−3), PIC concentration can be determined via a look up table (developed by Balch *et al.* 2005; Mitchell *et al.* 2017). The ratio between POC and PIC is sometimes used to infer whether an analysed region or waterbody could be a sink or source of atmospheric CO_2 (CRCSI 2021; Gerecht *et al.* 2014). PIC is therefore

also useful in ocean colour and water quality investigations (Balch *et al.* 2007; Hovland *et al.* 2013; Sadeghi *et al.* 2012).

In addition, a basic indicator of turbidity is useful in ocean colour remote sensing research to provide further context to and classification of coastal and open ocean waters. These measurements can indicate the relative amount of detrital material, suspended sediments, aquatic carbon and CDOM in coastal and open ocean waters. Several studies have concluded that the strongest relationship between suspended sediments and reflectance of water is observed in red and near infrared bands (Dogliotti *et al.* 2015). In fact, several studies have found strong correlations between the MODIS red band centred at wavelength 645 nm and general estimates of turbidity or suspended matter in waters (e.g. Aurin *et al.* 2013; Babin *et al.* 2012; Dogliotti *et al.* 2015; Kirk 1994). Indeed, a range of useful ocean colour algorithms and indicators are continually being developed, based on Earth observation data from local to global scales.

1.1.5.3 Remote sensing to investigate river discharge plumes and influence

River plumes can influence the salinity, temperature, water quality, vertical mixing and ambient velocities of the aquatic regions to which they discharge (Hamidi *et al.* 2017). They can also deliver harmful land-based pollutants and pathogens to coastal ecosystems (Costanzini *et al.* 2014; Hamidi *et al.* 2017). It is in this context that most remote sensing based research on river plumes has been conducted. It is clear that identifying the spatial extent of river plumes and the scale of their influence is important for management policy and environmental restoration plans. Remote sensing of water quality and turbidity is an efficient way of monitoring the spatial extent of river plumes over time when compared to traditional *in situ* based sampling. Studies that have employed remote sensing methods to determine the spatial and temporal extents of river plumes, usually under high flow conditions, have used a range of approaches and data products (e.g. Alvarez-Romero *et al.* 2013; Costanzini *et al.* 2014; Hopkins *et al.* 2013; Masotti *et al.* 2018; Petus *et al.* 2014a; Petus *et al.* 2014b). Both Alvarez-Ramero *et al.* (2013) and Petus *et al.* (2014b) used supervised classification methods on MODIS ocean colour imagery

(including true colour imagery) to investigate potential risk to the Great Barrier Reef due to several river plumes. Similarly, Guo *et al.* (2017) used surface reflectance products from MODIS and the Geostationary Ocean Colour Imager (GOCI) satellite to investigate inter and intra-daily variation in coastal water salinity and turbidity due to Yellow River discharge. These studies have importantly improved the knowledge of river discharge influence on phytoplankton and productivity (including harmful algal blooms) in a number of regions. However, their methods are not necessarily transferrable to other systems in other locations because they have been tuned in accordance with both local knowledge, *in situ* measurements or with a level of subjective classification.

It is important to understand the consequences of high nutrient loadings and pollutants delivered to coastal environments, including how damming and subsequent changes to suspended sediment in coastal waters will affect productivity (Chen *et al.* 2017) and to determine the inter- and intra-annual variation in river plume direction, extent, concentration and persistence. In many regions, the basic characterisation or identification of the maximum spatial extent of the coastal waters which rivers may influence, is not necessarily known (Fredston-Hermann *et al.* 2016). This lack of local knowledge contributes to a lack of knowledge on the influence of river plumes at the broader, global context. There is also a paucity of knowledge on the potential consequences if these flows remain low or are lost entirely for prolonged periods (Cloern *et al.* 2016; Masotti *et al.* 2018). This is critical as reduction of river flow volume and further changes in timing of peak river flow is likely to continue and become more severe due to climate and increasing anthropogenic dependency and interruption, as future projections suggest (Masotti *et al.* 2018). This research is increasingly important, as flows of many coastally discharging rivers around the world continue to change.

1.1.6 Previous global scale ocean colour research

The accuracy of climate change impact predictions on coastal marine ecosystems, depends on estimates of change in global scale ocean productivity (Behrenfeld *et al.* 2016a; Boyce *et al.* 2010). Of global scale ocean productivity research which has been

conducted, most studies have effectively used satellite imagery ocean colour products. For example, a study by Polovina *et al.* (2008) used 9 years of SeaWIFS imagery products to investigate the world's oligotrophic waters, where chl-*a* concentrations fall below 0.07 mg m^{-3}. The authors found that these oligotrophic regions of the world's ocean were expanding by 1-4% per year. These findings are consistent with the hypothesis that rising sea surface temperatures (SST products were also analysed in this study) will increase thermal stratification of ocean waters and reduce chl-*a* or phytoplankton biomass, and thus expansion of oligotrophic subtropical open ocean regions. While these global scale studies have advanced global climate predictions, coastal ocean regions or potential stimulative influence of river discharge on ocean productivity are often not considered.

Coastal ocean regions make up only a small fraction of ocean area, yet disproportionately contribute to marine resources and biogeochemical processes. These regions therefore have important roles in several different global biogeochemical cycles (Charette *et al.* 2016; Simpson and Sharples 2012). Despite this knowledge, these productive coastal regions are often excluded from global Earth system models that are used to project climate change impacts on marine ecosystems (Van Oostende *et al.* 2018). For example, Boyce *et al.* (2010) estimated the productivity of the global oceans but masked shallow (< 25 m deep) and coastal ocean regions from imagery (using a ~ 1 km buffer around continents). Most other global scale ocean productivity studies have taken similar approaches, excluding coastal data from analysis (e.g. Behrenfeld *et al.* 2016b; Gregg and Rousseaux 2019; Hammond *et al.* 2020). The purpose of this is usually to reduce overestimations due to optical errors in satellite derived products, which are more likely to be affected by bottom-reflectance or land contamination in shallow, near coastal areas. In the study by Boyce *et al.* (2010), the authors acknowledged that some influences on productivity, including that due to coastal runoff and river discharge, was outside the scope of their analysis. However, given that several global rivers have such large volumes of discharge that river plumes can extend several kilometres into open ocean regions (Babin *et al.* 2012; Constantin *et al.* 2018), river discharge may have a greater influence on ocean productivity than is currently recognised. Therefore, river discharge may effect

global scale estimates of ocean productivity, but this has not been studied explicitly to date and requires improved spatial analysis, methodology and approaches.

1.1.7 Summary of knowledge gaps

It is clear that although there has been increasing interest and need for investigation of river discharge influence on coastal waters, where this research has occurred, it has often been temporally or spatially limited. There is a clear paucity of knowledge on the effects of river discharge on coastal water quality and productivity in many regions of the globe, particularly under low or no flow conditions. However, this information is important to predict potential changes in coastal environmental conditions under a range of scenarios. A severe lack of long-term analyses on the prevalence and influence of river discharge on coastal water quality and productivity from local to global scales, also underpins our misunderstanding of the link between river discharge and coastal ecosystems, and undermines the sustainable management of these systems. Therefore, investigation of the relationship between these systems, and the development of new tools to enable long-term analysis at moderate spatial and temporal resolution are both required. Given that global scale studies of damming, river flow and climate projections indicate global scale change in river flow, it is logical to suggest this will have global scale consequences for the conditions of coastal ocean waters and thus, ecosystems.

In addition, the investigation of long-term trends in river flow in relation to the area of river discharge influence may indicate where nutrient ratios within river discharges have changed. For example, if a river's discharge is reduced due to impacts of damming and water extraction but the area of river discharge influence is increasing, this may indicate a change in nutrient concentrations from river flow modification. This kind of research can also assist in estimating global scale changes in ocean productivity due to river discharge or due to changes in river discharge. This information is increasingly important, in order to predict and understand potential changes to occur in the future with changes to climate, river discharge and flow volumes and concentrations.

1.2 Aims and objectives of the research

The overarching aim of this thesis is to investigate and build on the knowledge of the influence of river discharge on coastal waters from local to the broader, global scale. I develop novel, objective and simple tools and approaches using free, broad scale remote sensing ocean colour products to investigate the presence, absence, strength and spatial influence of river discharge on coastal water quality and productivity. Several major rivers are investigated, representing a range of global climates and discharge volumes, to demonstrate how river discharge may influence coastal waters across space and time under different flow conditions and across broad spatial and long temporal scales.

The specific objectives of the research chapters are to:

- Apply MODIS ocean colour imagery at the local scale for the purpose of investigating Murray River discharge (Australia), with particular interest in the contrasting effects of drought and high-flow periods and how they may influence the primary productivity and water quality of the adjacent coastal ocean.
- Develop a per-pixel spatiotemporal analysis method based on MODIS satellite ocean colour products to objectively identify coastal ocean regions where water quality and productivity are most influenced by river discharge.
- Use this method to determine whether the influence of river discharge on coastal chl-*a* and turbidity has changed over time in several global river systems via extraction and trend analysis of time series.

These objectives also address the hypotheses that:

- River discharge from the Murray is required for offshore stimulation of productivity. I.e. zero river-outflow from the Murray River (e.g. due to an extreme drought period in the South Australian region) results in greatly reduced coastal ocean productivity, whereas high flow periods result in high productivity in the coastal ocean.

- A strong positive relationship between river discharge and coastal productivity exists at the global scale - larger rivers with greater volumes of river discharge will have stronger influence on receiving coastal ocean waters indicated by higher concentrations and larger regions of elevated chl-*a* concentration.
- Where declining trends in river discharge are present, declining trends in chl-*a* and turbidity in pre-identified regions of river influence will also be present due to positive relationships between these variables.

1.3 Thesis structure

The thesis is organised into five chapters, with chapters 2 - 4 each presented in manuscript format. Chapters 2 and 3 have been published in peer-reviewed journals. The current chapter (Chapter 1) presents a general introduction to river discharge and the ecological significance of river plumes, knowledge gaps in the literature and remote sensing techniques for river plume and water quality monitoring. The broad, overarching aims and objectives driving the research are also described in this chapter. Due to the overlapping themes and literature used to investigate these aims, there is some necessary repetition of ideas and literature throughout the thesis. The final concluding chapter, Chapter 5, synthesizes the findings, summarises the significance and implications of the research work herein, describes limitations and suggests important avenues for future research.

Chapter 2 is the first of three research chapters and investigates the implications of reduced Murray River flow due to a severe drought period and flooding events on coastal productivity and water quality. This chapter serves as a first approach towards understanding the influence of river discharge at a regional scale on South Australia's coastal waters, where little is known about the effect of discharge, or lack thereof due to hydrological drought, on coastal water quality and productivity as indicated by chl-*a*.

Chapter 3 develops a novel satellite imagery product based method to map, with greater objectivity, where coastal productivity (chl-*a*) is most strongly influenced by river discharge. Regions where chl-*a* is strongly linked to river discharge are identified for several rivers around the globe.

Chapter 4 delves deeper, applying the method developed in Chapter 3 to further characterise changes in productivity and turbidity levels of coastal waters due to river discharge, for six river discharge receiving coastal regions around the world, representing a diversity of systems. Trend analysis is also conducted on time series of river discharge, chl-*a* and turbidity in this chapter.

1.4 References

Ab Lah, N.Z., Reba, M.N.M., and EkoSiswanto (2014) An improved MODIS standard chlorophyll-a algorithm for Malacca Straits Water. In 8th International Symposium of the Digital Earth. Vol. 18.

Acker, J.G., Lawrence, W.H., Leptoukh, G., Zhu, T., and Shen, S. (2005) Remotely-sensed chl *a* at the Chesapeake Bay mouth is correlated with annual freshwater flow to Chesapeake Bay. *Geophysical Research Letters* **32**(5), 1-4.

Akbarzadeh, Z., Maavara, T., Slowinski, S., and Van Cappellen, P. (2019) Effects of Damming on River Nitrogen Fluxes: A Global Analysis. *Global Biogeochemical Cycles* **33**(11), 1339-1357.

Alvarez-Romero, J.G., Devlin, M., da Silva, E.T., Petus, C., Ban, N.C., Pressey, R.L., Kool, J., Roberts, J.J., Cerdeira-Estrada, S., Wenger, A.S., and Brodie, J. (2013) A novel approach to model exposure of coastal-marine ecosystems to riverine flood plumes based on remote sensing techniques. *Journal of Environmental Management* **119**, 194-207.

Aurin, D., Mannino, A., and Franz, B. (2013) Spatially resolving ocean color and sediment dispersion in river plumes, coastal systems, and continental shelf waters. *Remote Sensing of Environment* **137**, 212-225.

Babin, M., Doxaran, D., Ehn, J., Matsuoka, A., Belanger, S., and Hooker, S. (2012) Optical Characterisation of Suspended Particles in the Mackenzie River Plume (Canadian Arctic Ocean) and Implications for Ocean Colour Remote Sensing. Vol. 9. pp. 3213-3229.

Baird, M.E., Mongin, M., Skerratt, J., Margvelashvili, N., Tickell, S., Steven, A.D.L., Robillot, C., Ellis, R., Waters, D., Kaniewska, P., and Brodie, J. (2021) Impact of catchment-derived nutrients and sediments on marine water quality on the Great Barrier Reef: An application of the eReefs marine modelling system. *Marine Pollution Bulletin* **167**, 112297.

Balch, W.M, Drapeau, D., Bowler, B., and Booth, E. (2007) Prediction of pelagic calcification rates using satellite measurements. *Deep-Sea Research Part Ii-Topical Studies in Oceanography* **54**(5-7), 478-495.

Balch, W.M., Gordon, H.R., Bowler, B.C., Drapeau, D.T., and Booth, E.S. (2005) Calcium carbonate measurements in the surface global ocean based on Moderate-Resolution Imaging Spectroradiometer data. *Journal of Geophysical Research: Oceans* **110**(C7).

Barale, V., and Schlittenhardt, P.M. (1993) 'Ocean colour: theory and applications in a decade of CZCS experience.' (Springer Dordrecht)

Barnes, B.B., Hu, C., Holekamp, K.L., Blonski, S., Spiering, B.A., Palandro, D., and Lapointe, B. (2014) Use of Landsat data to track historical water quality changes in Florida Keys marine environments. *Remote Sensing of Environment* **140**, 485-496.

Barrera-Guevara, J.C. (1990). The conservation of *Totoaba macdonaldi* (Gilbert), (Pisces: Sciaenidae) in the Gulf of California, Mexico. *Journal of Fish biology, 37*, 201-202

Bebars, M.I., & Lasserre, G. (1983). Analysis of the Eqyptian marine and lagoon fisheries from 1962-1976, in relation to the construction of the Aswan Dam (completed in 1969). *Oceanologica Acta, 6*, 417-426

Behrenfeld, M.J., O'Malley, R.T., Boss, E.S., Westberry, T.K., Graff, J.R., Halsey, K.H., Milligan, A.J., Siegel, D.A., and Brown, M.B. (2016a) Revaluating ocean warming impacts on global phytoplankton. *Nature Climate Change* **6**(3), 323-330.

Behrenfeld, M.J., O'Malley, R.T., Boss, E.S., Westberry, T.K., Graff, J.R., Halsey, K.H., Milligan, A.J., Siegel, D.A., and Brown, M.B. (2016b) Revaluating ocean warming impacts on global phytoplankton. *Nature Climate Change* **6**(3), 323-330.

Bellier, E., Planque, B., and Petitgas, P. (2007) Historical fluctuations in spawning location of anchovy (Engraulis encrasicolus) and sardine (Sardina pilchardus) in the Bay of Biscay during 1967–73 and 2000–2004. *Fisheries Oceanography* **16**(1), 1-15.

Biemans, H., Haddeland, I., Kabat, P., Ludwig, F., Hutjes, R.W.A., Heinke, J., von Bloh, W., & Gerten, D. (2011). Impact of reservoirs on river discharge and irrigation water supply during the 20th century. Water Resources Research, 47, n/a-n/a

Bierman, P.E. (2010) Remote sensing to montior interactions between aquaculture and the environment of Spencer Gulf, South Australia. PhD Thesis, The University of Adelaide, Adelaide.

Block, B.A., Jonsen, I.D., Jorgensen, S.J., Winship, A.J., Shaffer, S.A., Bograd, S.J., Hazen, E.L., Foley, D.G., Breed, G.A., Harrison, A.L., Ganong, J.E., Swithenbank, A., Castleton, M., Dewar, H., Mate, B.R., Shillinger, G.L., Schaefer, K.M., Benson, S.R., Weise, M.J., Henry, R.W., and Costa, D.P. (2011) Tracking apex marine predator movements in a dynamic ocean. *Nature* **475**(7354), 86-90.

Blondeau-Patissier, D., Gower, J.F.R., Dekker, A.G., Phinn, S.R., & Brando, V.E. (2014). A review of ocean color remote sensing methods and statistical techniques for the detection, mapping and analysis of phytoplankton blooms in coastal and open oceans. *Progress in Oceanography, 123*, 123-144

Boyce, D.G., Lewis, M.R., and Worm, B. (2010) Global phytoplankton decline over the past century. *Nature* **466**(7306), 591-596.

Chai, C., Yu, Z., Shen, Z., Song, X., Cao, X., and Yao, Y. (2009) Nutrient characteristics in the Yangtze River Estuary and the adjacent East China Sea before and after impoundment of the Three Gorges Dam. *Science of The Total Environment* **407**(16), 4687-4695.

Charette, M.A., Lam, P.J., Lohan, M.C., Kwon, E.Y., Hatje, V., Jeandel, C., Shiller, A.M., Cutter, G.A., Thomas, A., Boyd, P.W., Homoky, W.B., Milne, A., Thomas, H.,

Andersson, P.S., Porcelli, D., Tanaka, T., Geibert, W., Dehairs, F., and Garcia-Orellana, J. (2016) Coastal ocean and shelf-sea biogeochemical cycling of trace elements and isotopes: lessons learned from GEOTRACES. *Philosophical Transactions of the Royal Society A: Mathematical, Physical and Engineering Sciences* **374**(2081), 20160076.

Chaves, J.E., Werdell, P.J., Proctor, C.W., Neeley, A.R., Freeman, S.A., Thomas, C.S., & Hooker, S.B. (2015). Assessment of ocean color data records from MODIS-Aqua in the western Arctic Ocean. Deep Sea Research Part II: Topical Studies in Oceanography, 118, Part A, 32-43

Chen, C., Mao, Z., Tang, F., Han, G., and Jiang, Y. (2017) Declining riverine sediment input impact on spring phytoplankton bloom off the Yangtze River Estuary from 17-year satellite observation. *Continental Shelf Research* **135**, 86-91.

Chen, J., and Quan, W.T. (2013) An improved algorithm for retrieving chlorophyll-a from the Yellow River Estuary using MODIS imagery. *Environmental Monitoring and Assessment* **185**(3), 2243-2255.

Cisneros-Mata, M.A., Montemayor-Lopez, G., & Roman-Rodriquez, M.J. (1995). Life-history and conservation of Totoaba macdonaldi. Conservation Biology, 9, 806-814

Cloern, J.E., Abreu, P.C., Carstensen, J., Chauvaud, L., Elmgren, R., Grall, J., Greening, H., Johansson, J.O.R., Kahru, M., Sherwood, E.T., Xu, J., and Yin, K.D. (2016) Human activities and climate variability drive fast-paced change across the world's estuarine-coastal ecosystems. *Global Change Biology* **22**(2), 513-529.

Colombelli-Négrel, D. (2015) Low survival rather than breeding success explains little penguin population decline on Granite Island. *Marine and Freshwater Research* **66**(11), 1057-1065.

Constantin, S., Doxaran, D., Derkacheva, A., Novoa, S., and Lavigne, H. (2018) Multi-temporal dynamics of suspended particulate matter in a macro tidal river Plume (the Gironde) as observed by satellite data. *Estuarine Coastal and Shelf Science* **202**, 172-184.

Costanzini, S., Teggi, S., and Ghermandi, G. Remote sensing and GIS for the modeling of persistent organic pollutant in the marine environment. In 'Remote Sensing of the Ocean, Sea Ice, Coastal Waters, and Large Water Regions 2014', 24 - 25 September 2014, Amsterdam, Netherlands,

CRCSI (2021) 'Earth Observation: Data, Processing and Application.' (CRCSI: Melbourne)

CSIRO (2008). Water availability in the Murray-Darling Basin. In Sumary of a report to the Australian Government from the CSIRO Murray-Darling Basin Sustainable Yields Project. CSIRO. Australia

Darecki, M., Weeks, A., Sagan, S., Kowalczuk, P., and Kaczmarek, S. (2003) Optical characteristics of two contrasting Case 2 waters and their influence on remote sensing algorithms. *Continental Shelf Research* **23**(3), 237-250.

Devlin, M.J., Petus, C., da Silva, E., Tracey, D., Wolff, N.H., Waterhouse, J., & Brodie, J. (2015). Water Quality and River Plume Monitoring in the Great Barrier Reef: An Overview of Methods Based on Ocean Colour Satellite Data. Remote Sensing, 7, 12909-12941

Dogliotti, A.I., Ruddick, K.G., Nechad, B., Doxaran, D., and Knaeps, E. (2015) A single algorithm to retrieve turbidity from remotely-sensed data in all coastal and estuarine waters. *Remote Sensing of Environment* **156**, 157-168.

Drinkwater, K.F., and Frank, K.T. (1994) Effects of river regulation and diversion on marine fish and invertebrates. *Aquatic Conservation: Marine and Freshwater Ecosystems* **4**, 134-151.

Ekstrand, S. (1992) Landsat TM based quantification of chlorophyll-a during algae blooms in coastal waters. *International Journal of Remote Sensing* **13**(10), 1913-1926.

ESA (2006) MERIS Product Handbook. European Space Agency.

ESA (2022). Sentinel-3. Access via: https://sentinels.copernicus.eu/web/sentinel/missions/sentinel-3 Accessed: 19/07/2022

Esaias, W.E., Abbott, M.R., Barton, I., Brown, O.B., Campbell, J.B., Carder, K.L., Clark, R., Evans, R.H., Hoge, F.E., Gordon, H.R., Balch, W.M., Letelier, R.M., and Minnett, P.J. (1998) An overview of MODIS capabilities for ocean science observations. *IEEE Transactions on Geoscience and Remote Sensing* **36**, 1250-1265.

EUMETSAT (2018) Sentinel-3 OLCI Marine User Handbook. EUMETSAT, Darmstadt, Germany.

Fernández-Nóvoa, D., Costoya, X., deCastro, M., and Gómez-Gesteira, M. (2019) Dynamic characterization of the main Cantabrian river plumes by means of MODIS. *Continental Shelf Research* **183**, 14-27.

Fredston-Hermann, A., Brown, C.J., Albert, S., Klein, C.J., Mangubhai, S., Nelson, J.L., Teneva, L., Wenger, A., Gaines, S.D., and Halpern, B.S. (2016) Where Does River Runoff Matter for Coastal Marine Conservation? *Frontiers in Marine Science* **3**, 273.

Garcia, V.M.T., Signorini, S., Garcia, C.A.E., and McClain, C.R. (2006) Empirical and semi-analytical chlorophyll algorithms in the south-western Atlantic coastal region (25–40°S and 60–45°W). *International Journal of Remote Sensing* **27**(8), 1539-1562.

Garver, S.A., and Siegel, D.A. (1997) Inherent optical property inversion of ocean color spectra and its biogeochemical interpretation: 1. Time series from the Sargasso Sea. *Journal of Geophysical Research: Oceans* **102**(C8), 18607-18625.

Gerecht, A.C., Šupraha, L., Edvardsen, B., Probert, I., and Henderiks, J. (2014) High temperature decreases the PIC / POC ratio and increases phosphorus requirements in Coccolithus pelagicus (Haptophyta). *Biogeosciences* **11**(13), 3531-3545.

Gillanders, B.M., and Kingsford, M.J. (2002) Impact of changes in flow of freshwater on estuarine and open coastal habitats and the associated organisms. *Oceanography and Marine Biology* **40**, 233-309.

Gitelson, A.A., Gurlin, D., Moses, W.J., and Barrow, T. (2009) A bio-optical algorithm for the remote estimation of the chlorophyll- a concentration in case 2 waters. *Environmental Research Letters* **4**(4), 045003.

Gong, G.-C., Chang, J., Chiang, K.-P., Hsiung, T.-M., Hung, C.-C., Duan, S.-W., and Codispoti, L.A. (2006) Reduction of primary production and changing of nutrient ratio in the East China Sea: Effect of the Three Gorges Dam? *Geophysical Research Letters* **33**(7), 1-4.

Gordon, H.R. (1980) Remote sensing optical properties of a stratified ocean: an improved interpretation. *Applied Optics* **19**(20), 3428-3430.

Gornitz, V. (2000). Sea Level Rise: History and Consequences. San Diego, California: Academic Press

Gregg, W.W., and Rousseaux, C.S. (2019) Global ocean primary production trends in the modern ocean color satellite record (1998–2015). *Environmental Research Letters* **14**(12), 124011.

Grill, G., Lehner, B., Thieme, M., Geenen, B., Tickner, D., Antonelli, F., Babu, S., Borrelli, P., Cheng, L., Crochetiere, H., Ehalt Macedo, H., Filgueiras, R., Goichot, M., Higgins, J., Hogan, Z., Lip, B., McClain, M.E., Meng, J., Mulligan, M., Nilsson, C., Olden, J.D., Opperman, J.J., Petry, P., Reidy Liermann, C., Sáenz, L., Salinas-Rodríguez, S., Schelle, P., Schmitt, R.J.P., Snider, J., Tan, F., Tockner, K., Valdujo, P.H., van Soesbergen, A., and Zarfl, C. (2019) Mapping the world's free-flowing rivers. *Nature* **569**(7755), 215-221.

Grimes, C.B., and Kingsford, M.J. (1996) How do riverine plumes of different sizes influence fish larvae: do they enhance recruitment? *Marine and Freshwater Research* **47**, 191-208.

Guo, K., Zou, T., Jiang, D., Tang, C., and Zhang, H. (2017) Variability of Yellow River turbid plume detected with satellite remote sensing during water-sediment regulation. *Continental Shelf Research* **135**, 74-85.

Hamidi, S.A., Hosseiny, H., Ekhtari, N., and Khazaei, B. (2017) Using MODIS remote sensing data for mapping the spatio-temporal variability of water quality and river turbid plume. *Journal of Coastal Conservation* **21**(6), 939-950.

Hammond, M.L., Beaulieu, C., Henson, S.A., and Sahu, S.K. (2020) Regional surface chlorophyll trends and uncertainties in the global ocean. *Scientific Reports* **10**(1), 15273.

Hopkins, J., Lucas, M., Dufau, C., Sutton, M., Stum, J., Lauret, O., and Channelliere, C. (2013) Detection and variability of the Congo River plume from satellite derived sea surface temperature, salinity, ocean colour and sea level. *Remote Sensing of Environment* **139**, 365-385.

Hovis, W.A., Clark, D.K., Anderson, F., Austin, R.W., Wilson, W.H., Baker, E.T., Ball, D., Gordon, H.R., Mueller, J.L., El-Sayed, S.Z., Sturm, B., Wrigley, R.C., and Yentsch, C.S. (1980) Nimbus-7 Coastal Zone Color Scanner: System Description and Initial Imagery. *Science* **210**(4465), 60-63.

Hovland, E.K., Dierssen, H.M., Ferreira, A.S., and Johnsen, G. (2013) Dynamics regulating major trends in Barents Sea temperatures and subsequent effect on remotely sensed particulate inorganic carbon. *Marine Ecology Progress Series* **484**, 17-32.

Hu, C. (2009) A novel ocean color index to detect floating algae in the global oceans. *Remote Sensing of Environment* **113**(10), 2118-2129.

IOCCG (2000) Remote Sening of Ocean Colour in Coastal and other Optically-Complex Waters. IOCCG, Dartmouth, Canada.

Kampel, M., Gaeta, S.A., Lorenzzetti, J.A., Pompeu, M., Rudorff, F.M., and Frouin, R.J. (2007) Bio-optical variability in coastal waters of Southeast Brazil - art. no. 66800O. In Coastal Ocean Remote Sensing. Vol. 6680. (Eds. RJ Frouin and Z Lee) pp. O6800-O6800.

Kirk, J.T. (1994) 'Light and photosynthesis in aquatic ecosystems.' (Cambridge university press)

Lazure, P., Garnier, V., Dumas, F., Herry, C., and Chifflet, M. (2009) Development of a hydrodynamic model of the Bay of Biscay. Validation of hydrology. *Continental Shelf Research* **29**(8), 985-997.

Liu, B., D'Sa, E.J., Maiti, K., Rivera-Monroy, V.H., and Xue, Z. (2021) Biogeographical trends in phytoplankton community size structure using adaptive sentinel 3-OLCI chlorophyll a and spectral empirical orthogonal functions in the estuarine-shelf waters of the northern Gulf of Mexico. *Remote Sensing of Environment* **252**, 112154.

Lyu, H., Yang, Z., Shi, L., Li, Y., Guo, H., Zhong, S., Miao, S., Bi, S., and Li, Y. (2020) A Novel Algorithm to Estimate Phytoplankton Carbon Concentration in Inland Lakes

Using Sentinel-3 OLCI Images. *IEEE Transactions on Geoscience and Remote Sensing* **58**(9), 6512-6523.

Maritorena, S., Siegel, D.A., and Peterson, A.R. (2002) Optimization of a semianalytical ocean color model for global-scale applications. *Applied Optics* **41**(15), 2705-2714.

Masotti, I., Aparicio-Rizzo, P., Yevenes, M.A., Garreaud, R., Belmar, L., and Farías, L. (2018) The Influence of River Discharge on Nutrient Export and Phytoplankton Biomass Off the Central Chile Coast (33°–37°S): Seasonal Cycle and Interannual Variability. *Frontiers in Marine Science* **5**(423). [In English]

Milly, P.C.D., and Dunne, K.A. (2020) Colorado River flow dwindles as warming-driven loss of reflective snow energizes evaporation. *Science* **367**(6483), 1252-1255.

Milly, P.C.D., Dunne, K.A., & Vecchia, A.V. (2005). Global pattern of trends in streamflow and water availability in a changing climate. Nature, 438, 347-350

Mitchell, C., Hu, C., Bowler, B., Drapeau, D., and Balch, W.M. (2017) Estimating Particulate Inorganic Carbon Concentrations of the Global Ocean From Ocean Color Measurements Using a Reflectance Difference Approach. *Journal of Geophysical Research: Oceans* **122**(11), 8707-8720.

Morrison, J., Quick, M.C., & Foreman, M.G.G. (2002). Climate change in the Fraser River watershed: flow and temperature projections. Journal of Hydrology, 263, 230-244

Mosley, L.M., Barnett, L., Leyden, E., Fradley, K., Iacopetta, J., Jolley, A.-M., Mettam, P., Natt, A., Palmer, D., Scott, P., Spencer, J., Stone, D., & Zammit, B. (2013). Water quality in the Lower Lakes during a hydological drought: water quality monitoring report. Environment Protection Authority, South Australia.

Nilsson, C., Reidy, C.A., Dynesius, M., and Revenga, C. (2005) Fragmentation and flow regulation of the world's large river systems. *Science* **308**(5720), 405-408.

Nohara, D., Kitoh, A., Hosaka, M., and Oki, T. (2006) Impact of Climate Change on River Discharge Projected by Multimodel Ensemble. *Journal of Hydrometeorology* **7**(5), 1076-1089.

O'Reilly, J.E., Maritorena, S., Mitchell, B.G., Siegel, D.A., Carder, K.L., Garver, S.A., Kahru, M., & McClain, C. (1998). Ocean color chlorophyll algorithms for SeaWiFS. Journal of Geophysical Research: Oceans, 103, 24937-24953

Pereira, E.S., and Garcia, C.A.E. (2018) Evaluation of satellite-derived MODIS chlorophyll algorithms in the northern Antarctic Peninsula. *Deep Sea Research Part II: Topical Studies in Oceanography* **149**, 124-137.

Petus, C., da Silva, E.T., Devlin, M., Wenger, A.S., and Álvarez-Romero, J.G. (2014a) Using MODIS data for mapping of water types within river plumes in the Great Barrier Reef, Australia: Towards the production of river plume risk maps for reef and seagrass ecosystems. *Journal of Environmental Management* **137**, 163-177.

Petus, C., Marieu, V., Novoa, S., Chust, G., Bruneau, N., and Froidefond, J.-M. (2014b) Monitoring spatio-temporal variability of the Adour River turbid plume (Bay of Biscay, France) with MODIS 250-m imagery. *Continental Shelf Research* **74**, 35-49.

Phillips, E.M., Horne, J.K., Adams, J., and Zamon, J.E. (2018) Selective occupancy of a persistent yet variable coastal river plume by two seabird species. *Marine Ecology Progress Series* **594**, 245-261.

Phillips, E.M., Horne, J.K., and Zamon, J.E. (2017) Predator-prey interactions influenced by a dynamic river plume. *Canadian Journal of Fisheries and Aquatic Sciences* **74**, 1375-1390.

Planque, B., Bellier, E., and Lazure, P. (2007) Modelling potential spawning habitat of sardine (Sardina pilchardus) and anchovy (Engraulis encrasicolus) in the Bay of Biscay. *Fisheries Oceanography* **16**(1), 16-30.

Polikarpov, I., Al-Yamani, F., Petrov, P., Saburova, M., Mihalkov, V., and Al-Enezi, A. (2021) Phytoplankton bloom detection during the COVID-19 lockdown with remote sensing data: Using Copernicus Sentinel-3 for north-western Arabian/Persian Gulf case study. *Marine Pollution Bulletin* **171**, 112734.

Polovina, J.J., Howell, E.A., and Abecassis, M. (2008) Ocean's least productive waters are expanding. *Geophysical Research Letters* **35**(3).

Rowell, K., True, C., Flessa, K.W., & Dettman, D.L. (2008). Fish without water: Validation and application of δ18O in Totoaba macdonaldi otoliths. Ciencias Marinas, 34, 55-68

Ruddick, K.G., Gons, H.J., Rijkeboer, M., and Tilstone, G. (2001) Optical remote sensing of chlorophyll a in case 2 waters by use of an adaptivetwo-band algorithm with optimal error properties. *Applied Optics* **40**(21), 3575-3585.

Sadeghi, A., Dinter, T., Vountas, M., Taylor, B., Altenburg-Soppa, M., and Bracher, A. (2012) Remote sensing of coccolithophore blooms in selected oceanic regions using the PhytoDOAS method applied to hyper-spectral satellite data. *Biogeosciences* **9**(6), 2127-2143.

Shi, X., Qin, T., Nie, H., Weng, B., and He, S. (2019) Changes in Major Global River Discharges Directed into the Ocean. *International Journal of Environmental Research and Public Health* **16**(8).

Simpson, J.H., and Sharples, J. (2012) 'Introduction to the physical and biological oceanography of shelf seas.' (Cambridge University Press)

Smetacek, V.S. (1986). The Role of freshwater Outflow in Coastal Marine Ecosystems. Berlin: Springer

Soomets, T., Uudeberg, K., Kangro, K., Jakovels, D., Brauns, A., Toming, K., Zagars, M., and Kutser, T. (2020) Spatio-Temporal Variability of Phytoplankton Primary Production in Baltic Lakes Using Sentinel-3 OLCI Data. In Remote Sensing. Vol. 12.

Stahl, K., Hisdal, H., Hannaford, J., Tallaksen, L., Van Lanen, H., Sauquet, E., Demuth, S., Fendekova, M., and Jordar, J. (2010) Streamflow trends in Europe: evidence from a dataset of near-natural catchments. Hydrology and Earth System Sciences 14, p. 2367 - p. 2382. [In English]

Stramska, M. (2009) Particulate organic carbon in the global ocean derived from SeaWiFS ocean color. Deep Sea Research I 56, 1459-1470.

Stramski, D., Reynolds, R.A., Babin, M., Kaczmarek, S., Lewis, M.R., Röttgers, R., Sciandra, A., Stramska, M., Twardowski, M.S., Franz, B.A., and Claustre, H. (2008) Relationships between the surface concentration of particulate organic carbon and optical properties in the eastern South Pacific and eastern Atlantic Oceans. Biogeosciences 5(1), 171-201.

Swieca, K., Sponaugle, S., Briseño-Avena, C., Schmid, M.S., Brodeur, R.D., and Cowen, R.K. (2020) Changing with the tides: fine-scale larval fish prey availability and predation pressure near a tidally modulated river plume. Marine Ecology Progress Series 650, 217-238.

Thome, K. (2022) A message from the Project Scientist. In Terra Orbital Drift. Vol. 2022. (Ed. N Rayne). (NASA)

Tilstone, G.H., Lotliker, A.A., Miller, P.I., Ashraf, P.M., Kumar, T.S., Suresh, T., Ragavan, B.R., and Menon, H.B. (2013) Assessment of MODIS-Aqua chlorophyll-a algorithms in coastal and shelf waters of the eastern Arabian Sea. Continental Shelf Research 65, 14-26.

Tong, Y., Feng, L., Zhao, D., Xu, W., and Zheng, C. (2022) Remote sensing of chlorophyll-a concentrations in coastal oceans of the Greater Bay Area in China: Algorithm development and long-term changes. International Journal of Applied Earth Observation and Geoinformation 112, 102922.

Urquhart, E.A., and Schaeffer, B.A. (2020) Envisat MERIS and Sentinel-3 OLCI satellite lake biophysical water quality flag dataset for the contiguous United States. Data in Brief 28, 104826.

Van Oostende, N., Dussin, R., Stock, C.A., Barton, A.D., Curchitser, E., Dunne, J.P., and Ward, B.B. (2018) Simulating the ocean's chlorophyll dynamic range from coastal upwelling to oligotrophy. Progress in Oceanography 168, 232-247.

van Vliet, M.T.H., Franssen, W.H.P., Yearsley, J.R., Ludwig, F., Haddeland, I., Lettenmaier, D.P., & Kabat, P. (2013). Global river discharge and water temperature under climate change. Global Environmental Change, 23, 450-464

Zarfl, C., Lumsdon, A.E., Berlekamp, J., Tydecks, L., and Tockner, K. (2015) A global boom in hydropower dam construction. Aquatic Sciences 77(1), 161-170.

Chapter 2

Have droughts and increased water extraction from the Murray River (Australia) reduced coastal ocean productivity?

Statement of Authorship

Title of Paper	Have droughts and increased water extraction from the Murray River (Australia) reduced coastal ocean productivity?
Publication Status	☒Published ☐Accepted for Publication ☐Submitted for Publication ☐Unpublished and Unsubmitted work written in manuscript style
Publication Details	Auricht, H.C.C., Clarke, K.D., Lewis, M.M., & Mosley, L.M. (2018). Have droughts and increased water extraction from the Murray River (Australia) reduced coastal ocean productivity? Marine and Freshwater Research, 69, 343-356

Principal Author

Name of Principal Author (Candidate)	Hannah Auricht	
Contribution to the paper	Conceptualization, methodology, data curation, formal analysis, writing – original draft preparation, writing – review and editing.	
Overall percentage (%)	70%	
Signature		Date: 21/11/2022

Co-author Contributions

By signing the Statement of Authorship, each author certifies that:

i. the candidate's stated contribution to the publication is accurate (as detailed above);

ii. permission is granted for the candidate in include the publication in the thesis; and

iii. the sum of all co-author contributions is equal to 100% less the candidate's stated contribution.

Name of Co-Author	Kenneth Clarke	
Contribution to the Paper	Methodology, formal analysis, writing – review and editing.	
Signature		Date: 28/Nov/2022

Name of Co-Author	Luke Mosley	
Contribution to the Paper	Methodology, formal analysis, writing – review and editing.	
Signature		Date: 2 Dec 2022

Name of Co-Author	Megan Lewis	
Contribution to the Paper	Methodology, formal analysis, writing – review and editing.	
Signature		Date: 30 Nov 2022

Abstract

River discharges are decreasing in many regions of the world; however, the consequences of this on water quality and primary productivity of receiving coastal oceans are largely unclear. We analysed satellite remote-sensing data (MODIS) of the coastal ocean zone that receives discharge from the Murray River, from 2002 to 2016. This system has experienced historical flow reductions and a recent extreme hydrological 'Millennium' drought. Remotely sensed chlorophyll-*a* and particulate organic carbon in the coastal ocean were strongly correlated with river discharge ($R^2 > 0.6$) in an 8 km radial buffer zone from the Murray Mouth, and the river influence extended up to 60 km from the Murray Mouth during high-flow periods. This distance was approximately three times greater than the freshwater plume extent during maximum flows in 2011, suggesting that new primary productivity was created. In contrast, there was no additional coastal ocean productivity above background levels from 2007 to 2010 when river discharge ceased. Hindcast calculations based on historical flows from 1962 to 2002 suggest that declining Murray River flows have greatly reduced primary productivity in adjacent coastal waters. This has potential consequences for higher trophic levels and should be considered in future management planning.

2.1 Introduction

Many river systems around the world are stressed because of excessive water extraction for irrigation, industrial use and river regulation. These stressors can affect the natural variability and volume of freshwater discharge from rivers to oceans. Climate change is further altering discharge patterns of many rivers, in terms of both magnitude and variability (Milly *et al.* 2005), as well as causing increasingly frequent and severe droughts (Dai 2012). This will undoubtedly result in increased frequency and length of extreme low-flow periods in many rivers in the future.

Changes in river discharge volumes and patterns influence coastal water quality and ecosystems by modifying the supply of dissolved (e.g. nutrients) and suspended material. Many previous studies have focused on the potential negative effects or risks of river discharge to marine ecosystems as a result of transport of land-based pollutants from rivers to oceans (Alvarez-Romero *et al.* 2013; Costanzini *et al.* 2014; Petus *et al.* 2014a, 2014b; Yu *et al.* 2014; Devlin *et al.* 2015; Fernández-Nóvoa *et al.* 2015). However, currently there is limited understanding of how altered, reduced or complete lack of flow of freshwater affects estuarine and open coastal marine systems (Gillanders and Kingsford 2002). Acker *et al.* (2005) found that phytoplankton biomass in the nutrient-limited region near the mouth of Chesapeake Bay was significantly higher during an extremely high flow period than during an extremely low flow drought period. This was due to delivery of excess nutrients by the Susquehanna River into the bay, leading to increased phytoplankton biomass, turbidity and eutrophication. The study by Acker *et al.* (2005) was temporally limited and investigated effects on productivity caused by flow only for 2 years. Gong *et al.* (2006) suggested that a reduction in primary productivity observed in the East China Sea was the indirect consequence of construction of the Three Gorges Dam, which altered and reduced discharge and nutrient contributions from the Yangtze River and, therefore, nutrient ratios in the sea. Similarly, Black *et al.* (2016) found that the highest abundances of pink snapper (*Chrysophrys auratus*) larvae in Port Phillip Bay (Australia) occurred during years of low to intermediate flow and nutrient inputs from the Yarra River, whereas the lowest larval abundances occurred in years of

very high, very low or no freshwater flows. Although studies such as these provide evidence of the effects of changes to discharge on coastal ocean productivity and water quality, these findings are neither directly comparable to the influences of prolonged drought nor the compounding effects of over allocation and extraction of river water over the longer term. The potential consequences of lack of flow on coastal ocean productivity is, therefore, poorly understood and requires more research.

Satellite remote sensing offers opportunities to monitor ocean and water quality across broader spatial and temporal scales than do traditional *in situ* sampling techniques. However, together with *in situ* sampling of water-quality parameters, satellite remotely sensed data have greatly enhanced our knowledge about composition, occurrence and extension of river discharge (indicated by river plumes) in coastal waters (Petus *et al.* 2014b). It is a useful tool that can quantify several biophysical variables to examine changes in ocean productivity (Alvarez-Romero *et al.* 2013). These variables include coloured dissolved organic matter (CDOM), sea-surface temperature (SST), particulate organic carbon (POC), particulate inorganic carbon (PIC) and chlorophyll-*a* (chl-*a*). Each of these components reflects, scatters and backscatters solar energy that can be measured by remote-sensing instruments. Remotely sensed chl-*a* concentration, for example, is widely used as a proxy for measuring phytoplankton biomass in the upper surface layers of the ocean (Acker *et al.* 2005; Rinaldi *et al.* 2014; Harvey *et al.* 2015). Monitoring these variables enables assessment of water quality over large areas and periods of time, as well as the response of variables to prolonged changes in environmental conditions such as drought.

The Murray River is Australia's largest and most important river system, and its flow regime has changed considerably over the past century with construction of weirs, dams and levees (Maheshwari *et al.* 1995). Large-scale water extraction predominantly for irrigated agriculture has also occurred and greatly reduced total flow through to the end of the river system and coastal ocean. The basin-wide water extraction has made the end of the river system increasingly susceptible to hydrological drought. Consumptive water

use has reduced the average annual discharge at the Murray Mouth by 61%. Water now ceases to flow from the Murray Mouth 40% of the time, compared with 1% of the time before water-resource development (CSIRO 2008). Discharge from the Murray River between 2001 and 2010 were extremely low in the period now known as the 'Millennium drought' (Geddes *et al.* 2016). From 2007 to 2009, the river flows were so low that the river ceased to discharge to the ocean (Mosley *et al.* 2012). Following the end of the Millennium drought, there was a large flooding event across the Murray– Darling Basin in 2011–2012 that resulted in a high discharge to the coastal ocean. The longer-term flow reductions and the Millennium drought have had severe ecological consequences on the Lower Lakes, Coorong (see Figure 2.1) and floodplain wetland systems at the end of the river system (Kingsford *et al.* 2011; Pittock and Finlayson 2011). However, the implications of reduced river discharge and flooding on coastal ocean productivity have not been assessed for this important river system.

The aim of the present study was to apply MODIS ocean colour imagery for the purpose of investigating Murray River discharge, with particular interest in the contrasting effects of drought and high-flow periods and how they may influence the primary productivity and water quality of the adjacent coastal ocean. We hypothesised that the zero river-discharge (extreme drought) period from 2007 to 2010 would result in greatly reduced coastal ocean productivity, whereas the high flow post-drought period (2011–2012) would result in high productivity in the coastal ocean. We use remotely sensed MODIS satellite imagery (available since 2002), hydrological data and hindcast simulations based on historical river flow, to address these questions. The findings are likely to be applicable to other large river systems that are experiencing reduced discharge as a result of water extraction, river regulation and climatic effects.

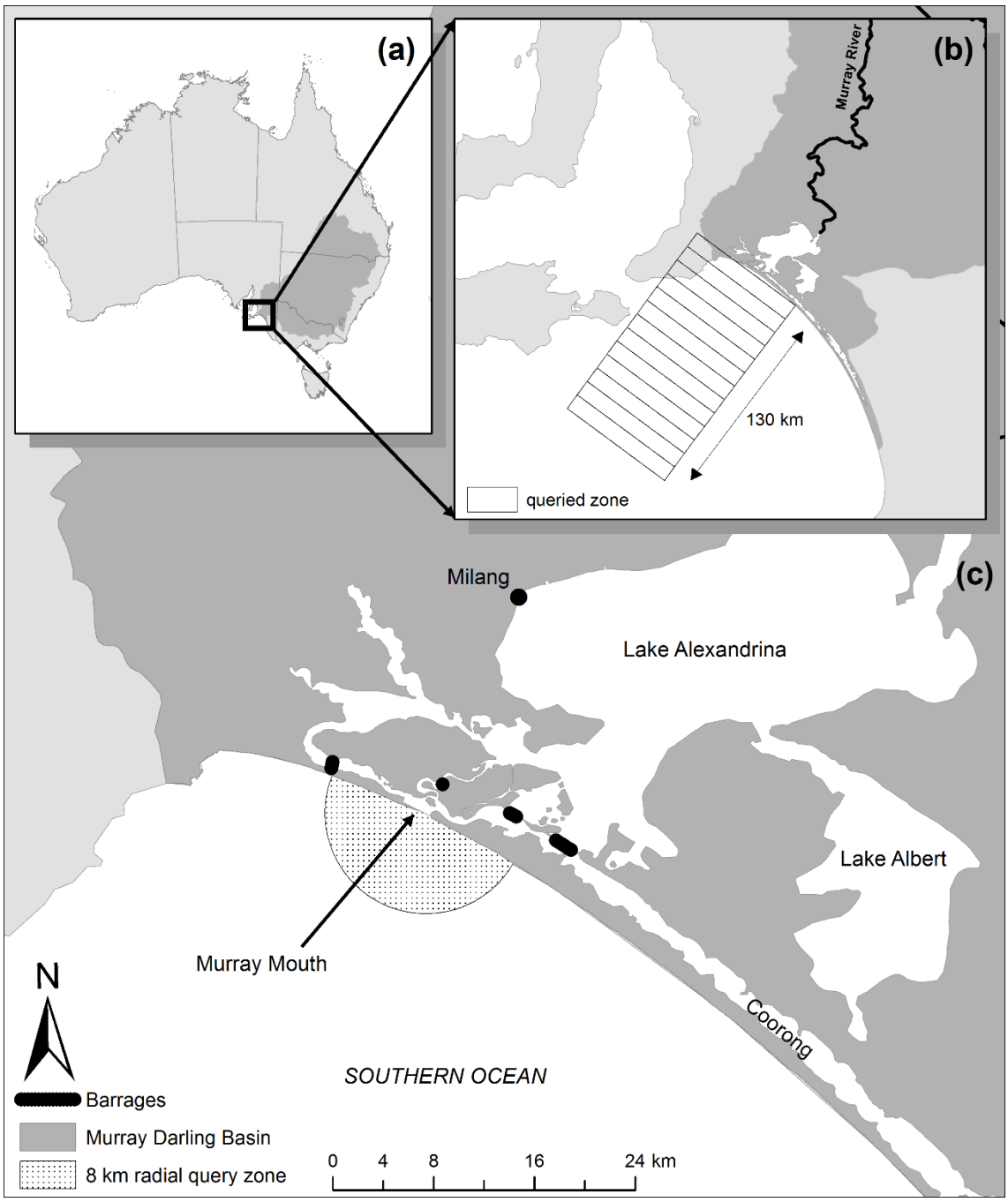

Figure 2.1: Study area showing location and extent of Australia's Murray–Darling Basin (a) and the course of the Murray River in South Australia and as it flows into the Lower Lakes (Lake Alexandrina and Lake Albert) and Coorong (b). Also depicted is the rectangular 130-km-long query zone, divided into 10-km increments. (c) The South Australian coast, indicating the location of the Murray Mouth where water from the Murray River and Lower Lakes drains into the Southern Ocean. The barrages and Milang are also depicted (sources of outflow and water-quality data) and the 8-km radial query zone.

2.2 Materials and Methods

2.2.1 Study area

The study area (Figure 2.1) comprised the coastal ocean zone outside of the Murray River Mouth, which is at the terminus of the Murray–Darling Basin and has a total catchment area of 1 061 469 km^2 (equivalent to 14% of Australia's total area). Prior to reaching the Murray Mouth, the river channel first discharges into two large (821.7-km^2 total surface area) and shallow freshwater lakes (Lakes Alexandrina and Albert, known as the Lower Lakes). Water levels in the Lower Lakes and discharges to the Murray Mouth area are regulated by a series of barrages completed in the late 1940s to prevent seawater intrusion into the lakes as water resource development in the Murray–Darling Basin began to exacerbate this effect.

2.2.2 Hydrological and water-quality data

A time series of daily discharge data from the barrages to the Murray Mouth was obtained from the Department of Environment, Water and Natural Resources (South Australia) for the period 1962–2017. The discharge was estimated from water levels measured upstream and downstream of the barrages, coupled with rating curves for the structures, and number of barrage gates opened. Unfortunately, it is not possible to measure discharge directly at the Murray Mouth site because of its shifting and dynamic nature. The accepted method for discharge estimations (used by The Department of Environment, Water and Natural Resources and SA Water) is based on the sum of estimated flow over all barrages. The majority of flow from the barrages exits directly out the Murray Mouth, some of the flow (particularly from the southern-most Tauwitchere barrage) can mix into the Coorong temporarily.

Nutrient loads exported with the water from the Murray Mouth were calculated. Long-term (2002–2017) water-quality data from Milang in Lake Alexandrina (Figure 2.2) were provided by the South Australian Environment Protection Authority (SA EPA). Unfortunately, sufficient data of nutrients exported at the Murray Mouth and barrages do not exist. This means that Milang, a long-term site for measurement of lake water-

quality parameters, is used to estimate nutrient loadings because (1) it has the longest water-quality record, (2) it has been found to best represent the mass balance of nutrients in the lake (Mosley *et al.* 2012) and (3) water in Lake Alexandrina has a short residence time and the water quality is generally similar to that in locations nearer the barrages, except during the 2007–2010 extreme low flow, drought period where there was saline seepage back into the lake from the barrages (Stone *et al.* 2016). These data were collected on an approximately fortnightly to monthly basis and analysed for total nitrogen (TN) and phosphorus (TP) by using methods described previously (Mosley *et al.* 2012). For the purposes of calculating daily loads through the Murray Mouth, daily water-quality concentrations were interpolated using a cubic interpolation in MATLAB (MathWorks Australia, Sydney, NSW, Australia) and multiplied by the estimated daily discharge volume. These interpolations showed good representation of the measured data (see Figure A1, Appendix A).

Additional coastal ocean water-quality data collected *in situ* along a transect on 25 February 2011 (high-flow period) were provided by the SA EPA. Continuously logged salinity data were collected by a calibrated water-quality sonde (YSI Pro Plus, Yellow Springs, OH, USA). Grab samples were also collected at 10 locations along the transect and analysed for turbidity by standard methods (Mosley *et al.* 2012).

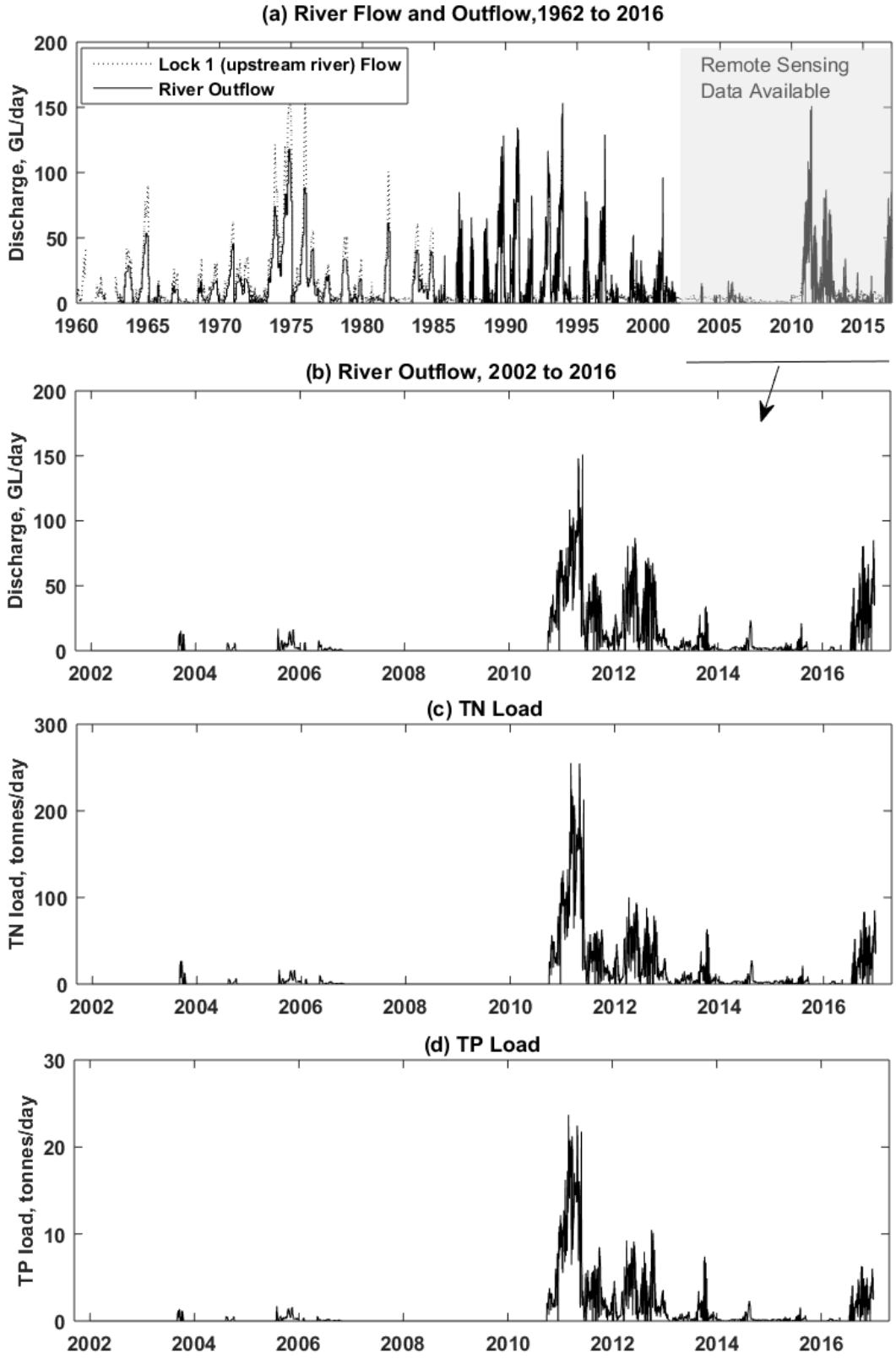

Figure 2.2: Murray River flow time series, total nitrogen and total phosphorous loadings. (a) River flow (upstream at Lock 1) and outflow to the Murray Mouth and coastal ocean (sum of barrage outflows) from 1962 to 2016, and (b) outflow, and (c) total nitrogen (TN)

and (d) total phosphorus (TP) loads from 2002 to 2016 to the Murray Mouth and coastal ocean.

2.2.3 MODIS-Aqua satellite image products

Imagery from the Moderate Resolution Imaging Spectroradiometer (MODIS) was used in the present study, and has been used previously in several other coastal-water studies (Bierman *et al.* 2011; Petus *et al.* 2014a; Chaves *et al.* 2015; Devlin *et al.* 2015; Liu *et al.* 2015). The MODIS sensor is aboard the polar orbiting satellite Aqua, launched in July 2002, and captures the entire Earth surface every 1–2 days.

We used the following four standard MODIS–Aqua Level-3 mapped data products: chl-*a*, POC, PIC and SST. These products are free to access on the NASA Ocean Colour website (https://oceancolor.gsfc.nasa.gov, accessed 6 November 2017) where details of their respective algorithms are also described (https://modis.gsfc.nasa.gov/data/dataprod/, accessed 6 November 2017). Briefly, the MODIS–Aqua chl-*a* product uses the OC3M formula, the standard chl-*a* algorithm distributed by NASA's Goddard Space Flight Centre based on the SeaWiFS OC4v4 algorithm (O'Reilly *et al.* 2000). It is calculated using an empirical relationship derived from *in situ* measurements of chl-*a* (a dataset consisting 2853 observations from a range of marine environments; O'Reilly *et al.* 2000) to the ratio of above-water reflectance at blue and green wavelengths (443–565 nm) and has been recommended for use in South Australian waters. Particulate organic carbon (POC) is calculated using an empirical relationship derived from *in situ* measurements of POC and blue-to-green band ratios of reflectances. Particulate organic carbon (POC) consists of autotrophic and heterotrophic microorganisms and biologically derived detrital particles suspended in seawater (Stramska 2009). The algorithm used to determine PIC from satellite imagery has been developed using observed *in situ* relationships among water leaving radiances, spectral backscattering coefficients and concentrations of calcium carbonate (Ackleson *et al.* 1988; Balch *et al.* 1989). This is the standard product algorithm included as part of the

standard MODIS Level-2 ocean-colour product suite and the Level-3 PIC product suite. The MODIS SST product was used to retrieve the temperature of the ocean surface; specifically, the 11-mm daytime product was used, which follows field-based measurements well in South Australia's coastal waters (Bierman 2010).

The OC3M algorithm is best suited for use in Case-1 waters (clear waters predominantly affected by phytoplankton) and is known to produce overestimates when used in Case-2 optically complex waters where visible amounts of suspended materials in the water column interfere. It has also been validated in South Australian waters by Bierman (2010). During high flows, suspended materials in the Murray River plume are visible close to the coast. However, these drop out quickly (i.e. within 10-km turbidity is, 4 NTU; see Figure A2, Appendix A). Our zone of interest encompassed a larger area, up to 130 km from the Murray Mouth, and, consequently, use of the OC3M algorithm was considered most appropriate.

2.2.4 Image analysis

In total, 174 monthly composite images at 4-km spatial resolution of each product were downloaded, where each image is an average of all clear observations for each calendar month. Together, the 174 images are a complete temporal coverage of MODIS–Aqua at the time of the study (July 2002 to December 2016). Although these products can also be obtained at daily and weekly temporal resolution, cloud cover results in significant numbers of missing pixels. Hence, we used monthly composite images as this temporal resolution was sufficient for our purpose and minimising missing pixels was a priority.

All MODIS data were projected to the geographical coordinate system WGS_1984. So as to determine the temporal characteristics of chl-*a*, POC, PIC and SST in the ocean adjacent to the Murray Mouth in relation to flow, the mean, maximum, minimum, range and standard deviation statistics were extracted from the data. First, an 8-km radius from the Murray Mouth was queried, which encapsulated the first six pixels nearest this point. In several instances, the closest two pixels to the Murray Mouth contained no data,

a result of their exclusion because of either extended periods of cloud cover or because the values are outside the range of the algorithm, because of land 'contamination'.

To create Hovmöller-type distance–time plots of each variable, a much larger area was assessed, which extended up to 130 km from the Murray Mouth, divided into 10-km incremental zones (see Figure 2.1b). A rectangular area or 'corridor' ensured that approximately the same number of pixels at each incremental zone was queried, with the exception of the first three zones (accounting for the first 30 km of the incremental query area closest to the mouth), which included some of the land mask. The extent and direction of the query area incorporated the direction of the river plume (interpreted from viewing monthly composite imagery across years of high flow). It also deliberately excluded a known near-shore area of seasonal upwelling, to the south-east of the study area (Auricht 2015; Kämpf2015; Kämpf and Kavi 2017) to further exclude contributions independent of discharge. Mean concentration statistics were then extracted for each distance-from-mouth zone, and every monthly composite image for all four of the variables. The means were then displayed in distance–time plots.

2.2.5 Extrapolation to historical flow dataset

Pearson's correlation was calculated for the 8-km query area to assess the strength of relationships between barrage flow and remotely sensed ocean variables. This was done, first, on each variable's complete dataset, including dates with no data or where flow was equal to zero, and, second, excluding dates with no data or where mean monthly flow was 10,000 ML. The aim of excluding values of flow below 10,000 ML per month was to reduce potential bias at low flows. However, because this did not result in any great change in strength of correlations (e.g. R^2 of 0.61 for POC increased to R^2 of 0.64 when data points below 10 000 ML were excluded), these data were not presented. The derived linear relationship from the correlation analysis for the 2002–2016 period was then used to predict historical chl-*a* and POC concentrations for the full historical barrage discharge dataset (December 1962 to January 2017).

2.3 Results

2.3.1 River discharge and nutrient loads

The discharge from the Murray River system to the coastal ocean from 1960 to 2016 showed that higher, more frequent discharge occurred before the 'Millennium' drought (2001– 2010, Figure 2.2a). The discharge in the 2002–2017 MODIS study period is shown in Figure 2.2b. Only minor discharges occurred from 2002 to 2006. There was zero discharge from river to the sea from 2007 to September 2010. A high-flow event occurred from 2011 to 2012, moderate flows from 2013 to 2015, and a recent high-flow event occurred in late 2016. Total nutrient (TN and TP) loads to the coastal ocean showed very similar patterns to the river water discharge (Figure 2.2c, d). This indicates that discharge is a good proxy for the total nutrient load to the coastal ocean.

2.3.2 Near-shore temporal patterns in water quality and primary productivity

A comparison of the MODIS POC and chl-*a* data products for the whole study area in a high-flow period (May 2011) and no-flow, extreme-drought period (May 2008) is shown in Figure 2.3. In the high-flow conditions (Figure 2.3b, d), there was elevated chl-*a* and POC in a plume extending, 50–60 km from the Murray Mouth, which was absent in the low-flow conditions (Figure 2.3a, c). Analysis of the full MODIS time series in the 8-km radial zone from the Murray Mouth showed that the monthly mean POC and chl-*a* concentrations were highest at times of large river discharge, namely between September

2010 and January 2013, and late 2016 (

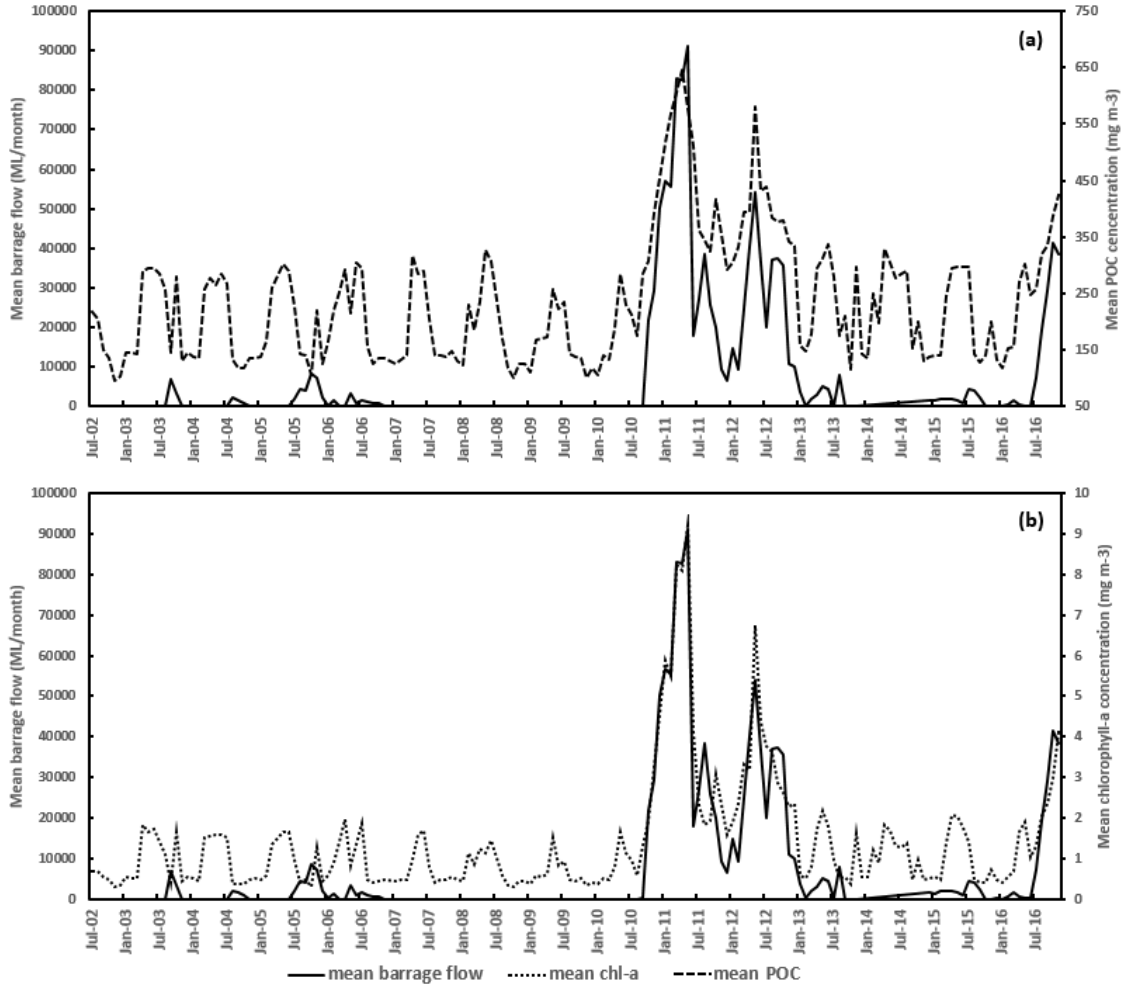

Figure 2.4). During no-flow and very low flow periods, there was a strong seasonal pattern for both POC and chl-*a* that is independent of flow from the Murray Mouth. However, small deviations above the seasonal cycling patterns were apparent during minor river-discharge periods (i.e. higher chl-*a* and POC concentrations occur during September and October 2003 and October and November 2005). In contrast, large increases in concentrations above the seasonal patterns were apparent during times in which mean barrage flow exceeded 10 000 ML per month. The linear regression analysis results further supported a strong relationship between barrage flow and primary productivity in the 8-km radial zone beyond the Murray Mouth (Figure 2.5). There was a strong correlation (R^2 = 0.83) between chl-*a* concentration in this zone and river discharge for the 2002 to late 2016 period (Figure 2.5a). There was also a linear relationship between barrage flow and POC concentration but this correlation (R^2 = 0.61)

was weaker than that for chl-*a* (Figure 2.5b). Correlations between both chl-*a* and POC with discharge decreased with an increasing distance from the Murray Mouth (refer to Figures A 3.1 and A 3.2 in Appendix A), but moderate correlations (R^2 > 0.2 for POC and R^2 > 0.4 for chl-*a*) were present up to the 50–60-km zone. Particulate inorganic carbon (PIC) showed a much more variable profile, with no clear relationship to discharge or season (Figure 2.6a). In contrast, the temporal profile for SST in the 8-km zone showed no clear relationship with river discharge (Figure 2.6b); however, a strong seasonal cycle was apparent, with high temperatures occurring between November and May and low temperatures between May and November.

The *in situ* water-quality monitoring conducted at the time of maximum discharge in the whole MODIS-data period (February 2011) showed that a discernible influence of the river discharge on ocean salinity occurred up to, 10–25 km from the Murray Mouth (Figure 2.7).

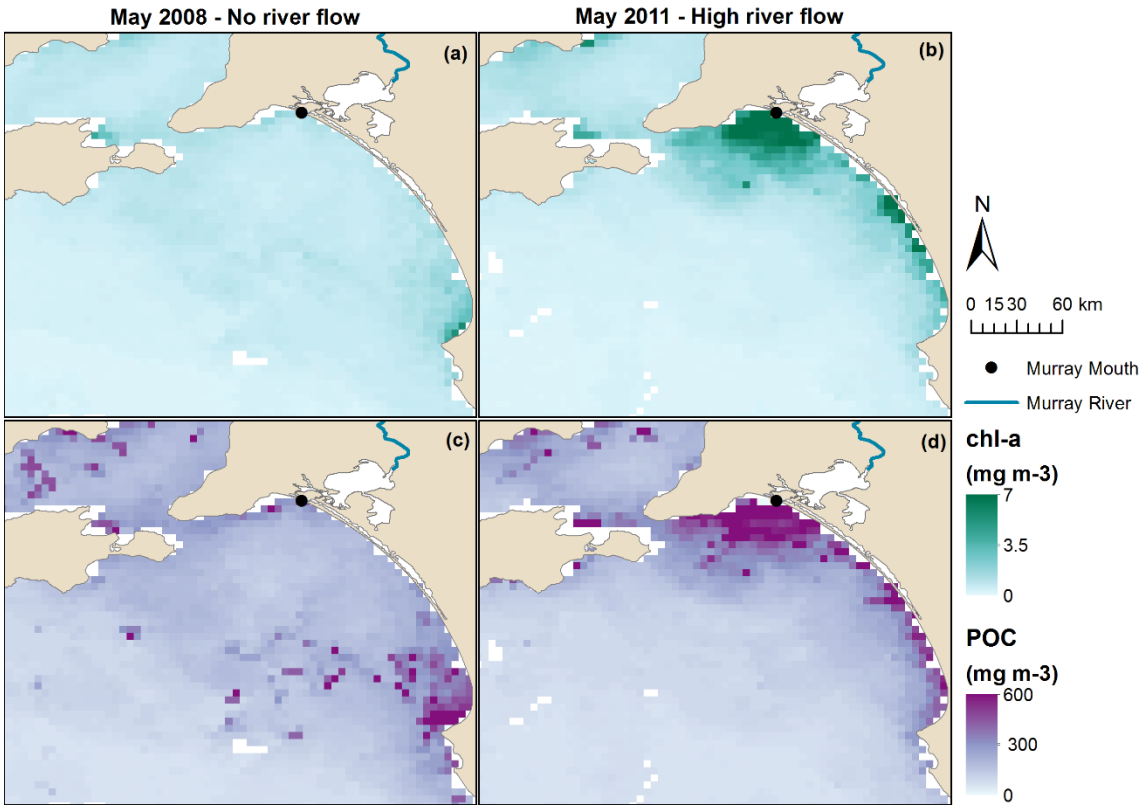

Figure 2.3: Example of MODIS–Aqua (monthly composite) satellite imagery products showing chlorophyll-*a* (chl-*a*) concentrations in the (a) no-flow period of May 2008, and (b) a high-flow period in May 2011, as well as particulate organic carbon (POC)

concentration for (c) the low-flow period in May 2008 and (d) high-flow period in May 2011.

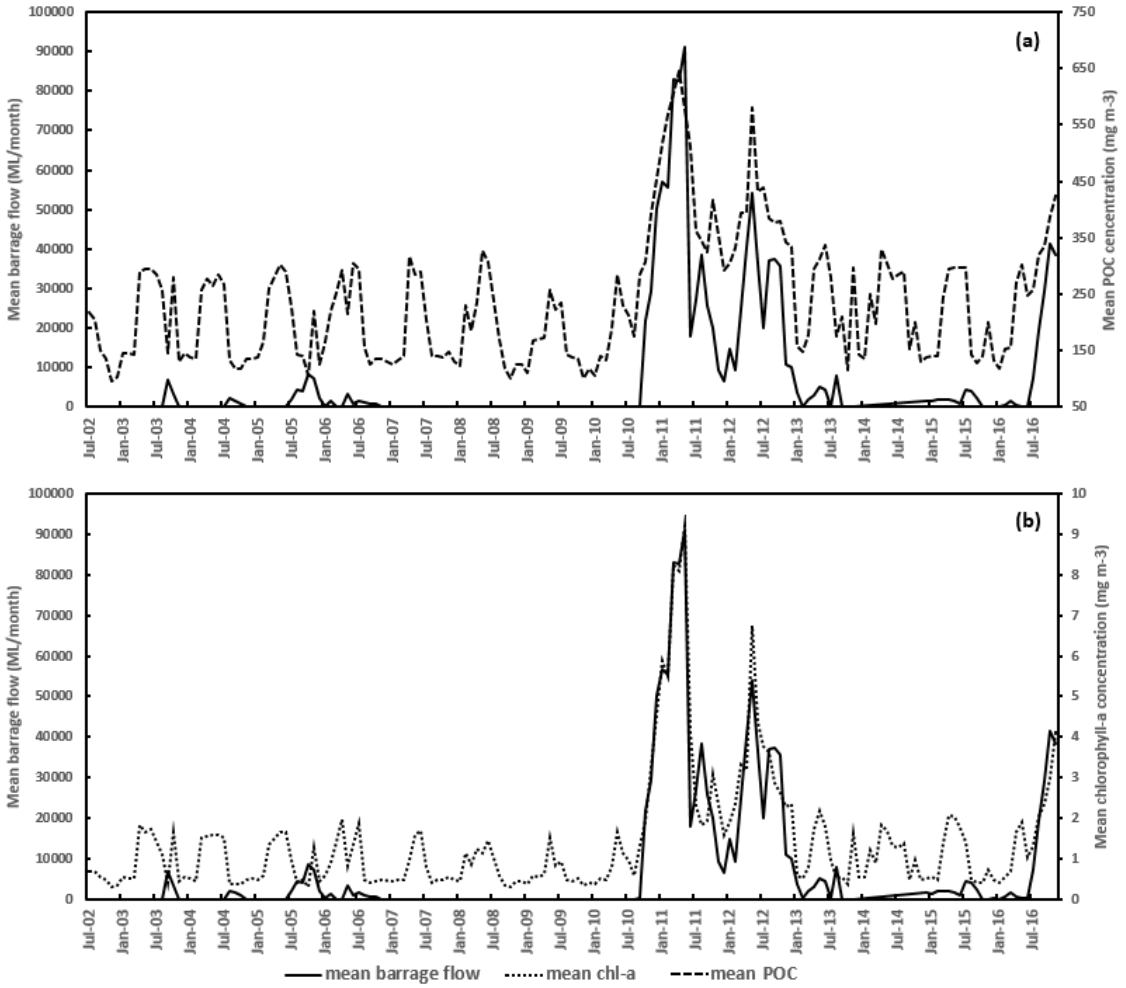

Figure 2.4: Temporal profiles for (a) mean chlorophyll-*a* (chl-*a*) concentration and (b) mean particulate organic carbon (POC) within an 8-km radial zone of the marine waters beyond the Murray River Mouth against river outflow for the period between July 2002 and December 2016.

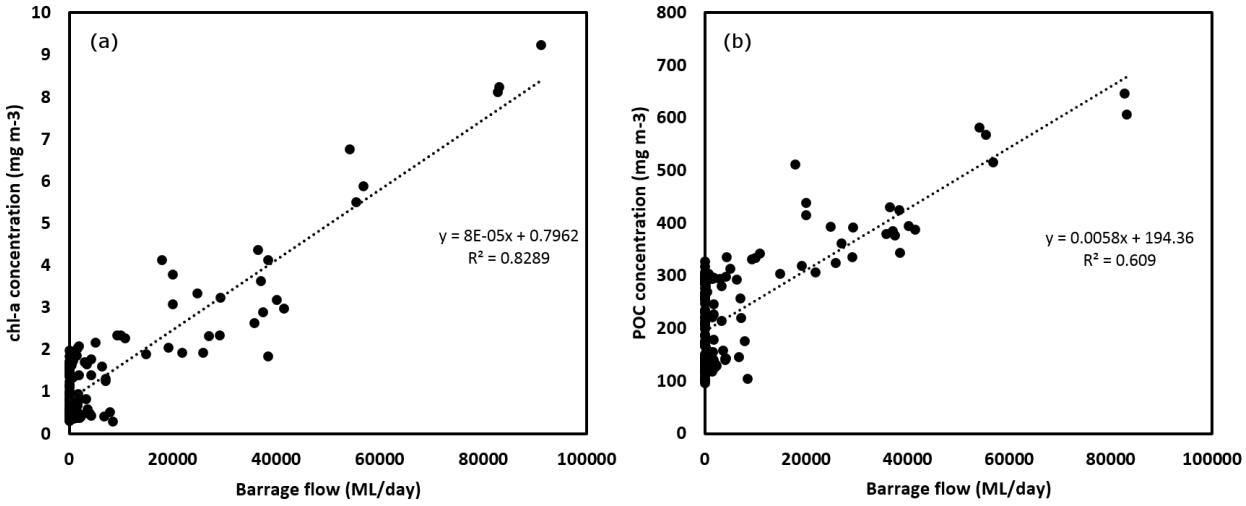

Figure 2.5: Relationship between (a) mean chlorophyll-*a* (chl-a) and (b) mean particulate organic carbon (POC) concentration with mean daily river (barrage) outflow within an 8-km radius of the Murray Mouth.

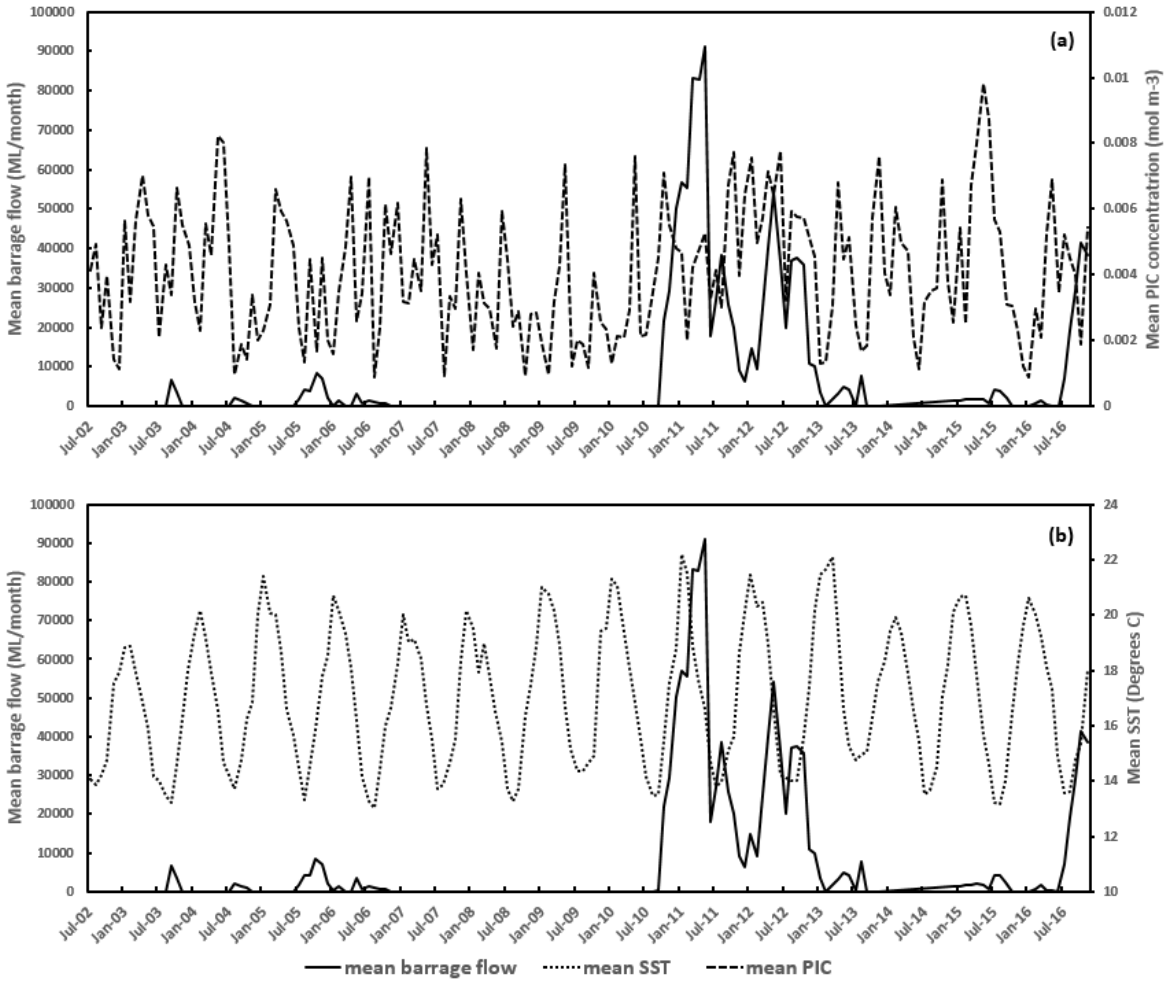

Figure 2.6: Temporal profiles for (a) the mean particulate inorganic carbon (PIC) concentration and (b) mean sea-surface temperature (SST) within an 8-km radial zone of the marine waters beyond the Murray River Mouth, showing against river barrage outflow for the period between July 2002 and December 2016.

Figure 2.7: Continuous in situ transect data for salinity taken on 25 February 2011 during a high-flow event.

2.3.3 Offshore temporal patterns in water quality and primary productivity

Hovmöller distance–time plots for the incremental query zone up to 130 km from the Murray Mouth showed strong increases in chl-*a* (Figure 2.8) and POC (Figure 2.9) concentrations during the high flow period of 2011, when compared with the extreme-drought period when there were no flows, in 2008. During the no-flow period, chl-*a* concentrations were very low, between 0 and 2 mg m^{-3}, within 30 km from the Murray Mouth and coast (Figure 2.8b). However, during the high-flow period in May 2011, chl-*a* concentrations up to 7 mg m^{-3} occurred as far as 20 km from the mouth and concentrations of 5–6 mg m^{-3} observed up to 30 km from the mouth (Figure 2.8c).

A very similar pattern to chl-*a* was observed for POC for the no-flow 2008 and high-flow 2011 periods (Figure 2.9). During the high-flow period, between February and July 2011,

mean concentration of POC was ~600 mg m^{-3} at 30 km from the Murray Mouth, with discernible influences up to ~60 km (Figure 2.9c). In contrast, mean concentration of POC was 300 mg m^{-3} in this zone during the extreme-drought (2008) period (Figure 2.9b).

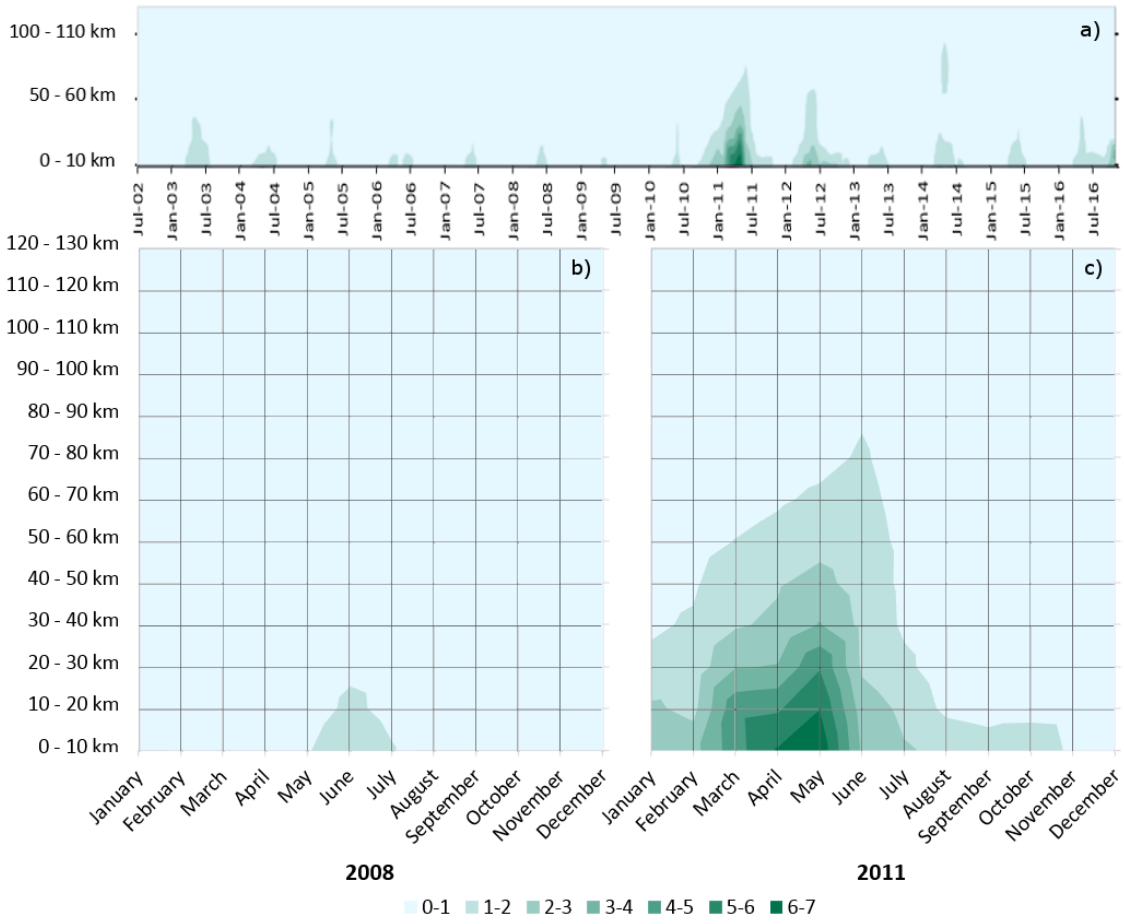

Figure 2.8: Hovmöller distance–time plots, showing the mean chlorophyll-a (chl-*a*) concentration (mg m^{-3}) in the incremental query zone (refer Figure 2.1) across (a) the whole MODIS–Aqua period, (b) the no-flow year 2008 and (c) high-flow year 2011.

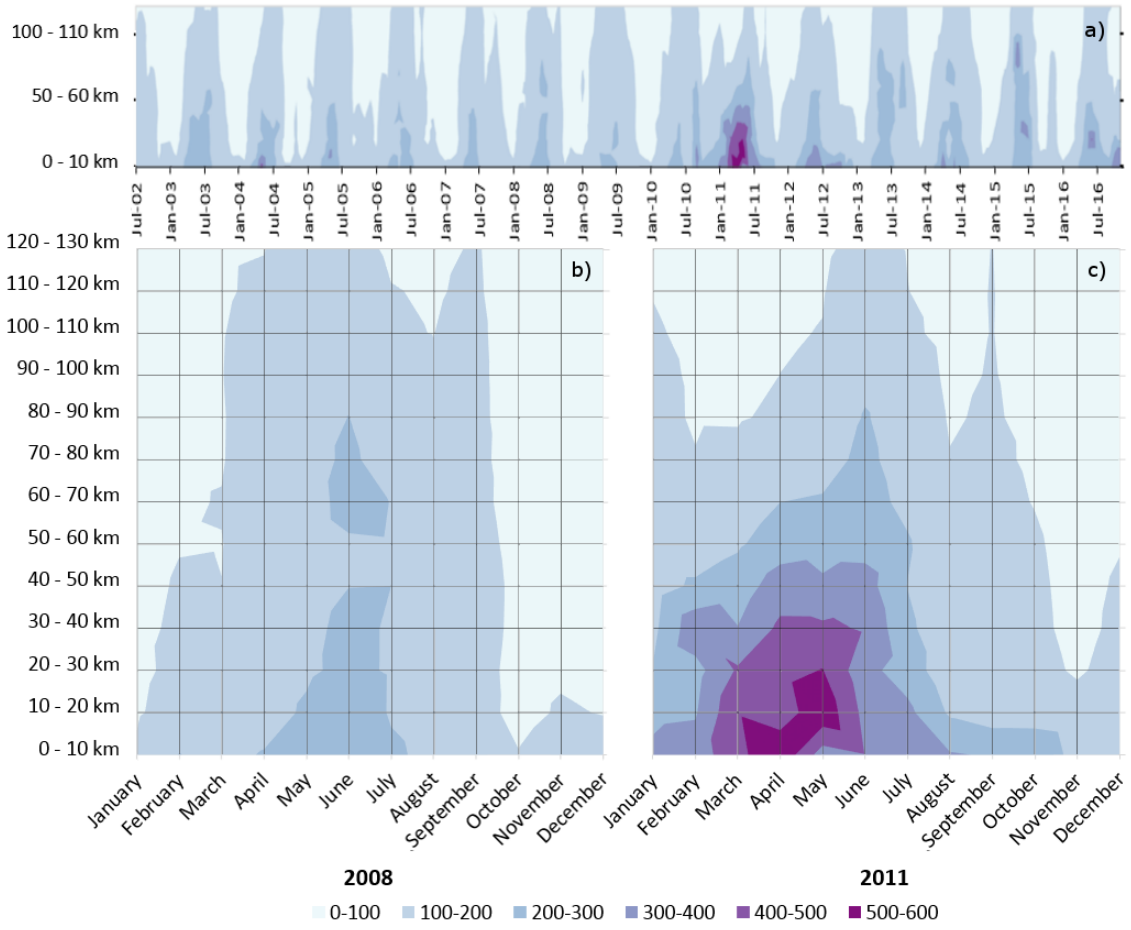

Figure 2.9: Hovmöller distance–time plots showing mean particulate organic carbon (POC) concentration (mg m^{-3}) for (a) the whole MODIS time series, (b) the no-flow year 2008 and (c) high-flow year 2011, in the incremental study area extending to 130 km offshore from the Murray Mouth (see Figure 2.1).

2.3.4 Hindcast mean chl-a and POC concentrations

Figure 2.10 shows hindcast prediction of chl-*a* (Figure 2.10a) and POC (Figure 2.10b) concentrations from 1962 to 2017, produced using the full historical discharge dataset and the regression equation derived from the correlation analysis (Figure 2.5). These results suggest that before the Millennium drought, which began in the early 2000s, both chl-*a* and POC concentrations were more frequently higher in the 8-km (and wider ~60 km) zone beyond the Murray Mouth (Figure 2.10a, b), because there were more regular high-flow periods at this time (Figure 2.2a). The hindcast also suggested that the more

recent, post-Millenium-drought high-flow events (2011 to 2012, and late 2016) had an influence of similar magnitude to the high flows in the pre-2000 period.

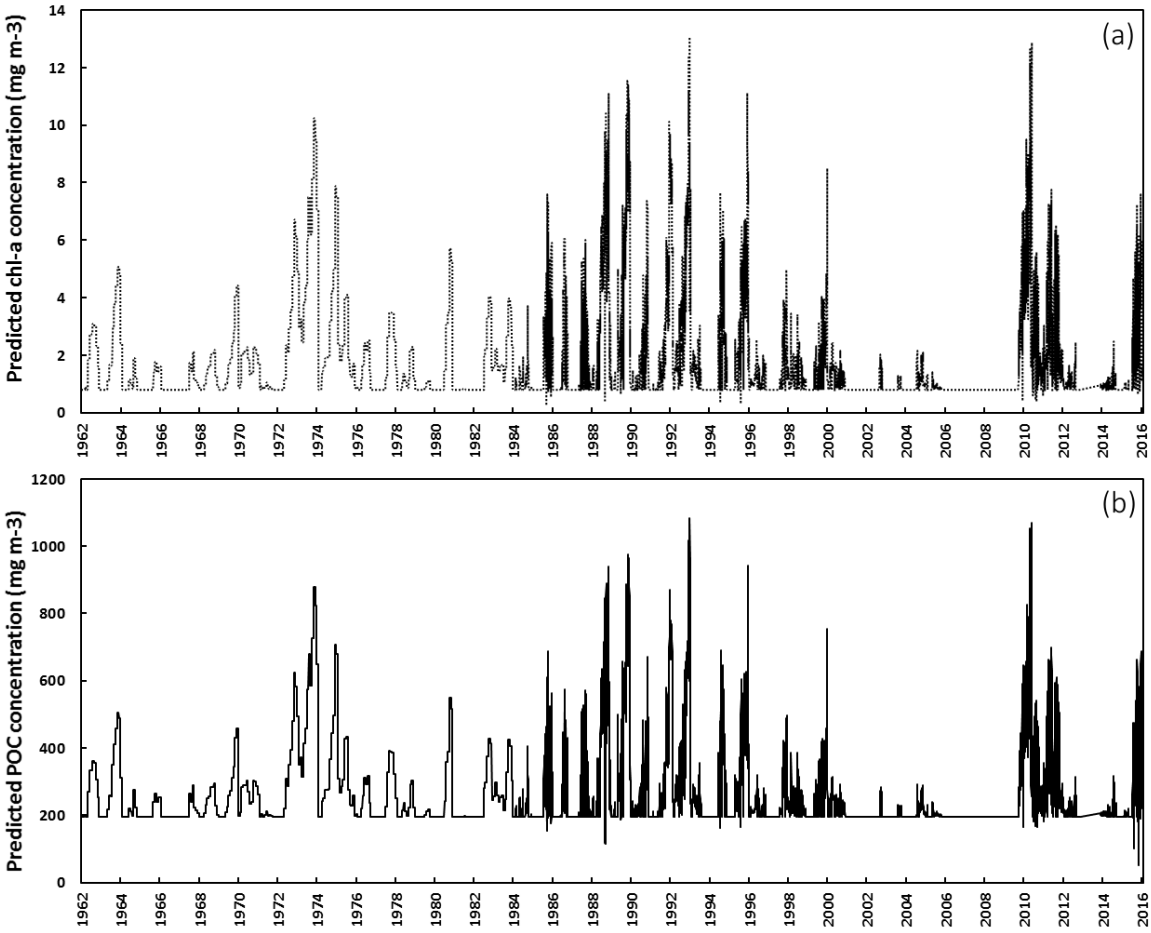

Figure 2.10: (a) Hindcast prediction of chlorophyll-a (chl-*a*) concentration in 8-km radial zone of Murray Mouth, produced using linear equation derived from linear regression analysis between barrage flow day1 and chl-*a* concentration, and (b) hindcast prediction of particulate organic carbon (POC) concentration, produced using equation derived from linear regression analysis between barrage flow/day and POC concentration.

2.4 Discussion

The results indicated that there are broad-scale temporal and spatial implications of reduced Murray River discharge on coastal ocean productivity. The MODIS–Aqua satellite-imagery time series enabled investigation of the effect of flow on coastal marine productivity beyond the Murray Mouth during the period from mid-2002 to late 2016, encompassing not only periods of prolonged drought (from early 2000 to August 2010) and including extreme drought (2007–2010), but also periods of high flow (2011–2012 and recently in late 2016). The results support our hypothesis that the coastal ocean environment beyond the Murray Mouth would have a much lower productivity (indicated by the chl-*a* concentration) during the prolonged period of drought with no contributions of freshwater flows, than during the high-flow, post-drought period.

A notable increase in chl-*a* and POC concentrations was observed within 8 km of the Murray Mouth at times of high flow, compared with low chl-*a* and POC concentrations during times of no flow. Correlation analysis revealed strong relationships between mean barrage flow and chl-*a* concentration ($R^2 = 0.83$) and POC concentration ($R^2 = 0.61$) in this area (Figure 2.5). It is likely that a larger proportion of the chl-*a* and POC sensed in this region during high flows could result directly from the export of freshwater from the eutrophic Lower Lakes upstream of the barrages, rather than from new coastal ocean phytoplankton activity. The *in situ* monitoring data available during maximum discharge (February 2011) supported this because they showed that the discharge diluted salinity from ambient marine values within ~10–15 km of the Murray Mouth.

It is possible that because of the shallow depth in the 8-km Murray Mouth zone (< 20 m, Geoscience Australia 2009), when flows are very low or cease, MODIS measurements may produce over-estimates of chl-*a* because of bottom reflectance (Bierman 2010). This would be less likely during times of high flow when the zone is turbid, because sources of error in these circumstances are more likely as a result of the presence of other constituents in the water column than bottom reflectance. Beyond, 10 km from the Murray Mouth, the depth of the water is greater than 20 m. Thus, ocean-colour estimates

should not be affected by bottom reflectance beyond this distance. Analysis of the MODIS data also showed that the influence of Murray River discharge on the coastal ocean is considerably far reaching, particularly during high flows. During the high-flow periods (from 2011 to 2012 and, more recently, late 2016), elevated bloom concentrations of both chl-*a* and POC extended up to >60 km beyond the Murray Mouth (Figure 2.8 and Figure 2.9). It may also be possible that apparent chl-*a* and POC estimations are compromised by CDOM from the river discharge (which can interfere with estimates of blue to green reflectance ratios; Garcia *et al.* 2006; Kämpf 2015; Shanmugam 2011), in which case, they may actually be an estimation of combined CDOM and phytoplankton biomass. However, the observed zone of Murray River influence was at least three times greater than was the measured maximum extent of salinity dilution caused by the freshwater river plume (indicated by salinity; see Figure 2.7), and turbidity was substantially lower beyond 10 km from the mouth. This indicated that new coastal ocean productivity had been stimulated by the discharge. Further study and *in situ* sampling would be useful to validate this and the MODIS data under high-flow conditions. Nevertheless, these findings are also consistent with previous findings of extensive spatial influence of river plumes on the productivity of the coastal ocean in other locations (e.g. Smith and DeMaster 1996).

The input of riverine dissolved nutrients can remove nutrient limitations that commonly provide a barrier to phytoplankton growth in the ocean (Acker *et al.* 2005), although removal of light limitations associated with high turbidity in near-shore areas may be required first (Smith and DeMaster 1996). Considering that much of the nutrient load exiting the Murray River system is in organic forms (Mosley *et al.* 2012), it appears likely that release of dissolved nutrients from breakdown of this organic material (e.g. by microbial breakdown and plasmolysis of freshwater phytoplankton cells as a result of osmotic shock; Hart *et al.* 1991) occurs and stimulates new ocean productivity. In contrast to POC, PIC showed no clear relationship with flow, which suggests that the PIC in the Murray River coastal zone is an insensitive indicator of the discharge of river water (usually unsaturated with $CaCO_3$; Mosley *et al.* 2013). This could be due to $CaCO_3$

mineral buffering mechanisms and suggests that PIC is a less useful variable for tracing riverine influences on the coastal ocean. Similarly, SST showed no discernible change as a result of the river flows, possibly because the river water temperature was either similar, or equilibrated quickly, to the coastal ocean water.

During the extreme-drought period where no discharge occurred, remotely sensed chl-*a* and POC concentrations in the coastal ocean were much lower and there was no plume detectable in the MODIS data. Lower flows are now much more frequent on the Murray River system because of large-scale water extraction for agriculture and river regulation (CSIRO 2008). Hindcast extrapolations of the remotely sensed data (based on correlation with flow from 2002 to late 2016) suggested that coastal ocean productivity is likely to have been much greater in the past, before large-scale water extraction and river regulation (Figure 2.10). In particular, it appears that the frequency of high-productivity conditions in the ocean beyond the mouth would likely have been much higher when flows were more frequent and voluminous than they have been in the past decade. In contrast, for long periods in the past 15 years, chl-*a* and POC have been within background seasonal concentrations.

Because phytoplankton biomass is the base of the marine food web, population dynamics and abundance of higher trophic levels and fishery resources are likely to be affected by reduced flows and extended drought periods. Although a limited number of studies reflect on potential implications of a complete lack of river discharge on marine environments, it is generally understood that changing the scale, frequency and seasonality of river discharge can have severe impacts on species that require food pulses for successful reproduction or larval survival (Drinkwater and Frank 1994; Whitfield and Marais 1999). Several studies have identified important relationships between discharge-stimulated productivity and populations of marine species and habitats as a result of these controls (Burrage *et al.* 2002; De Robertis *et al.* 2005; Burla *et al.* 2010; Brookes *et al.* 2015; Black *et al.* 2016). There is also a critical period at the point of first

feeding by larvae where the presence of suitable amounts and types of food determine year-class strength (Hjort 1914).

In the coastal Murray River region that we studied, there was evidence that reduced discharge during the Millennium-drought period negatively influenced the pipi (*Donax deltoides*) fishery in the region, where variability in freshwater flows explained 45% of the variability in the relative abundance of the bivalve mollusc (Ferguson *et al.* 2013). The declining abundance of mulloway fish (*Argyrosomus japonicus*) may also be partly explained by environmental limitations resulting from the lack of flow; these species show preference for turbid estuaries and are dependent on freshwater discharge to create environments suitable for recruitment (Ferguson *et al.* 2013). The relative rarity and diminishment of suitable freshwater flow into the remnant estuary and coastal ocean has thus placed high strain and pressure on the few strong year classes that have resulted from years of above average flow to continue the population (Ferguson *et al.* 2008). Considering this and the high age and size at maturity of A. japonicas (Griffiths 1996; Farmer 2008), extended periods of drought and reduced flow in the future could lead to a repeated failure of recruitment and, in an extreme scenario, cause local extinction of the species. These fisheries data strongly support wider implications of reduced Murray discharge and primary productivity on the adjacent coastal ocean. However, because the observed long-term decline in these species during the Millennium drought also occurred synchronously with severe overfishing (Ferguson *et al.* 2013), these additional effects on population dynamics also require consideration in management.

Past decision-making on water allocation and management on the Murray River, including large water volumes allocated for extraction by irrigators, has previously failed to consider impacts on coastal environments outside the river system. The focus has been on maintaining sufficient flows to maintain regulated water levels, water allocations for irrigators, and sufficient quality to meet irrigation and drinking-water requirements. Dredging has been undertaken for considerable periods over the past 15 years to keep the Murray Mouth open in the absence of sufficient flows. The Murray–Darling Basin

Plan (MDBA2010) that is currently being implemented is recovering water from irrigators, by buy-backs and efficiency improvements, to return it to the environment. 'Maintaining an open Murray Mouth' is an objective of the plan; however, beyond this, there is no consideration of the volume of discharge required to maintain coastal marine ecosystems. Of increasing concern are predictions that climate change will result in further discharge reductions (CSIRO 2008). Reducing discharge trends are occurring in many other global river systems as a result of climate change (10–40% reductions by 2050; Milly *et al.* 2005). Hence, significant reductions in coastal ocean productivity are likely to occur adjacent to many other river systems in the future, with flow-on effects on dependent species (e.g. invertebrates, fish, water birds) and industries (e.g. fisheries, tourism). The effects of discharge on the health and resilience of coastal ocean ecosystems require improved consideration in river management plans.

2.5 Conclusions

The present study investigated, for the first time, how discharge reductions and drought on the Murray River affect primary productivity in the adjacent coastal ocean. MODIS–Aqua ocean-colour products were analysed and chl-*a* and POC concentrations in the coastal ocean showed a strong positive correlation with river discharge, up to 60 km from the Murray River Mouth. The increases in chl-*a* and POC during high flows were far greater than was the freshwater-plume extent, indicating that the discharge stimulated new ocean productivity. Hindcast simulations indicated that flow reductions on the Murray River have greatly reduced the productivity of the coastal ocean over the past few decades because of the largescale water extraction and a severe drought. This effect on the Murray River and coastal ocean and other large global river systems is likely to become more common as a result of climate change and other anthropogenic pressures. Higher trophic level (e.g. fish, shellfish, birds) productivity, recruitment and migration could also be greatly affected by declining primary productivity and could have severe implications for fisheries and, possibly, lead to the extinction of particular species. It would, therefore, be worthwhile in future research to also include investigation on these wider ecological impacts.

2.6 References

Acker, J.G., Lawrence, W.H., Leptoukh, G., Zhu, T., and Shen, S. (2005) Remotely-sensed chl-*a* at the Chesapeake Bay mouth is correlated with annual freshwater flow to Chesapeake Bay. Geophysical Research Letters 32(5), 1-4.

Ackleson, S.G., Balch, W.M., and Holligan, P.M. (1988) White waters of the Gulf of Maine. Oceanography 1, 18-22.

Alvarez-Romero, J.G., Devlin, M., da Silva, E.T., Petus, C., Ban, N.C., Pressey, R.L., Kool, J., Roberts, J.J., Cerdeira-Estrada, S., Wenger, A.S., and Brodie, J. (2013) A novel approach to model exposure of coastal-marine ecosystems to riverine flood plumes based on remote sensing techniques. Journal of Environmental Management 119, 194-207.

Auricht, H. (2015) Monitoring sea surface temperature and phytoplankton in the Spencer Gulf using MODIS satellite imagery. BSc (Hons) Thesis, University of Adelaide, Adelaide.

Balch, W.M., Eppley, R.W., Abbott, M.R., and Reid, F.M.H. (1989) Bias in satellite-derived pigment measurements due to coccolithophores and dinoflagellates. Journal of Plankton Research 11, 575-581.

Bierman, P., Lewis, M., Ostendorf, B., and Tanner, J. (2011) A review of methods for analysing spatial and temporal patterns in coastal water quality. Ecological Indicators 11(1), 103-114.

Bierman, P.E. (2010) Remote sensing to monitor interactions between aquaculture and the environment of Spencer Gulf, South Australia. PhD Thesis, The University of Adelaide, Adelaide.

Black, K.P., Longmore, A.R., Hamer, P.A., Lee, R., Swearer, S.E., and Jenkins, G.P. (2016) Linking nutrient inputs, phytoplankton composition, zooplankton dynamics and the recruitment of pink snapper, *Chrysophrys auratus*, in a temperate bay. Estuarine Coastal and Shelf Science 183, 150-162.

Brookes, J.D., Aldridge, K.T., Bice, C.M., Deegan, B., Ferguson, G.J., Paton, D.C., Sheaves, M., Ye, Q., and Zampatti, B.P. (2015) Fish productivity in the lower lakes and Coorong, Australia, during severe drought. Transactions of the Royal Society of South Australia 139(2), 189-215.

Burla, M., Baptista, A.M., Casillas, E., Williams, J.G., and Marsh, D.M. (2010) The influence of the Columbia River plume on the survival of steelhead (*Oncorhynchus mykiss*) and Chinook salmon (*Oncorhynchus tshawytscha*): a numerical exploration. Canadian Journal of Fisheries and Aquatic Sciences 67, 1671-1684.

Burrage, D.M., Heron, M.L., Hacker, J.M., Stieglitz, T.C., Steinberg, C.R., and Prytz, A. (2002) Evolution and dynamics of tropical river plumes in the Great Barrier Reef: An integrated remote sensing and in situ study. Journal of Geophysical Research: Oceans 107(C12), SRF 17-1-SRF 17-22.

Chaves, J.E., Werdell, P.J., Proctor, C.W., Neeley, A.R., Freeman, S.A., Thomas, C.S., and Hooker, S.B. (2015) Assessment of ocean color data records from MODIS-Aqua in the western Arctic Ocean. Deep Sea Research Part II: Topical Studies in Oceanography 118, Part A, 32-43.

Costanzini, S., Teggi, S., and Ghermandi, G. Remote sensing and GIS for the modelling of persistent organic pollutant in the marine environment. In 'Remote Sensing of the Ocean, Sea Ice, Coastal Waters, and Large Water Regions 2014', 24 - 25 September 2014, Amsterdam, Netherlands.

CSIRO (2008) Water availability in the Murray-Darling Basin. CSIRO, Australia.

Dai, A.G. (2013) Increasing drought under global warming in observations and models. Nature Climate Change 3(1), 52-58.

De Robertis, A., Morgan, C.A., Schabetsberger, R.A., Zabel, R.W., Brodeur, R.D., Emmett, R.L., Knight, C.M., Krutzikowsky, G.K., and Casillas, E. (2005) Columbia River plume fronts. II. Distribution, abundance and feeding ecology of juvenile salmon. Marine Ecology Progress Series 299, 33-44.

Devlin, M.J., Petus, C., da Silva, E., Tracey, D., Wolff, N.H., Waterhouse, J., and Brodie, J. (2015) Water Quality and River Plume Monitoring in the Great Barrier Reef: An Overview of Methods Based on Ocean Colour Satellite Data. Remote Sensing 7(10), 12909-12941.

Drinkwater, K.F., and Frank, K.T. (1994) Effects of river regulation and diversion on marine fish and invertebrates. Aquatic Conservation: Marine and Freshwater Ecosystems 4, 134-151.

Farmer, B.M. (2008) Comparisons of the biological and genetic characteristics of the Mulloway *Argyrosomus japonicus* (sciaenidae) in different regions of Western Australia. PhD Thesis, Murdoch University, Western Australia.

Ferguson, G.J., Ward, T.M., and Geddes, M.C. (2008) Do recent age structures and historical catches of mulloway, *Argyrosomus japonicus* (Temminck & Schlegel, 1843), reflect freshwater inflows in the remnant estuary of the Murray River, South Australia? Aquatic Living Resources 21, 145-152.

Ferguson, G.J., Ward, T.M., Ye, Q.F., Geddes, M.C., and Gillanders, B.M. (2013) Impacts of Drought, Flow Regime, and Fishing on the Fish Assemblage in Southern Australia's Largest Temperate Estuary. Estuaries and Coasts 36(4), 737-753.

Fernández-Nóvoa, D., Mendes, R., deCastro, M., Dias, J.M., Sánchez-Arcilla, A., and Gómez-Gesteira, M. (2015) Analysis of the influence of river discharge and wind on the Ebro turbid plume using MODIS-Aqua and MODIS-Terra data. Journal of Marine Systems 142, 40-46.

Garcia, V.M.T., Signorini, S., Garcia, C.A.E., and McClain, C. (2006) Empirical and semianalytical chlorophyll-*a* algorithms in the southwestern Atlantic coastal region (25-40 S and 60-45 W). International Journal of Remote Sensing 27(1539-1562).

Geddes, M.C., Shiel, R.J., and Francis, J. (2016) Zooplankton in the Murray estuary and Coorong during flow and no-flow periods. Transactions of the Royal Society of South Australia 140(1), 74-89.

Geoscience Australia (2009) Australian Bathymetry and Topography Grid, June 2009. Geoscience Australia, Canberra. Available at: https://ecat.ga.gov.au/geonetwork/srv/eng/search#!a05f7892-fae9-7506-e044-00144fdd4fa6 [accessed 18 September 2017].

Gillanders, B.M., and Kingsford, M.J. (2002) Impact of changes in flow of freshwater on estuarine and open coastal habitats and the associated organisms. In Oceanography and Marine Biology. Vol. 40. (Eds. RN Gibson, M Barnes and RJA Atkinson) pp. 233-309.

Gong, G.-C., Chang, J., Chiang, K.-P., Hsiung, T.-M., Hung, C.-C., Duan, S.-W., and Codispoti, L.A. (2006) Reduction of primary production and changing of nutrient ratio in the East China Sea: Effect of the Three Gorges Dam? Geophysical Research Letters 33(7), 1-4.

Griffiths, M.H. (1996) Life history of the Dusky kob *Argyrosomus japonicus* (Sciaenidae) off the east coast of South Africa. South African Journal of Marine Science 17, 135-154.

Hart, B.T., Bailey, P., Edwards, R., Hortle, K., James, K., McMahon, A., Meredith, C., and Swadling, K. (1991) A review of the salt sensitivity of the Australian freshwater biota. Hydrobiologia 210(1), 105-144.

Harvey, E.T., Kratzer, S., and Philipson, P. (2013) Satellite-based water quality monitoring for improved spatial and temporal retrieval of chlorophyll-a in coastal waters. Remote Sensing of Environment 158, 417-430.

Hjort, J. (1914) 'Fluctuations in the Great Fisheries of Northern Europe, Viewed in the Light of Biological Research.' (Andr. Fred. Høst & Fils: Copenhagen, Denmark)

Kämpf, J. (2015) Phytoplankton blooms on the western shelf of Tasmania: Evidence of a highly productive ecosystem. Ocean Science 11, 1-11.

Kämpf, J., and Kavi, A. (2017) On the "hidden" phytoplankton blooms on Australia's southern shelves. Geophysical Research Letters 44(3), 1466-1473.

Kingsford, R.T., Walker, K.F., Lester, R.E., Young, W.J., Fairweather, P.G., Sammut, J., and Geddes, M.C. (2011) A Ramsar wetland in crisis - the Coorong Lower Lakes and Murray Mouth, Australia. Marine and Freshwater Research 62(3), 255-265.

Liu, D., Pan, D.L., Bai, Y., He, X.Q., Wang, D.F., Wei, J.A., and Zhang, L. (2015) Remote Sensing Observation of Particulate Organic Carbon in the Pearl River Estuary. Remote Sensing 7(7), 8683-8704.

Maheshwari, B.L., Walker, K.F., and McMahon, T.A. (1995) Effects of regulation on the flow regime of the River Murray, Australia. Regulated Rivers: Research and Management 10, 15-38.

MDBA (2010) Guide to the proposed Basin Plan: Technical background. Murray-Darling Basin Authority, Canberra.

Milly, P.C.D., Dunne, K.A., and Vecchia, A.V. (2005) Global pattern of trends in streamflow and water availability in a changing climate. Nature 438(7066), 347-350.

Mosley, L.M., Barnett, L., Leyden, E., Fradley, K., Iacopetta, J., Jolley, A.-M., Mettam, P., Natt, A., Palmer, D., Scott, P., Spencer, J., Stone, D., and Zammit, B. (2013) Water quality in the Lower Lakes during a hydological drought: water quality monitoring report. Environment Protection Authority, South Australia.

Mosley, L.M., Zammit, B., Leyden, E., Heneker, T.M., Hipsey, M.R., Skinner, D., and Aldridge, K.T. (2012) The Impact of Extreme Low Flows on the Water Quality of the Lower Murray River and Lakes (South Australia). Water Resources Management 26(13), 3923-3946.

O'Reilly, J.E.S., Maritorena, S., Seigel, D., O'Brien, M., Toole, D., Mitchell, B.G., Kahru, M., Chavez, F.P., Strutton, P., Cota, G.F., Hooker, S.B., McClain, C.R., Carder, K.L., Muller-Karger, F.E., Harding, L., Magnuson, A., Phinney, D., Moore, G.F., Aiken, J., Arrigo, K.R., Letelier, R.M., and Culver, M.E. (2000) Ocean Color Chlorophyll-a Algorithms for SeaWiFS, OC2 and OC4: Version 4.

Petus, C., da Silva, E.T., Devlin, M., Wenger, A.S., and Álvarez-Romero, J.G. (2014a) Using MODIS data for mapping of water types within river plumes in the Great Barrier Reef, Australia: Towards the production of river plume risk maps for reef and seagrass ecosystems. Journal of Environmental Management 137, 163-177.

Petus, C., Marieu, V., Novoa, S., Chust, G., Bruneau, N., and Froidefond, J.-M. (2014b) Monitoring spatio-temporal variability of the Adour River turbid plume (Bay of Biscay, France) with MODIS 250-m imagery. Continental Shelf Research 74, 35-49.

Pittock, J., and Finlayson, C.M. (2011) Australia's Murray-Darling Basin: freshwater ecosystem conservation options in an era of climate change. Marine and Freshwater Research 62(3), 232-243.

Rinaldi, E., Nardelli, B.B., Volpe, G., and Santoleri, R. (2014) Chlorophyll distribution and variability in the Sicily Channel (Mediterranean Sea) as seen by remote sensing data. Continental Shelf Research 77, 61-68.

Shanmugam, P. (2011) A new bio-optical algorithm for the remote sensing of algal blooms in complex ocean waters. Journal of Geophysical Research 116(C4), 2156-2202.

Smith, W.O., and DeMaster, D.J. (1996) Phytoplankton biomass and productivity in the Amazon River plume: correlation with seasonal river discharge. Continental Shelf Research 16(3), 291-319.

Stone, D., Palmer, D., Hamilton, B., Cooney, C., Mosley, L.M., (2016) Coorong, Lower Lakes and Murray Mouth water quality monitoring program 2009-2016; Summary report. Environment Protection Authority, South Australia. Available at: www.epa.sa.gov.au/files/12070_cllmm_final_2016.pdf [accessed 18 September 2017].

Stramska, M. (2009) Particulate organic carbon in the global ocean derived from SeaWiFS ocean color. Deep Sea Research I 56, 1459-1470.

Whitfield, A.K., and Marais, J.F.K. (1999) The Ichthyofauna. In 'Estuaries of South Africa'. (Eds. BR Allanson and D Baird). (Cambridge University Press: Cambridge)

Yu, Y.Y., Zhang, H., and Lemckert, C. (2014) Numerical analysis on the Brisbane River plume in Moreton Bay due to Queensland floods 2010-2011. Environmental Fluid Mechanics 14(1), 1-24.

Appendix A

A.1 Nutrient loading interpolations

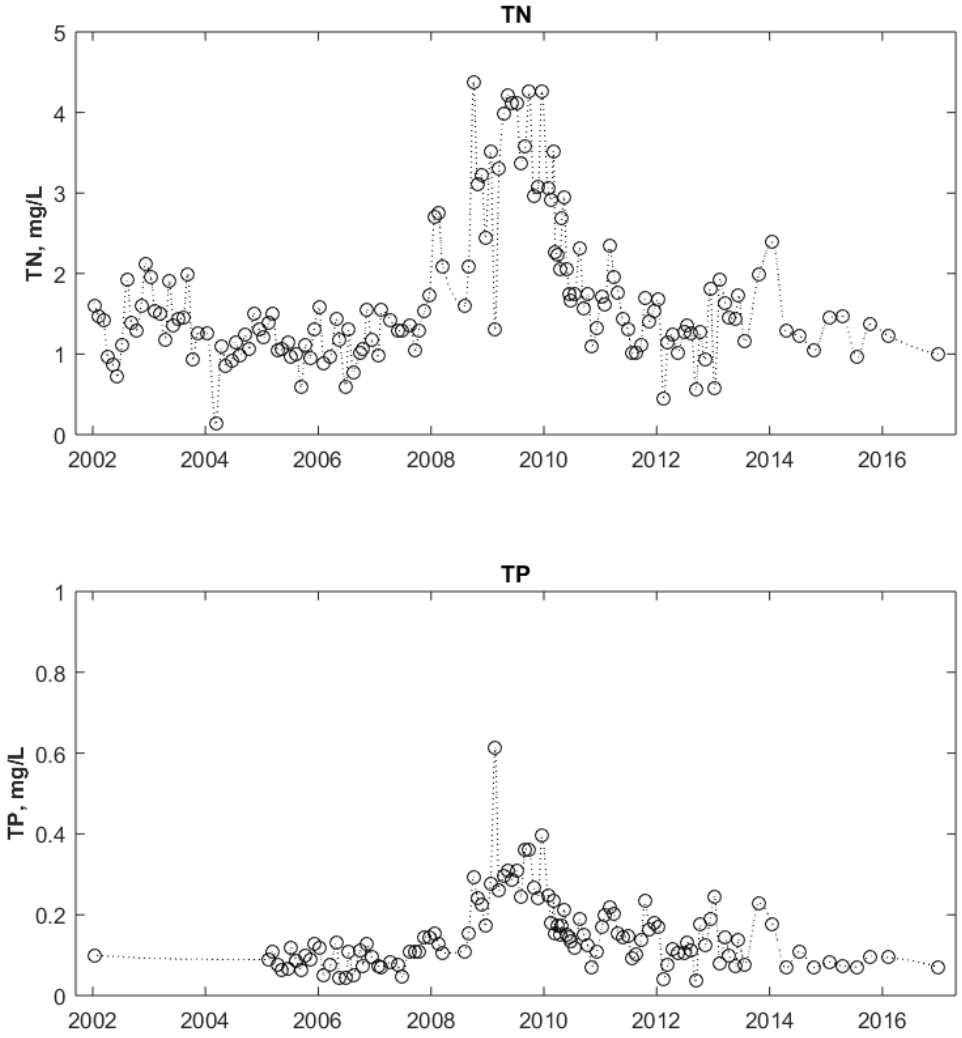

Figure A.1: Total Nitrogen (TN) and Phosphorus (TP) at Milang in Lake Alexandrina. The hollow circles are the measured data and the dashed line is the interpolated daily data using a shape-preserving piecewise cubic interpolation ("interp1" function) in MATLABTM.

Figure A1 shows the interpolated TP and TN loadings represent the measured data very well.

A.2 Coastal Ocean in situ water quality

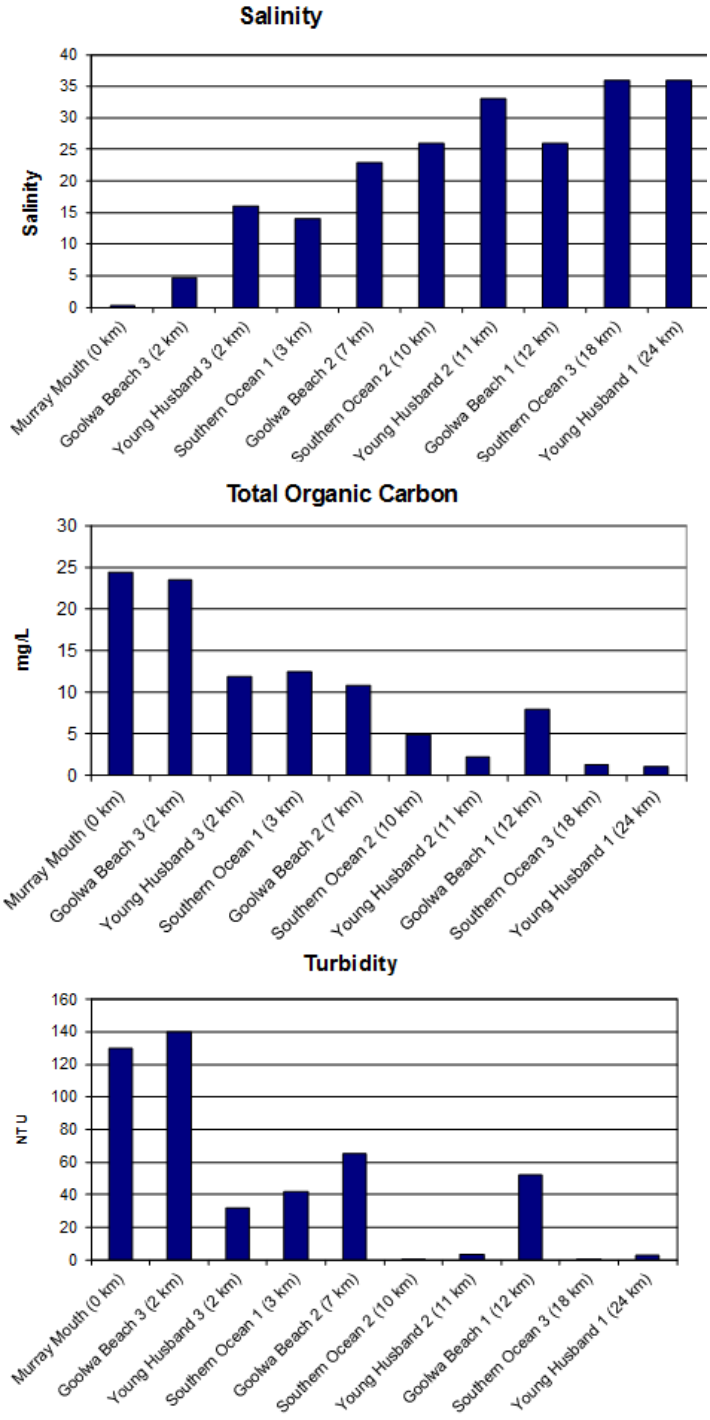

Figure A.2: Salinity, turbidity and total organic carbon measured in samples collected from the coastal ocean during a high flow period (Feb-Mar 2011). The distance from the River Murray Mouth is indicated in the brackets after the sample site name. Source: Environment Protection Authority (South Australia).

A.3 Relationships at incremental distances from Murray Mouth

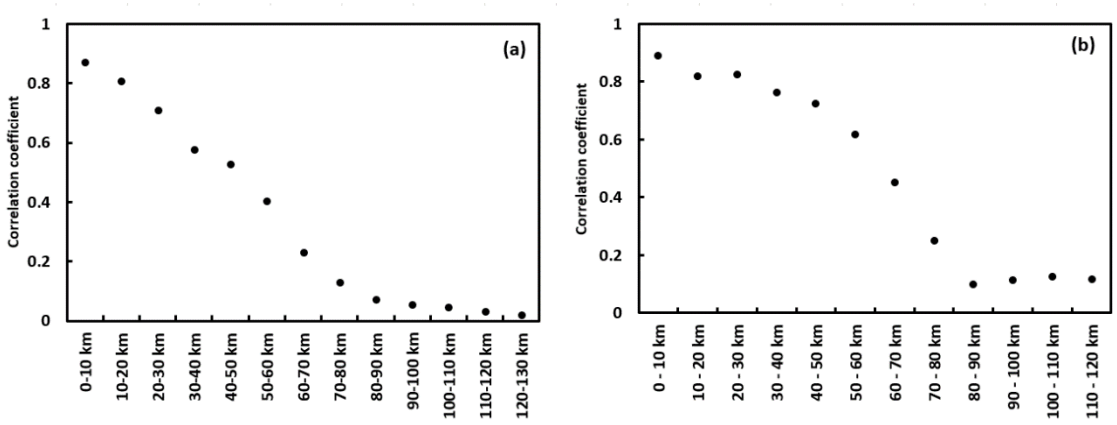

Figure A.3.1: correlation coefficient between (a) mean barrage flow per month and mean chl-a concentration and (b) mean barrage flow (when >10,000ML) per month and chl-a concentration for each incremental distance from the Murray Mouth.

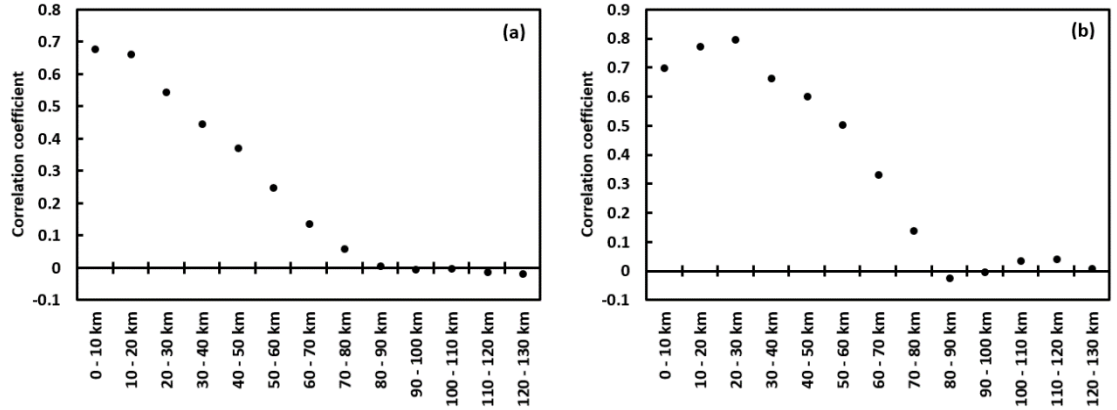

Figure A.3.2: correlation coefficient between (a) mean barrage flow per month and mean POC concentration and (b) mean barrage flow (when >10,000ML) per month and POC concentration for each incremental distance from the Murray Mouth.

Analysis of correlations at each incremental distance from the Murray Mouth demonstrates a stronger relationship between chl-a concentration and barrage flow closer to the Murray Mouth. Correlations are greatest in surface waters up to the 50-60 km zone from the Murray Mouth (where R2 > 0.4) (Figure A.3.1). This is also the

observable trend for POC concentration in surface waters where the correlation decreases with increasing distance from the mouth (Figure A.3.2).

Chapter 3

Mapping the long-term influence of river discharge on coastal ocean chlorophyll-*a*.

Statement of Authorship

Title of Paper	Mapping the long-term influence of river discharge on coastal ocean chlorophyll-a
Publication Status	☒Published ☐Accepted for Publication ☐Submitted for Publication ☐Unpublished and Unsubmitted work written in manuscript style
Publication Details	Auricht, H., Mosley, L., Lewis, M., & Clarke, K. (2022). Mapping the long-term influence of river discharge on coastal ocean chlorophyll-a. Remote Sensing in Ecology and Conservation, 8, 629-643.

Principal Author

Name of Principal Author (Candidate)	Hannah Auricht	
Contribution to the paper	Conceptualization, methodology, data curation, formal analysis, writing – original draft preparation, writing – review and editing.	
Overall percentage (%)	70%	
Signature		Date: 21/11/2022

Co-author Contributions

By signing the Statement of Authorship, each author certifies that:

i. the candidate's stated contribution to the publication is accurate (as detailed above);

ii. permission is granted for the candidate in include the publication in the thesis; and

iii. the sum of all co-author contributions is equal to 100% less the candidate's stated contribution.

Name of Co-Author	Kenneth Clarke	
Contribution to the Paper	Methodology, formal analysis, writing – review and editing.	
Signature		Date: 28/Nov/2022

Name of Co-Author	Megan Lewis	
Contribution to the Paper	Methodology, formal analysis, writing – review and editing.	
Signature		Date: 30 Nov 2022

Name of Co-Author	Luke Mosley	
Contribution to the Paper	Methodology, formal analysis, writing – review and editing.	
Signature		Date: 2 Dec 2022

Abstract

Although the potential of river discharge to support ocean productivity and marine ecosystems is known, the specifics of this relationship are poorly understood in many regions of the world. Global estimates of river flow indicate that river discharge is decreasing due to the increasing fragmentation, extraction and regulation of rivers. This likely means that the contribution of river flow to coastal productivity and water quality is changing, potentially leading to fewer and smaller magnitude ocean fertilisation events. We developed a simple analysis method, based on Earth observation data, to investigate where coastal ocean chlorophyll-*a* is most strongly influenced by river discharge. The per-pixel spatiotemporal correlation technique (implemented using Python) correlates chlorophyll-*a* concentration (a proxy for phytoplankton biomass and indicator of primary productivity) from MODIS ocean colour data with river discharge data. The method was tested globally on 11 different rivers discharging into coastal ocean regions. Our findings suggest some of the world's largest river systems, such as the Amazon River, have zones of elevated coastal chl-*a* which extend hundreds to thousands of km from the river mouth. These findings suggest the influence of river discharge may have been underestimated in many coastal regions of the world. The method appears more effective for larger river systems discharging to ocean waters with less complex nutrient dynamics and weaker seasonal productivity patterns, most notably in temperate regions. Increasing our understanding of the specific areas influenced by river discharge, and the degree of influence over space and time, is an important step towards improved river and coastal management. This method will increase the capacity of researchers to monitor how, when and where coastal waters are affected as river discharge continues to change into the future.

3.1 Introduction

By delivering dissolved nutrients to coastal ocean regions, river discharge not only supplements primary productivity by stimulating phytoplankton growth, but also contributes to the long-term biological productivity of the ocean and hence ocean carbon

storage (Gomes *et al.* 2018; Jickells *et al.* 2017). This effect can subsidize the functioning of marine food webs, supporting marine ecosystems (Connolly *et al.* 2009; Matsumoto *et al.* 2016; Schlacher *et al.* 2008). Some fish species utilise river plumes as juveniles, or as signals for migration (Abrantes and Sheaves 2010; Black *et al.* 2016; Burla *et al.* 2010; Drinkwater and Frank 1994; Grimes 2001). There is increasing evidence to show that river plumes affect predator-prey interactions, particularly for larval fishes, their planktonic prey and predators (Akester 2019; Black *et al.* 2016; Dowidar 1984; Nixon 2003; Phillips *et al.* 2017; Ware and Thomson 2005). For example, Swieca *et al.* (2020) observed substantially higher concentrations of zooplankton in the Columbia River plume, with chl-*a* and surface salinity the most influential factors. The plume was found to enhance spatial overlap between larval fishes and their prey, relative to open oceanic waters. Studies like these illustrate the importance of river discharge and river plumes for marine food-web and ecosystem functioning and stability. Consequently, river plumes can affect fisheries stability (e.g. (Chai *et al.* 2009; Grimes and Kingsford 1996; Sharaf El Din 1977)). However, there is limited understanding of how altered, reduced or complete lack of freshwater flow affects estuarine and open coastal marine systems (Gillanders and Kingsford 2002), especially over longer time scales.

Remote sensing has increased our understanding of the effect of river discharge on coastal ocean water quality, and is a less expensive and more spatially and temporally comprehensive approach than ship-borne and other *in situ* based methods (Acker *et al.* 2005; Alvarez-Romero *et al.* 2013; Colella *et al.* 2016; Devlin *et al.* 2015). While many remote sensing studies have mapped river plumes, usually from true-colour imagery, few have investigated the specific spatial and temporal relationship between increases in river discharge with increases in chl-*a* concentrations. In general, most research has been limited to investigating mixing of turbid plumes during high flow events. Few have investigated any potential increases in chl-*a* beyond the extent of the turbid plume. There is also a paucity of research which can comment on the strength of this relationship across space and time, or under varying flow conditions. This is likely because it is difficult to distinguish background increases in phytoplankton from typical fluctuations

that result from seasonality, as well as challenges of obtaining accurate optical measurements from satellite imagery in shallow and coastal waters. There is currently no broadly accepted method to identify areas where ocean chl-*a*, as a proxy for phytoplankton biomass and an indicator of productivity, may be attributed specifically to river discharge. However, this information is crucial to our understanding of the influence of river discharge on coastal environments. Such information allows the scale of spatial and temporal influence to be monitored over time, under various flow, climate and management conditions.

This paper presents a method based on Earth observation data to objectively identify coastal ocean regions where water quality and productivity is most influenced by river discharge. A per-pixel spatiotemporal analysis of freely available MODIS ocean colour imagery products is developed to achieve this goal. Eleven rivers, representing a broad range of river volume, flow volume, seasonality and location, are used to demonstrate our approach for investigating the long-term relationship between river flow and coastal water productivity.

3.2 Methods

3.2.1 Ocean colour products

NASA's Moderate Resolution Imaging Spectroradiometer (MODIS) sensor, on board the sun-synchronous, polar-orbiting satellite "Aqua", became operational in 2002 and is still operational today. Monthly composite MODIS ocean colour chl-*a* products were obtained at 4 km spatial resolution via: https://oceancolor.gsfc.nasa.gov/. These products are effectively 'ready to use.' Spectral contamination due to land, atmospheric effects, probable ice or cloud cover, or areas where radiance is saturated or values suggest sunglint are masked from final chl-*a* products products (BoM 2014; IOCCG 2000). Some of these masked pixels include those near the coast on some dates in the imagery (e.g. near the mouths of the Mekong and Amazon rivers).

The primary focus of this study was to develop a more objective and broadly applicable method for identifying coastal ocean regions where chl-*a* is influenced by river discharge.

MODIS OC3M chl-*a* products are generally considered more accurate when used to estimate concentrations of chl-*a* in clear open ocean waters where the main contribution to ocean colour is phytoplankton (Case 1 waters) (IOCCG 2000). MODIS chl-*a* products in the nearshore environment can also be affected by high sediment loading (turbidity) from river discharge, leading to overestimations of chl-*a* concentrations. However obtaining precise measurements of chl-*a* is not essential to achieve the aim of this paper, and chl-*a* response can extend a large distance from near-shore turbidity plumes (Auricht *et al.* 2018). With this understanding, MODIS chl-*a* products are appropriate for assessing the relationship between river discharge and coastal water quality at a broad, global scale.

3.2.2 River flow data and Selection

Eleven rivers and adjacent ocean regions, including several major river systems, were chosen to demonstrate the applicability of the spatiotemporal method (Table 3.1 and Figure 3.1). Rivers across all populated continents were selected, covering a range of flow rates and climatic systems, although river choice was limited by flow data availability. All the rivers had at least three years of flow data over the period of MODIS data availability. The temporal resolution of river discharge data was mean monthly discharge (m3/s), to match the temporal resolution of the monthly composite MODIS ocean colour chl-*a* products. This was supplied from some sources such as the Global Runoff Data Centre (GRDC) but was calculated from daily flow data for others (e.g. the Amazon).

Table 3.1: River flow data used in this study.

River name	Station(s)	Approx. location of station(s) (Latitude and Longitude)	Ocean	Record ends (MM/YYYY)	Max no. data pairs compared per pixel	Approx. catchment area (km^2)	Mean annual discharge at station (m^3/s)[1]	Data Source
Amazon	Óbidos	(-1.9472, -55.5111)	Atlantic	04/2018	190	4,680,000	175,024.35	ANA[4]
Mississippi	Vicksburg	(32.315, -90.9058)	Gulf of Mexico	03/2019	201	2,964,255	21,428.67	GRDC[2]
Parana	Timbues	(51.4154, 0.3077)	Atlantic	08/2014	146	2,346,000	17,291.12	GRDC
Mekong	Sum of discharge at Can Tho & MyThuan	Can Tho (10.02361, 105.7692) MyThuan (10.275, 105.295)	South China Sea	12/2007	66	795,000	13,970.35	MRC[3]
St. Lawrence	Cornwall	(45.0062, 74.7949)	Atlantic	06/2017	180	773,892	7,184.99	GRDC
Niger	Lokoja	(7.8, 6.7667)	Atlantic	10/2011	120	1,270,000[6]	5,983.31	GRDC
Columbia	Dallas	(45.6073, -121.1734)	Pacific	11/2016	161	613,830	4,890.51	GRDC
Rhone	Chancy, Aux Ripes	(46.153, 5.9707)	Mediterranean	12/2014	150	10,323	320.68	GRDC
Pearl	Bogalusa	(30.7932, -89.8209)	Gulf of Mexico	05/2017	179	17,024	282.70	GRDC
Murray	Sum of discharge over barrages	e.g. (-35.5577, 138.8778)	Southern	03/2019	201	1,059,000	72.90	DEW[5]
Thames	Kingston	(51.415443, -0.30771)	North Sea	09/2015	159	9,948	62.96	GRDC

[1]Calculated from monthly averaged data from July 2002 to record end. [2]Global Runoff Data Centre, [3]Mekong River Commission, [4]National Water Agency of Brazil, [5]Department of Environment and Water (South Australian Government), [6]Aich *et al.* (2016)

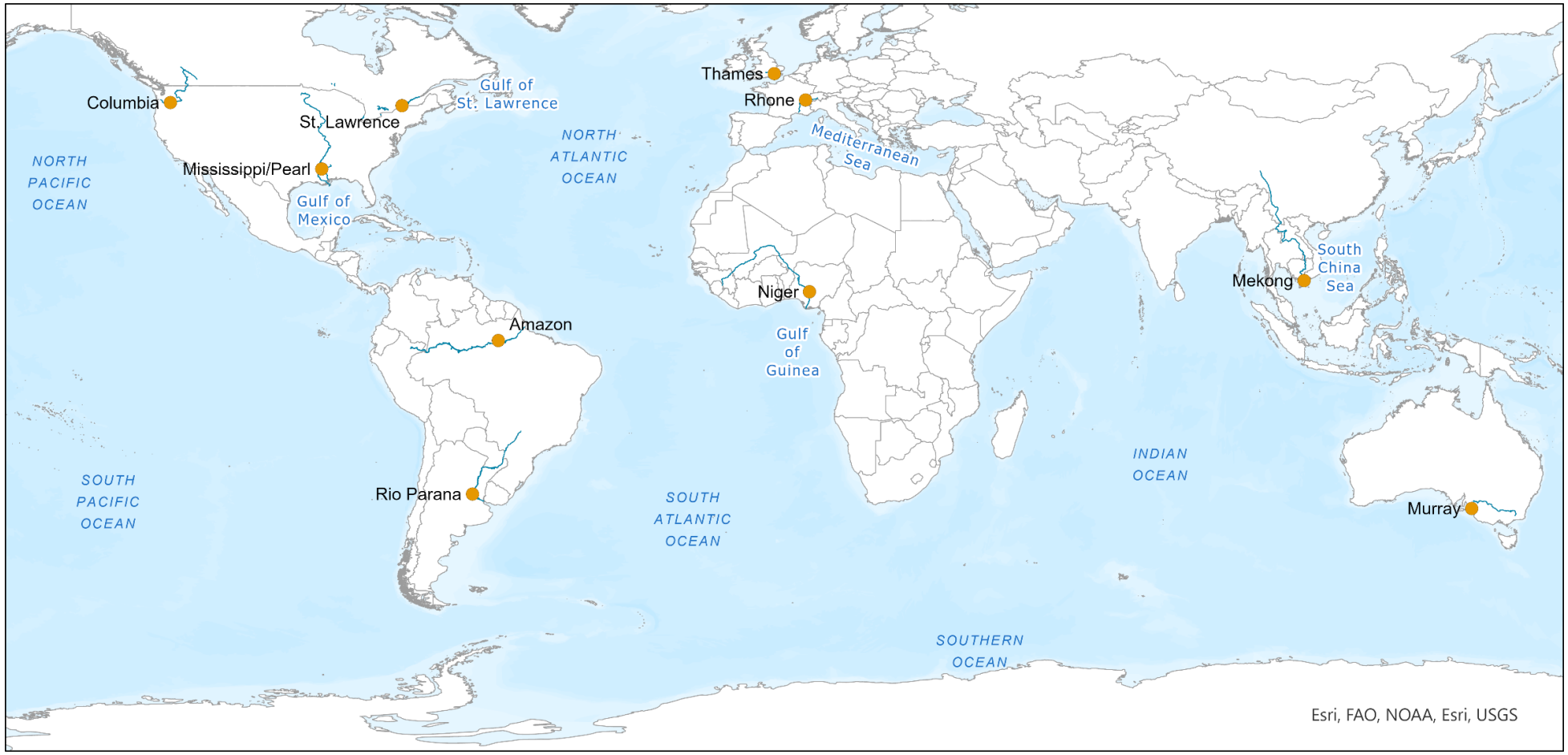

Figure 3.1: Map of flow stations for rivers investigated in this paper. Orange points indicate the location of river discharge stations (refer Table 3.1).

3.2.3 Spatiotemporal correlation analysis

A spatiotemporal, non-parametric correlation analysis was used to identify and map pixels in the MODIS imagery where change in chl-*a* is correlated with and likely influenced or driven predominantly by river discharge from the nearby river. This analysis was developed in Python 3 language, using packages including but not limited to pandas, numpy, xarray, gdal and rasterio. An example of the python script is available on request. Figure 3.2 shows a summary of the methods. For each river, a study area (ranging from ~260 km x 220 km to ~6,600 km x 4,800 km) of surrounding coastal ocean centred on the river mouth was examined. Time series data were extracted for each pixel in the imagery captured over these areas. Where data were missing from either the time series of river discharge or chl-*a* for pixels (due to cloud cover or land contamination), the corresponding dates for both datasets were removed. This ensured that the data for river discharge and for chl-*a* was temporally synchronised.

As much of the flow and MODIS time series data were not normally distributed, a non-parametric Spearman rank correlation test was used to test correlations between chl-*a* and river discharge for each pixel across the study areas. A significance test was also conducted on these time series to determine where in the scene a significant relationship between river discharge and chl-*a* products could be detected. These scenes were then masked by significant p-values ($p<0.01$) and where Spearman's rho (r_s) >= 0. Final information products then indicated areas where a significant long-term, positive relationship between river discharge and chl-*a* concentrations was present. Maps showing the proportion of valid observations per pixel used to perform these analyses were also produced for each scene and are presented in Supplementary Material (Figures B3.1 and B3.2, Appendix B).

Correlation was also calculated between residual chl-*a* and river flow datasets (refer Appendix B and Figures B to S3). These datasets were produced with the aim of removing seasonality from both the river discharge data and the chl-*a* data, respectively.

This involved calculating the long-term mean (river discharge or chl-*a*) of each month, and subtracting these values from that observed in the corresponding month. This resulted in a residual time series for every pixel of the chl-*a* data, and river discharge data.

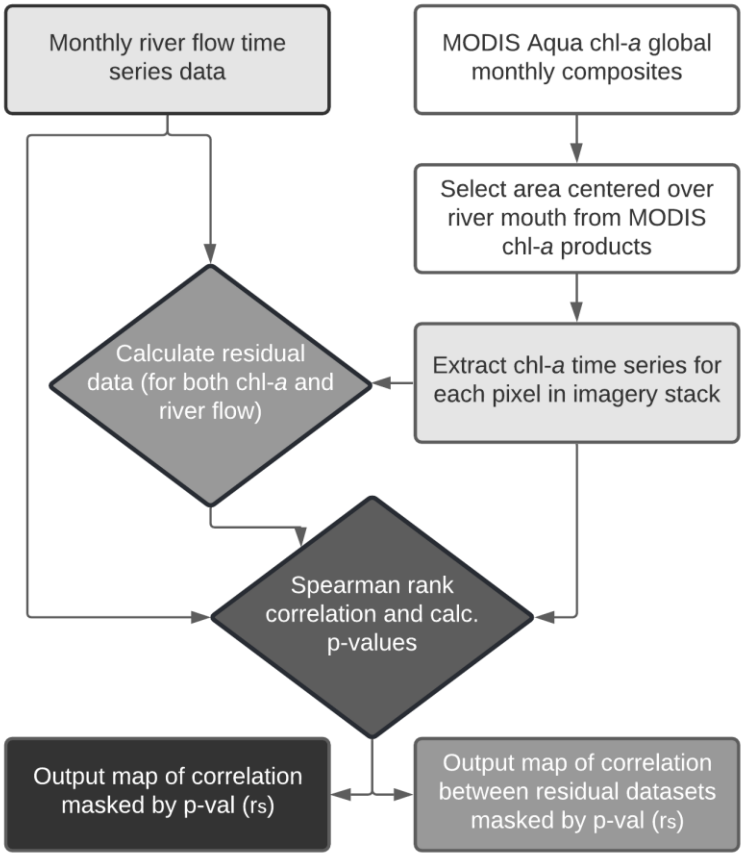

Figure 3.2: Flow chart summarising the overall process for the spatiotemporal correlation analysis. These processes were implemented using python scripting language. This methodology is used to produce maps showing correlation between chl-a concentration (derived from MODIS satellite imagery) in coastal ocean waters and river discharge data from nearby rivers.

3.3 Results and Discussion

The spatiotemporal correlation analysis developed in this paper enabled us to identify areas of long term river influence on coastal ocean chl-*a* in a diversity of locations. The analysis also revealed that these relationships can be complex and that the method is more useful for particular kinds of river systems, as presented and discussed below.

3.3.1 Clear patterns of influence in temperate regions

The spatiotemporal correlation analysis was most useful when applied to identify riverine influences on temperate coastal ocean regions. It identified areas with positive, moderate to strong monotonic relationships (r_s >= 0.5) to river discharge, distinguishable from background processes and consistent with previous studies in these regions. This was most evident for the Murray and Rhone rivers, respectively. These rivers also have highly variable river flow time series.

Off the coast of the Murray River mouth, elevated chl-*a* also correlated with river flow up to roughly 25 km (Figure 3.3a) in a location consistent with results from our previous research (Auricht *et al.* 2018). The Murray River is an arid to semi-arid river system and flow is highly variable with weak seasonal patterns (Figure 3.3a). The quality of the temperate Southern Ocean waters (or more specifically, Great Australian Bight waters) below the Murray mouth has been little researched to date. However, previous studies that have investigated upwelling on the west of Kangaroo Island and the South Eastern Bonney coast, suggest that phytoplankton growth is nutrient limited and that coastal waters in this location have relatively lower nutrient concentrations compared to northern, tropical Australian waters (Doubell *et al.* 2018; McClatchie *et al.* 2006; Motoda *et al.* 1978; van Ruth *et al.* 2018). This is a significant finding given that little research has been conducted on the response of coastal waters to Murray River discharge, even though the Murray is Australia's largest river. Management of Murray River flow is often a contentious issue due to the sheer number of stakeholders and the length of the river. Therefore, identifying regions where chl-*a* is strongly influenced, and

perhaps even dependent on river discharge is of interest to both river and coastal managers.

Positive correlation values between ocean chl-*a* and Rhone River discharge (r_s = 0.2 - 0.4) extend up to ~90 km south west beyond the river mouth (more specifically, into the Gulf of Lion) (Figure 3.3b). These results can be explained by the characteristics of the Mediterranean Sea to which the Rhone River discharges. This sea has relatively oligotrophic waters and is semi-enclosed (Mena *et al.* 2019; Tanhua *et al.* 2013). The Rhone is one of the main rivers contributing dissolved and undissolved nutrients to the Mediterranean north coast via its discharge (e.g. simulated total N of 88,531 ton/year and simulated total P of 1,938 ton/year (Malagó *et al.* 2019)) and is largely responsible for primary productivity in this region (Colella *et al.* 2016; Malagó *et al.* 2019; Piroddi *et al.* 2017). However, it should be noted that the Gulf of Lion, compared with the rest of the Mediterranean, undergoes deep wintertime convection and mixing. These processes are well studied in this region, increasing phytoplankton biomass and productivity leading to spring blooms (Barale and Gade 2008; Macias *et al.* 2018). Chl-*a* concentrations in the broader Gulf and Mediterranean are therefore driven predominantly by climate related changes (e.g. wind, temperature), rather than river discharge alone. These factors should be considered alongside the findings of this paper. Nevertheless, the correlation between river flow and chl-*a* is stronger (r_s > 0.4) within ~30 km of the river mouth and shore (Figure 3.3b). The long term analysis and correlation between chl-*a* and river flow in the Mediterranean shows a region of similar shape and extent to previous studies which have mapped the turbid plume under high flow conditions (e.g. Devenon *et al.* 1992; Estournel *et al.* 2001; Forget *et al.* 1990). These findings suggest the analysis successfully identified the coastal waters where chl-*a* is influenced by river discharge. The increased coastal productivity due to Rhone River discharge is understood to affect fishery yields in the Gulf of Lion (Piroddi *et al.* 2017; Salen-Picard *et al.* 2002). However, policies such as the EU Nitrates Directive and an Urban Waste Water Directive have been employed to reduce the concentrations of nutrients in discharge from the Rhone. As a result, chl-*a* concentrations have reduced in

more recent years in the Gulf of Lion (Colella *et al.* 2016; Malagó *et al.* 2019). This region can be more closely monitored for change, as river discharge volume and concentrations are altered into the future, and for assessment of the success of implementation of these policies. These findings illustrate the importance of the method in identifying coastal waters where chl-*a* concentrations are largely controlled by river discharge, as it is information relevant to both river and coastal managers.

Because both the Murray and Rhone rivers discharge into generally low nutrient waters, a strong, measurable response by phytoplankton, contrasting with surrounding waters, is therefore more easily and objectively identified using the spatiotemporal analysis developed in this study. In addition, the flow time series for both rivers do not have dominant seasonal patterns. This means that large increases in chl-*a* are more easily identified with larger freshwater pulses from river mouths. These results demonstrate the applicability of the methodology for lower nutrient ocean regions for identifying regions which have been influenced by river discharge across the longer term.

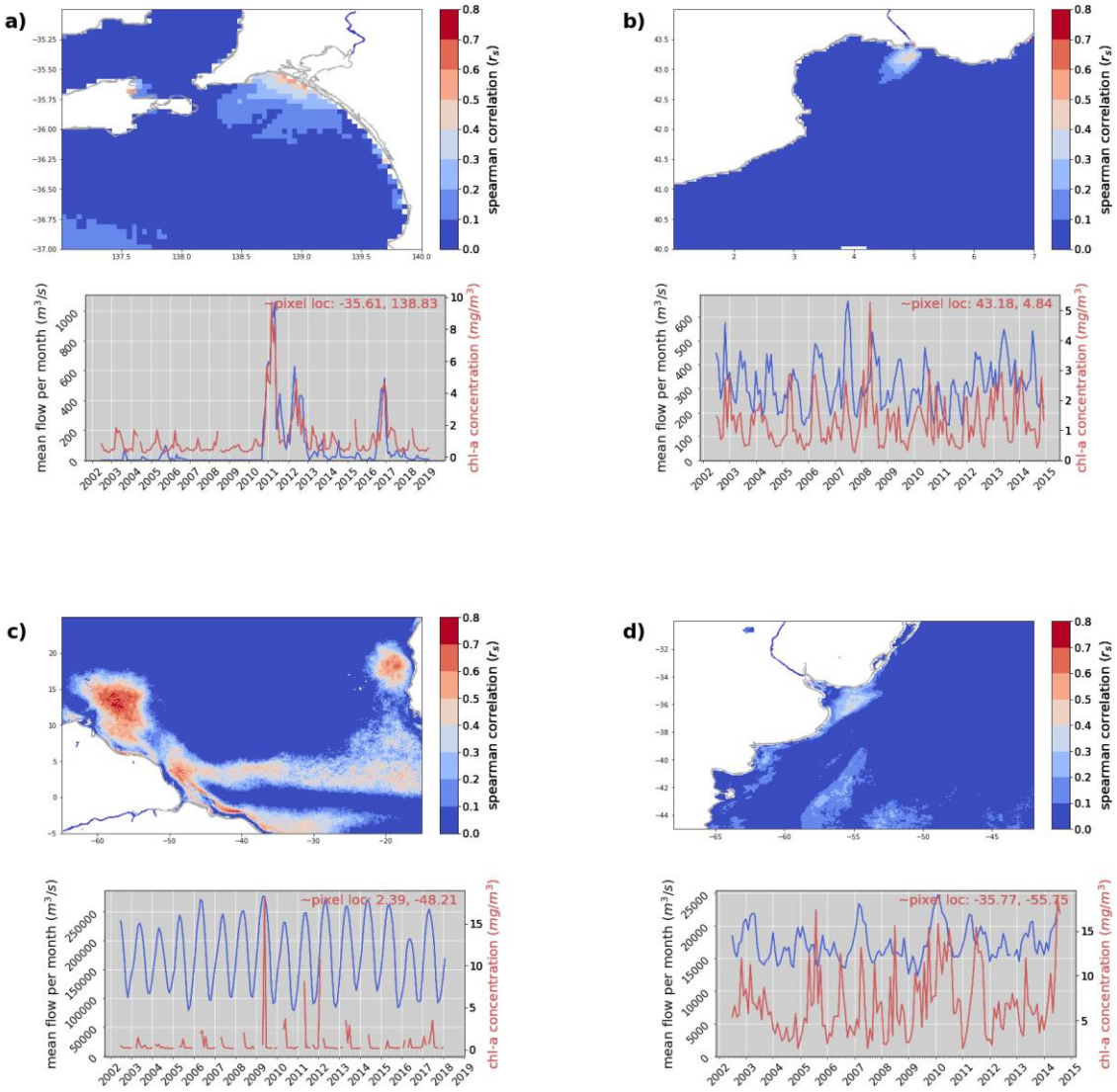

Figure 3.3: Maps of river discharge influence based on Spearman correlation analysis on remotely sensed MODIS chl-a concentrations and corresponding river flow time series and chl-a concentrations at pixel (with location on top right of time series plot) for the a) Murray River on the coastal waters in the Southern Ocean of South Australia, b) Rhone River in the Gulf of Lion, France, c) Amazon River on the mid-Atlantic Ocean and along the northeastern coast of South America and d) Parana River on the Southern Atlantic Ocean.

3.3.2 Patterns of influence in tropical and subtropical regions

Very large coastal ocean regions (> 2,000 km north west from the Amazon River mouth and > ~250 km south east from the Mekong delta coast) are influenced by discharge from their respective rivers (r_s > 0.5) (Figure 3.3c and Figure 3.4a). Both the Amazon and Mekong rivers (Figures 3c and 4a) have strong seasonal and predictable river flow patterns.

There is a two-fold seasonal variation in river water discharge rate from the Amazon, with peaks in discharge rate occurring reliably between March and June (> 250,000 m3/s) and lows between July and December (Figure 3.3c). Moderate to high r_s values (> 0.5 and > 528,598 km2 within the scene) are identified along the coast extending both north and south of the Amazon River mouth, and a large radial area near to the Caribbean is also visible (Figure 3.3c). These findings suggest that Amazon river discharge has a moderate to strong influence on coastal ocean phytoplankton and marine productivity in the open ocean, thousands of kilometres from the river mouth (Figure 3.3c). These findings are consistent with previous studies, including *in situ* sampling, tracking with buoys and ship based cruises which have tracked terrestrially derived nutrients and sediments, thousands of km from the river mouth (Coles *et al.* 2013; Hu *et al.* 2004). The Amazon discharges at the equator and on the western boundary of the Atlantic Ocean. Because of this location, the Amazon river plume becomes synchronized with a number of seasonally varying energetic boundary currents (Coles *et al.* 2013). During winter and spring months (April - May) discharge reaches its peak (Figure 3.3c). Previous research has shown that during winter, the plume is carried with the North Brazil Current along the north-eastern coast of Brazil, while from spring to autumn (September - October) it is entrained with the North Equatorial Counter Current (NECC) which travels eastward (Coles *et al.* 2013; Gomes *et al.* 2018; Muller-Karger *et al.* 1998; Weber *et al.* 2017). The latter may explain the distinct band of ocean between 0 and 5 degrees latitude where correlation is positive (r_s > 0.2), in addition to higher temperatures and circulation in this equatorial region. However, some authors debate that the plume travels persistently northward throughout the year, rather than only during winter months eastward (Coles

et al. 2013; Gomes *et al.* 2018; Muller-Karger *et al.* 1998; Weber *et al.* 2017). The results of this paper suggest plume waters and productivity is elevated due to discharge along the north coast towards the Caribbean with the North Brazil Current (NBC), as well as to the east, with the NECC. These findings show the influence of Amazon River discharge is much farther reaching than the shelf itself, and may settle some of the debate about the predominant direction and influence of the plume across the long term.

South of the Amazon, the Parana River is the most important tributary of the Rio de la Plata, contributing more than 80% of Rio de la Plata streamflow (Camilloni and Barros 2003). However, the Parana River discharge is very irregular with no easily predictable seasonal trends (Figure 3.3d). Over the last several decades, despite no significant rainfall increases in the basin, river discharges have increased. The range between high and low flow is narrower than that of the Amazon (between ~12,000 m^3 s^{-1} and 25,000 m^3 s^{-1}), but still of great magnitude (Table 3.1). This is due to concomitant changes in forest cover, as deforestation has been a major issue in this region since the 1970s (Carvalho *et al.* 2011; Lee *et al.* 2018). This seems to have also changed peak discharge timing of the Parana (Lee *et al.* 2018). The results of our analysis suggest that chl-*a* concentrations off the coast of the river mouth in the Atlantic Ocean are likely influenced by the river discharge of the Parana, indicated by positive correlation values > 0.4 in a region within ~ 300 km from the mouth (Figure 3.3d). It is possible that volume and concentrations of the Parana River flow is increasing, and that the relationship may increase or cover a large area of the scene in the future. Calls to consider these factors for forecasting hydropower generation (which supplies up to 80% of Brazil's energy) have been made (Lee *et al.* 2018), but how they will affect coastal ocean productivity and water quality in the future should also be considered.

Much of the ocean in the scene in Figure 3.4a is occupied by pixels with a positive correlation with Mekong river discharge. Of these, an area covering around ~8,402 km^2 have relatively strong correlation values (r_s > 0.6). These positive pixels cover a region south east from the mouth, but other positively correlated pixels also extend northeast

and southwest along the coast. River discharge from the Mekong is known to contribute terrestrial nutrients during summer, increasing productivity near the western coasts of the South China Sea (SCS) (Dai 2012; Gan *et al.* 2010; Lu *et al.* 2020). Highest flow in the Mekong usually occurs between August and October, while lower flow rates occur between January and April (Figure 3.4a). In winter, when there is lower river discharge, the turbid river plume generally flows south west under a north-easterly monsoon Lu *et al.* 2020). The region of elevated correlation in the SCS region of this study displays patterns which fit somewhat with this known phenomenon (Figure 3.4a). However, the region of apparent influence (Figure 3.4a) is far more extensive than what is perhaps expected from Mekong discharge alone, and it is likely that other rivers in this region and other factors which co-vary with the seasonal river flow (e.g. seasonality of sea surface temperatures) are also responsible for the correlation seen here, rather than Mekong River discharge explicitly. It is also possible that the spatiotemporal method may overestimate the strength of the relationship in the broader SCS due to the lower number of dates available for comparison (Table 3.1), which are a result of a short available temporal record further reduced by extensive cloud cover. Additionally, several pixels are masked in the nearshore of the Mekong and Amazon from the MODIS 4 km products, likely because of high turbidity and land interference contributing to chl-*a* estimations (Figure 3.4a and Figure 3.3c).

Mean monthly Mississippi discharge rates from the Vicksburg, Mississippi station ranged between ~ 10,000 $m^3 s^{-1}$ and ~ 50,000 $m^3 s^{-1}$ between 2002 and 2019 with highs generally occurring between February and July, following the northern hemisphere's winter and spring months (Figure 3.4b). However, in some years, high flows occur in later months of the year, during winter (e.g. 2004, 2009, 2011, 2015 and 2018). The spatiotemporal analysis results between Mississippi river flow and chl-*a* show positive correlations which 'hug' the northern Gulf of Mexico coast. The influenced area where $r_s > 0.4$, extends more than ~ 280 km east and ~ 530 km west of the river mouth (Figure 3.4b). These highlight a known area of increased productivity to the east and west of the river mouth and delta, an area characterized by a seasonally shifting eastwards or

westwards along-shelf surface current (Figure 3.4b) (Nowlin *et al.* 1998; Walker 1996; Wiseman *et al.* 1999; Yuan *et al.* 2004). These shelf currents generally confine the river plume and productivity to the northern continental shelf of the Gulf.

The open Gulf of Mexico is subtropical, permanently stratified and oligotrophic (Yuan *et al.* 2004). Consequently, discharge from the Mississippi River to the northern coast promotes phytoplankton growth (Ritter and Chitikela *et al.* 2020) on a scale which can be detected easily using the methodology used in this paper. This is crucial information because discharges from Mississippi and Atchafalaya rivers have repeatedly resulted in far-reaching algae blooms which deplete oxygen from the water column with the devastating consequence of mass fish kills. The 'dead zone' region occurs reliably, on an annual basis at the Mississippi River mouth (Rabalais *et al.* 2002; Scavia *et al.* 2019). The extent of these anoxic zones can be extreme. In 2019, after several years under implementation of a Hypoxia Task Force by the US Environmental Protection Authority, the Gulf of Mexico hypoxic zone covered an area of ~18,005 km^2. This was the eighth largest extent recorded since 1985 and was far larger than the goal of 5,000 km^2 set by the task force (Ritter and Chitikela 2020). Usually, the coverage of the anoxic area is estimated by conducting cruises off the coast, and taking *in situ* measurements (Fennel and Laurent 2018; Lohrenz *et al.* 2008; Walker 1996). Occasionally, sampling is informed by analysis of true colour satellite imagery (Board 2007; Walker and Rabalais 2006). These approaches can determine finer scale characteristics and diagnostics of the river plume and anoxic zones, useful for future predictions. However, the method developed and demonstrated here helps identify where we can expect, generally, to see response of phytoplankton to river discharge and could be used to constrain or target *in situ* sampling and track changes in the response of coastal waters to river discharge over a broader spatiotemporal scale.

The results from the analysis for the Mississippi suggest a region of influence consistent with plume mapping in previous studies (Figure 3.4b). The analysis provides additional contextual information on the dependency and relationship between productivity

(indicated by chl-*a* concentrations) and river discharge from the Mississippi. This information is also important considering that fisheries productivity in the Gulf of Mexico is strongly linked to Mississippi discharge by several studies (Grimes 2001; Lindall and Saloman 1977; Mickle *et al.* 2018; Rakocinski *et al.* 1996).

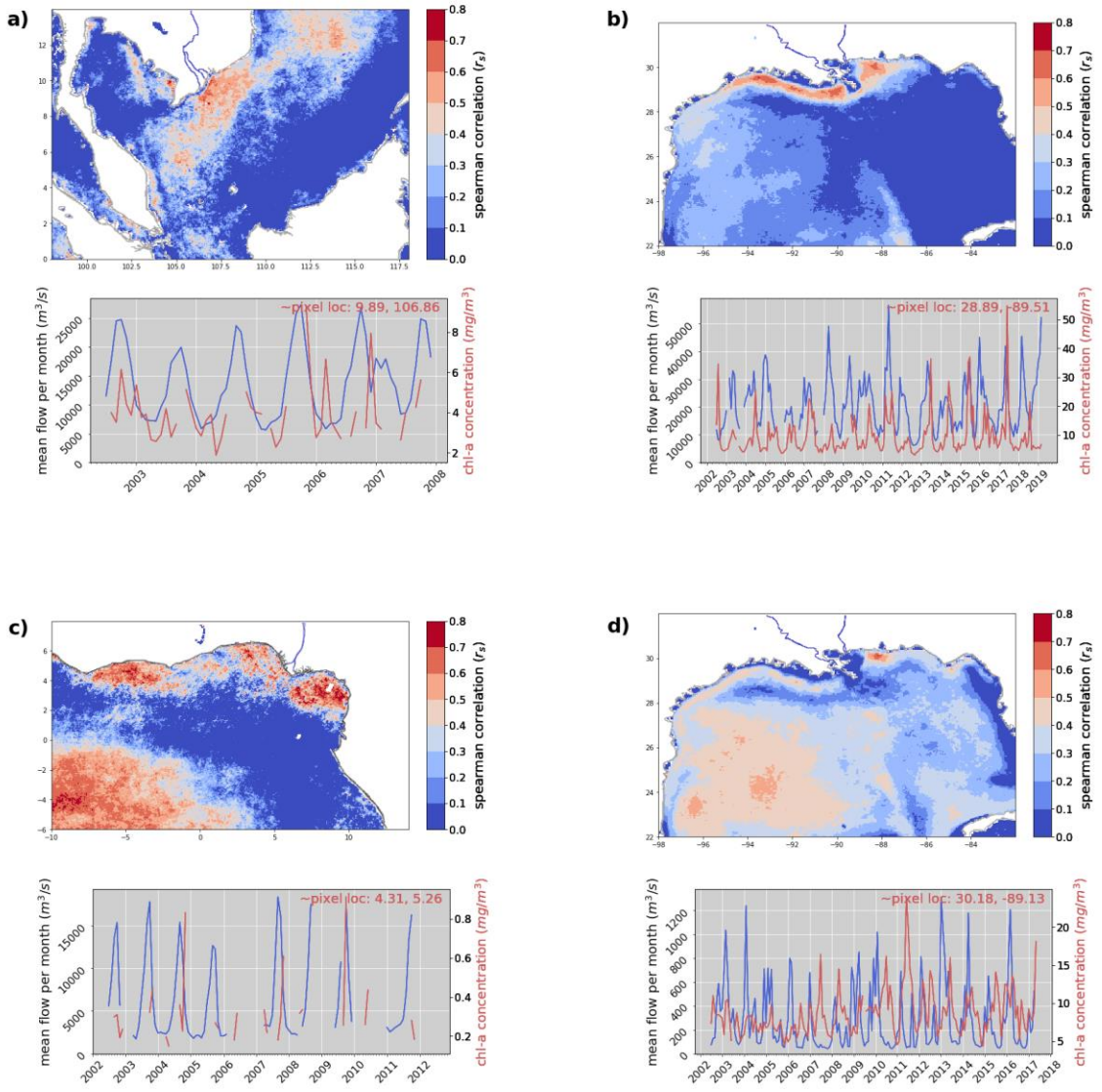

Figure 3.4: Maps of river discharge influence based on Spearman correlation analysis on remotely sensed MODIS chl-a concentrations and corresponding river flow time series and chl-a concentrations at pixel (with location on top right of time series plot) for the (a) Mekong River on the South China Sea, (b) Mississippi River on the northern Gulf of Mexico, (c) the Niger River on the coastal waters in the Gulf of Guinea and (d) the Pearl River in the Gulf of Mexico.

3.3.3 Complex coastal regions with unclear responses to river discharge

The remaining rivers investigated in this paper did not have clear areas of influence, or areas where chl-*a* was strongly correlated to nearby river discharge detected using the spatiotemporal correlation method. This is most likely due to the added complexities of the systems to which they export freshwater, or the relative volume of river discharge.

The St. Lawrence River has the third greatest average discharge of the rivers investigated for this paper (Table 3.1). Flow to the Gulf of St. Lawrence increases in warm months with snow melt. Sea ice forms in the Gulf in December and begins to spread seaward (east), eventually covering most of the Gulf, reaching its maximum extent in March, thereafter beginning to melt (Urrego-Blanco and Sheng 2014). The lack of distinctive areas of moderate to high correlation in the Gulf of St. Lawrence from the spatiotemporal analysis are likely due to a lack of data due to cloud cover and masking or inaccurate estimates of chl-*a* due to ice cover (Figure 3.5a) melt (Urrego-Blanco and Sheng 2014). The Gulf of St. Lawrence is known to be highly productive, but higher productivity in the eastern region, has previously been attributed to upwelling (Savenkoff *et al.* 2001). Using ocean colour satellite imagery from the Coastal Zone Colour Scanner and *in situ* measurements, Fuentes-Yaco, *et al.* (1997) confirmed a strong seasonal cycle in the Gulf of St. Lawrence, with increases in chl-*a* in late summer to early fall, consistent with timing of sea-ice melt, and not in spring months. However, the study was temporally limited, only analysing 80 images covering a 2 year time span (April 1979 to 1981). Findings of this paper indicate a region with positive correlation due to river discharge in the western Gulf of St. Lawrence, nearer the river estuary, consistent with these previous studies. Importantly, while chl-*a* estimates in MODIS products may have been affected in this location due to sea ice cover, they are derived from more than 14 years of monthly satellite imagery. Considering this, these results may still be a reasonable and adequate representation of the long term pattern in chl-*a* in relation to river discharge in this region, but this requires further investigation.

Although the Niger River has relatively high discharge in terms of volume, several months of river flow data were missing from this record, and this may have contributed to inconclusive results (Figure 3.4c). Figure 3.4c shows the correlation between the Niger River discharge and chl-*a* in waters in the Gulf of Guinea and wider Atlantic Ocean. This shows very high positive correlation values ($r_s > 0.6$) in a large portion of the scene (~ 515,920 km^2), especially below the equator towards the South, but it is unlikely that chl-*a* in this location is linked to Niger River discharge. In reality, these results are likely a consequence of a limited river discharge dataset, and high seasonality.

Findings for the Columbia River (Figure 3.5c), despite many years of river discharge data, do not show a clear area of influence. Several rivers discharge to the coast in this region, and open ocean productivity of the Pacific also appears to correlate to flow, most likely because of the seasonality of the flow record. This coastline experiences high energy wave action and relatively strong tidal and wave-driven currents and circulation (Elias *et al.* 2012; Jay *et al.* 2010). These factors also affect the capacity of any method to detect a clear area of influence on coastal productivity due independently to Columbia River discharge.

The Pearl and Thames rivers have very low river discharge rates and smaller catchment areas (Table 3.1, Figure 3.4d and Figure 3.5b). Despite large areas of positive correlation with these respective rivers, it is likely these are coincidental or due to other circulation or seasonal factors. These are examples of rivers for which the spatiotemporal analysis needs refinement or further development in order to provide useful results, and demonstrates relative to other rivers in this paper, where it is best applied. For example, ocean colour products of finer spatial resolution than used here may be able to detect a response from coastal waters to river discharge from these rivers. The Pearl River also drains to an area, where several other, considerably larger rivers drain (e.g. the Mississippi) which further complicates interpretation. The method proposed here is therefore not suitable for rivers with very low contributions to coastal waters, particularly if those coastal waters are highly dynamic and complex, and have other influential factors

such as upwelling, have strong patterns in phytoplankton production *in situ* and independent of river flow or there are other complex circulation patterns (e.g. due to wind and tides).

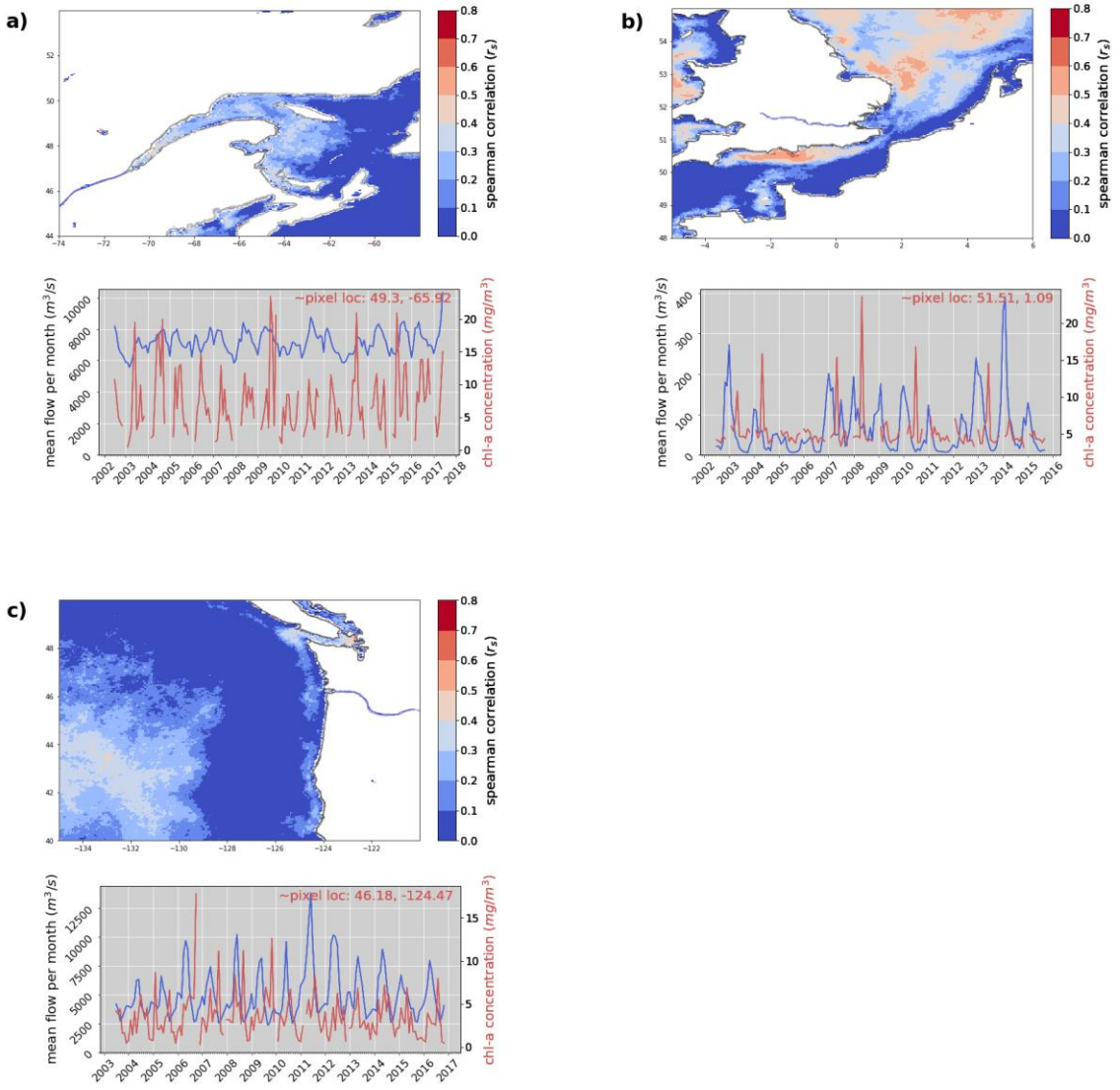

Figure 3.5: Maps of river discharge influence based on Spearman correlation analysis on remotely sensed MODIS chl-a concentrations and corresponding river flow time series and chl-a concentrations at pixel (with location on top right of time series plot) for the (a) St. Lawrence River draining to the Gulf of St. Lawrence, (b) the Thames River draining to the North Sea and (c) Columbia River on the Pacific Ocean.

s

3.3.4 Limitations

Future research would benefit from including or developing a measurement of spatial-temporal decay. All pixels representing chl-*a* estimates are compared to river discharge equally, regardless of their proximity to the river mouth. In reality, we expect that pixels closer to a river mouth would respond relatively quickly to a change in river discharge (possibly hours) while those further from the river mouth would take longer (possibly days, weeks or months). Further development of our method could incorporate a measure of spatial-temporal decay which accounts for this temporal lag, or perhaps to attempt to measure this relationship. This may require data of greater temporal and spatial resolution than was used in this study, although some research shows peaks in chl-*a* have occurred several months after peaks in river discharge (e.g. Hopkins, *et al.* (2013)). For example, in Chesapeake Bay, a system similar to the Rio de la Plata estuary, the strongest correlation between flow and chl-*a* occurred at a one month temporal lag Acker *et al.* 2005). Kim, *et al.* (2009) also observed a similar relationship between chl-*a* of the East China Sea and summertime freshwater discharge from the Yangtze (Changjiang) River of China and regulated by the Three Gorges Dam. A lag between 1 and 2 months was determined between freshwater discharge and higher chl-*a* ocean concentrations. Such a refinement could more adequately map the progression of the influence of river discharge over space and time and determine the temporal lag at which the strongest relationship between river discharge and productivity is most important between rivers.

Co-varying seasonality of both river flow and background chl-*a* in some coastal waters reduced the ability of the spatiotemporal correlation approach to clearly separate out the specific zones of river influence (including for the Niger, Pearl and Columbia rivers). In another case (e.g. the Thames), discharge rates were relatively low and no influence of discharge was detected at this spatial and temporal resolution (4 km and monthly composite data). The results of the correlation on the residual data did not provide useful additional information to discern river influence zones. Spatial and temporal patterns were no clearer or more enhanced with this approach (refer Figures B2.1, B2.2, B2.3,

Appendix B). Nevertheless, results from analyses conducted on the original, unaltered datasets suggest that river discharge from some rivers has a greater influence on coastal productivity than may have been realised previously.

Additionally, the ocean colour chl-*a* products used in this analysis have a spatial resolution of 4 km^2. This means the method is sometimes unable to accurately detect the zone of influence of very low volume river discharge (e.g. as seen in the results for the Thames River). The spatio-temporal correlation approach could be performed on satellite imagery of higher spatial and temporal resolution, depending on the research question or needs of the end users.

3.4 Conclusions

The spatiotemporal per-pixel analysis method developed in this study, utilising MODIS chl-*a* products and river discharge data, successfully enabled identification of coastal ocean regions that are influenced by river discharge long term. The method appears most useful when applied to larger river discharges to nutrient-limited coastal zones, most notably in temperate regions, although there are exceptions (e.g. the Amazon). Some of the identified ocean zones where chl-*a* concentration has stronger relationships to river discharge are much more extensive than previously documented. These findings indicate that global river discharge plays a larger role on global open ocean productivity than has been considered in the past. The world's rivers are becoming increasingly regulated, with many seeing reduced volume of flow and discharge, disconnected from oceans and with flows becoming increasingly concentrated. The way coastal ocean environments respond to these changes in flow volume, timing and concentration in the future is still uncertain and requiring further attention in research. The ability to identify regions directly influenced by river discharge enables monitoring of these regions for change over time. Development of knowledge and awareness of the importance of river discharge on coastal ocean productivity will enable people to more effectively protect and conserve these incredibly important environments in the future.

3.5 References

Abrantes, K.G., and Sheaves, M. (2010) Importance of freshwater flow in terrestrial–aquatic energetic connectivity in intermittently connected estuaries of tropical Australia. Marine Biology 157(9), 2071-2086.

Acker, J.G., Lawrence, W.H., Leptoukh, G., Zhu, T., and Shen, S. (2005) Remotely-sensed chl a at the Chesapeake Bay mouth is correlated with annual freshwater flow to Chesapeake Bay. Geophysical Research Letters 32(5), 1-4.

Aich, V., Liersch, S., Vetter, T., Fournet, S., Andersson, J.C.M., Calmanti, S., van Weert, F.H.A., Hattermann, F.F., and Paton, E.N. (2016) Flood projections within the Niger River Basin under future land use and climate change. Science of The Total Environment 562, 666-677.

Akester, M.J. (2019) Productivity and coastal fisheries biomass yields of the northeast coastal waters of the Bay of Bengal Large Marine Ecosystem. Deep Sea Research Part II: Topical Studies in Oceanography 163, 46-56.

Alvarez-Romero, J.G., Devlin, M., da Silva, E.T., Petus, C., Ban, N.C., Pressey, R.L., Kool, J., Roberts, J.J., Cerdeira-Estrada, S., Wenger, A.S., and Brodie, J. (2013) A novel approach to model exposure of coastal-marine ecosystems to riverine flood plumes based on remote sensing techniques. Journal of Environmental Management 119, 194-207.

Auricht, H.C.C., Clarke, K.D., Lewis, M.M., and Mosley, L.M. (2018) Have droughts and increased water extraction from the Murray River (Australia) reduced coastal ocean productivity? Marine and Freshwater Research 69(3), 343-356.

Barale, V., and Gade, M. Multisensor study of wind patterns and algal blooms in near-coastal gyres of the Mediterrannean sea. In 'Remote Sensing for a Changing Europe', 2008, Istanbul, Turkey. (Ed. D Maktav), pp. 32-39

Black, K.P., Longmore, A.R., Hamer, P.A., Lee, R., Swearer, S.E., and Jenkins, G.P. (2016) Linking nutrient inputs, phytoplankton composition, zooplankton dynamics and

the recruitment of pink snapper, Chrysophrys auratus, in a temperate bay. Estuarine Coastal and Shelf Science 183, 150-162.

Board, E.S.A. (2007) Hypoxia in the Northern Gulf of Mexico: An update by the EPA Science Advisory Board

United States Environmental Protection Agency, Washington, D. C.

BoM (2014) eReefs Marine Water Quality Dashboard Data Product Specification. Melbourne, Australia.

Burla, M., Baptista, A.M., Casillas, E., Williams, J.G., and Marsh, D.M. (2010) The influence of the Columbia River plume on the survival of steelhead (Oncorhynchus mykiss) and Chinook salmon (Oncorhynchus tshawytscha): a numerical exploration. Canadian Journal of Fisheries and Aquatic Sciences 67, 1671-1684.

Camilloni, I.A., and Barros, V.R. (2003) Extreme discharge events in the Paraná River and their climate forcing. Journal of Hydrology 278(1), 94-106.

Carvalho, L.M.V., Jones, C., Silva, A.E., Liebmann, B., and Silva Dias, P.L. (2011) The South American Monsoon System and the 1970s climate transition. International Journal of Climatology 31(8), 1248-1256.

Chai, C., Yu, Z., Shen, Z., Song, X., Cao, X., and Yao, Y. (2009) Nutrient characteristics in the Yangtze River Estuary and the adjacent East China Sea before and after impoundment of the Three Gorges Dam. Science of The Total Environment 407(16), 4687-4695.

Colella, S., Falcini, F., Rinaldi, E., Sammartino, M., and Santoleri, R. (2016) Mediterranean Ocean Colour Chlorophyll Trends. PLOS ONE 11(6), e0155756.

Coles, V.J., Brooks, M.T., Hopkins, J., Stukel, M.R., Yager, P.L., and Hood, R.R. (2013) The pathways and properties of the Amazon River Plume in the tropical North Atlantic Ocean. Journal of Geophysical Research: Oceans 118, 6894-6913.

Connolly, R.M., Schlacher, T.A., and Gaston†, T.F. (2009) Stable isotope evidence for trophic subsidy of coastal benthic fisheries by river discharge plumes off small estuaries. Marine Biology Research 5(2), 164-171.

Dai, A.G. (2012) Increasing drought under global warming in observations and models. Nature Climate Change 3(1), 52-58.

Devenon, J.L., Broche, P., de Maistre, J.C., Forget, P., Gaggelli, J., and Rougier, G. (1992) VHF radar measurements in the Rhone river plume. Water Pollution Research reports 28, 75-87.

Devlin, M.J., Petus, C., da Silva, E., Tracey, D., Wolff, N.H., Waterhouse, J., and Brodie, J. (2015) Water Quality and River Plume Monitoring in the Great Barrier Reef: An Overview of Methods Based on Ocean Colour Satellite Data. Remote Sensing 7(10), 12909-12941.

Doubell, M.J., Spencer, D., van Ruth, P.D., Lemckert, C., and Middleton, J.F. (2018) Observations of vertical turbulent nitrate flux during summer in the Great Australian Bight. Deep Sea Research Part II: Topical Studies in Oceanography 157-158, 27-35.

Dowidar, N.M. (1984) Phytoplankton biomass and primary productivity of the south-eastern Mediterranean. Deep Sea Research Part A. Oceanographic Research Papers 31(6), 983-1000.

Drinkwater, K.F., and Frank, K.T. (1994) Effects of river regulation and diversion on marine fish and invertebrates. Aquatic Conservation: Marine and Freshwater Ecosystems 4, 134-151.

Elias, E.P.L., Gelfenbaum, G., and Van der Westhuysen, A.J. (2012) Validation of a coupled wave-flow model in a high-energy setting: The mouth of the Columbia River. Journal of Geophysical Research: Oceans 117(C9).

Estournel, C., Broche, P., Marsaleix, P., Devenon, J.L., Auclair, F., and Vehil, R. (2001) The Rhone River Plume in Unsteady Conditions: Numerical and Experimental Results. Estuarine, Coastal and Shelf Science 53(1), 25-38.

Fennel, K., and Laurent, A. (2018) N and P as ultimate and proximate limiting nutrients in the northern Gulf of Mexico: implications for hypoxia reduction strategies. Biogeosciences 15(10), 3121-3131.

Forget, P., Devenon, J.L., De Maistre, J.C., Broche, P., and Leveau, M. (1990) VHF remote sensing for mapping river plume circulation. Geophysical Research Letters 17(8), 1097-1100.

Fuentes-Yaco, C., Vézina, A.F., Larouche, P., Vigneau, C., Gosselin, M., and Levasseur, M. (1997) Phytoplankton pigment in the Gulf of St. Lawrence, Canada, as determined by the Coastal Zone Color Scanner—Part I: spatio-temporal variability. Continental Shelf Research 17(12), 1421-1439.

Gan, J., Lu, Z., Dai, M., Cheung, A.Y.Y., Liu, H., and Harrison, P. (2010) Biological response to intensified upwelling and to a river plume in the northeastern South China Sea: A modeling study. Journal of Geophysical Research: Oceans 115(C9).

Gillanders, B.M., and Kingsford, M.J. (2002) Impact of changes in flow of freshwater on estuarine and open coastal habitats and the associated organisms. Oceanography and Marine Biology 40, 233-309.

Gomes, H.d.R., Xu, Q., Ishizaka, J., Carpenter, E.J., Yager, P.L., and Goes, J.I. (2018) The Influence of Riverine Nutrients in Niche Partitioning of Phytoplankton Communities–A Contrast Between the Amazon River Plume and the Changjiang (Yangtze) River Diluted Water of the East China Sea. Frontiers in Marine Science 5(343). [In English]

Grimes, C.B. (2001) Fishery Production and the Mississippi River Discharge. Fisheries 26(8), 17-26.

Grimes, C.B., and Kingsford, M.J. (1996) How do riverine plumes of different sizes influence fish larvae: do they enhance recruitment? Marine and Freshwater Research 47, 191-208.

Hopkins, J., Lucas, M., Dufau, C., Sutton, M., Stum, J., Lauret, O., and Channelliere, C. (2013) Detection and variability of the Congo River plume from satellite derived sea surface temperature, salinity, ocean colour and sea level. Remote Sensing of Environment 139, 365-385.

Hu, C.E., Montgomery, E.T., Schmitt, R.W., and Muller-Karger, F.E. (2004) The dispersal of the Amazon and Orinoco River water in the tropical Atlantic and Caribbean Sea: Observation from space and S-PALACW floats. Deep Sea Research Part II: Topical Studies in Oceanography 51(10-11), 1151-1171.

IOCCG (2000) Remote Sening of Ocean Colour in Coastal and other Optically-Complex Waters. IOCCG, Dartmouth, Canada.

Jay, D.A., Zaron, E.D., and Pan, J. (2010) Initial expansion of the Columbia River tidal plume: Theory and remote sensing observations. Journal of Geophysical Research: Oceans 115(C2), n/a-n/a.

Jickells, T.D., Buitenhuis, E., Altieri, K., Baker, A.R., Capone, D., Duce, R.A., Dentener, F., Fennel, K., Kanakidou, M., LaRoche, J., Lee, K., Liss, P., Middelburg, J.J., Moore, J.K., Okin, G., Oschlies, A., Sarin, M., Seitzinger, S., Sharples, J., Singh, A., Suntharalingam, P., Uematsu, M., and Zamora, L.M. (2017) A reevaluation of the magnitude and impacts of anthropogenic atmospheric nitrogen inputs on the ocean. Global Biogeochemical Cycles 31(2), 289-305.

Kim, H.-C., Yamaguchi, H., Yoo, S., Zhu, J., Okamura, K., Kiyomoto, Y., Tanaka, K., Kim, S.-W., Park, T., Oh, I.S., and Ishizaka, J. (2009) Distribution of Changjiang Diluted Water detected by satellite chlorophyll-a and its interannual variation during 1998–2007. Journal of Oceanography 65(1), 129-135.

Lee, E., Livino, A., Han, S.-C., Zhang, K., Briscoe, J., Kelman, J., and Moorcroft, P. (2018) Land cover change explains the increasing discharge of the Paraná River. Regional Environmental Change 18(6), 1871-1881.

Lentz, S.J., and Limeburner, R. (1995) The Amazon River Plume during AMASSEDS: Spatial characteristics and salinity variability. Journal of Geophysical Research: Oceans 100(C2), 2355-2375.

Lindall, W.N., Jr., and Saloman, C.H. (1977) Alterations and destruction of estuaries affecting fishery resources of the Gulf of Mexico. Marine Fisheries Review 39(9), 1-7.

Lohrenz, S.E., Redalje, D.G., Cai, W.-J., Acker, J., and Dagg, M. (2008) A retrospective analysis of nutrients and phytoplankton productivity in the Mississippi River plume. Continental Shelf Research 28(12), 1466-1475.

Lu, Z., Gan, J., Dai, M., Zhao, X., and Hui, C.R. (2020) Nutrient transport and dynamics in the South China Sea: A modeling study. Progress in Oceanography 183, 102308.

Macias, D., Garcia-Gorriz, E., and Stips, A. (2018) Deep winter convection and phytoplankton dynamics in the NW Mediterranean Sea under present climate and future (horizon 2030) scenarios. Scientific Reports 8(1), 6626.

Malagó, A., Bouraoui, F., Grizzetti, B., and De Roo, A. (2019) Modelling nutrient fluxes into the Mediterranean Sea. Journal of Hydrology: Regional Studies 22, 100592.

Matsumoto, S., Yamamoto, T., Kawabe, R., Ohshimo, S., and Yoda, K. (2016) The Changjiang River discharge affects the distribution of foraging seabirds. Marine Ecology Progress Series 555, 273-277.

McClatchie, S., Middleton, J.F., and Ward, T.M. (2006) Water mass analysis and alongshore variation in upwelling intensity in the eastern Great Australian Bight. Journal of Geophysical Research: Oceans 111(C8).

Mena, C., Reglero, P., Hidalgo, M., Sintes, E., Santiago, R., Martín, M., Moyà, G., and Balbín, R. (2019) Phytoplankton Community Structure Is Driven by Stratification in the Oligotrophic Mediterranean Sea. Frontiers in Microbiology 10(1698). [In English]

Mickle, P.F., Herbig, J.L., Somerset, C.R., Chudzik, B.T., Lucas, K.L., and Fleming, M.E. (2018) Effects of Annual Droughts on Fish Communities in Mississippi Sound Estuaries. Estuaries and Coasts 41(5), 1475-1485.

Motoda, S., Kawamura, T., and Taniguchi, A. (1978) Differences in productivities between the Great Australian Bight and the Gulf of Carpentaria. Marine Biology 46, 93-99.

Muller-Karger, F.E., Mcclain, C.R., and Richardson, P.L. (1998) The dispersal of the Amazon's water. Nature 333, 56-59.

Nixon, S.W. (2003) Replacing the Nile: Are anthropogenic nutrients providing the fertility once brought to the Mediterranean by a great river? Ambio 32(1), 30-39.

Nowlin, W.D.J., Jochens, A.E., Reid, R.O., and DiMarco, S.F. (1998) Texas-Lousisiana shelf circulation and transport process study: Synthesis report. New Orleans, Louisiana.

Philander, S.G.H., and Pacanowski, R.C. (1986) The mass and heat budget in a model of the tropical Atlantic Ocean. Journal of Geophysical Research: Oceans 91(C12), 14212-14220.

Phillips, E.M., Horne, J.K., and Zamon, J.E. (2017) Predator-prey interactions influenced by a dynamic river plume. Canadian Journal of Fisheries and Aquatic Sciences 74, 1375-1390.

Piroddi, C., Coll, M., Liquete, C., Macias, D., Greer, K., Buszowski, J., Steenbeek, J., Danovaro, R., and Christensen, V. (2017) Historical changes of the Mediterranean Sea ecosystem: modelling the role and impact of primary productivity and fisheries changes over time. Scientific Reports 7(1), 44491.

Rabalais, N.N., Turner, R.E., Dortch, Q., Justic, D., Bierman, V.J., and Wiseman, W.J. (2002) Nutrient-enhanced productivity in the northern Gulf of Mexico: past, present and future. In Nutrients and Eutrophication in Estuaries and Coastal Waters: Proceedings of the 31st Symposium of the Estuarine and Coastal Sciences Association (ECSA), held in Bilbao, Spain, 3–7 July 2000. (Eds. E Orive, M Elliott and VN de Jonge) pp. 39-63. (Springer Netherlands: Dordrecht)

Rakocinski, C.F., Lyczkowski-Shultz, J., and Richardson, S.L. (1996) Ichthyoplankton assemblage structure in Mississippi Sound as revealed by canonical correspondence analysis. Estuarine, Coastal and Shelf Science 43(2), 237-257.

Richardson, P.L., Hufford, G.E., Limeburner, R., and Brown, W.S. (1994) North Brazil Current retroflection eddies. Journal of Geophysical Research: Oceans 99(C3), 5081-5093.

Ritter, W.F., and Chitikela, S.R. (2020) The Mississippi River Basin Nitrogen Problem: Past History and Future Challenges to Solve It. In Watershed Management 2020. pp. 109-123.

Salen-Picard, C., Darnaude, A.M., Arlhac, D., and Harmelin-Vivien, M.L. (2002) Fluctuations of macrobenthic populations: a link between climate-driven river run-off and sole fishery yields in the Gulf of Lions. Oecologia 133, 380-388.

Savenkoff, C., Vézina, A.F., Smith, P.C., and Han, G. (2001) Summer Transports of Nutrients in the Gulf of St. Lawrence Estimated by Inverse Modelling. Estuarine, Coastal and Shelf Science 52(5), 565-587.

Scavia, D., Justić, D., Obenour, D.R., Craig, J.K., and Wang, L. (2019) Hypoxic volume is more responsive than hypoxic area to nutrient load reductions in the northern Gulf of Mexico—and it matters to fish and fisheries. Environmental Research Letters 14(2), 024012.

Schlacher, T.A., Skillington, A.J., Connolly, R.M., Robinson, W., and Gaston, T.F. (2008) Coupling between Marine Plankton and Freshwater Flow in the Plumes off a Small Estuary. International Review of Hydrobiology 93(6), 641-658.

Schott, F.A., and Böning, C.W. (1991) The WOCE model in the western equatorial Atlantic: Upper layer circulation. Journal of Geophysical Research: Oceans 96(C4), 6993-7004.

Sharaf El Din, S.H. (1977) Effect of the Aswan High Dam on the Nile flood and on the estuarine and coastal circulation pattern along the Mediterranean coast. Limnology and Oceanography 22, 194-207.

Swieca, K., Sponaugle, S., Briseño-Avena, C., Schmid, M.S., Brodeur, R.D., and Cowen, R.K. (2020) Changing with the tides: fine-scale larval fish prey availability and predation pressure near a tidally modulated river plume. Marine Ecology Progress Series 650, 217-238.

Tanhua, T., Hainbucher, D., Schroeder, K., Cardin, V., Álvarez, M., and Civitarese, G. (2013) The Mediterranean Sea system: a review and an introduction to the special issue. Ocean Sci. 9(5), 789-803.

Urrego-Blanco, J., and Sheng, J. (2014) Formation and distribution of sea ice in the Gulf of St. Lawrence: A process-oriented study using a coupled ocean-ice model. Journal of Geophysical Research: Oceans 119(10), 7099-7122.

van Ruth, P.D., Patten, N.L., Doubell, M.J., Chapman, P., Rodriguez, A.R., and Middleton, J.F. (2018) Seasonal- and event-scale variations in upwelling, enrichment and primary productivity in the eastern Great Australian Bight. Deep Sea Research Part II: Topical Studies in Oceanography 157-158, 36-45.

Walker, N.D. (1996) Satellite assessment of Mississippi River plume variability: Causes and predictability. Remote Sensing of Environment 58(1), 21-35.

Walker, N.D., and Rabalais, N.N. (2006) Relationships among satellite chlorophylla, river inputs, and hypoxia on the Louisiana Continental shelf, Gulf of Mexico. Estuaries and Coasts 29(6), 1081-1093.

Ware, D.M., and Thomson, R.E. (2005) Bottom-up ecosystem trophic dynamics determine fish production in the northeast Pacific. Science 308(5726), 1280-1284.

Weber, S.C., Carpenter, E.J., Coles, V.J., Yager, P.L., Goes, J., and Montoya, J.P. (2017) Amazon River influence on nitrogen fixation and export production in the western tropical North Atlantic. Limnology and Oceanography 62(2), 618-631.

Wiseman, W.J., Rabalais, N.N., Dagg, M.J., and Whitledge, T.E. (1999) Nutrient enhanced coastal ocean productivity in the northern Gulf of Mexico : understanding the effects of nutrients on a coastal ecosystem.

Yuan, J., Miller, R.L., Powell, R.T., and Dagg, M.J. (2004) Storm-induced injection of the Mississippi River plume into the open Gulf of Mexico. Geophysical Research Letters 31(9).

Appendix B

B.1 Additional river discharge station information

Table B.1:Distances of river discharge measuring stations to coastal ocean.

River name	Station(s)	Ocean	Approx. distance of station(s) from coastline in direct line (km)
Amazon	Óbidos	Atlantic	660
Niger	Lokoja	Atlantic	400
Mississippi	Vicksburg	Gulf of Mexico	390
Rhone	Chancy, Aux Ripes	Mediterranean	320
Parana	Timbues	Atlantic	257
Columbia	Dallas	Pacific	195
Mekong	Sum of discharge at Can Tho & MyThuan	South China Sea	83 (from Can Tho) 45 (My Thuan)
Pearl	Bogalusa	Gulf of Mexico	73
Thames	Kingston	North Sea	50
St Lawrence	Cornwall	Atlantic	3
Murray	Sum of discharge over barrages	Southern	3

B.2 Residual analyses

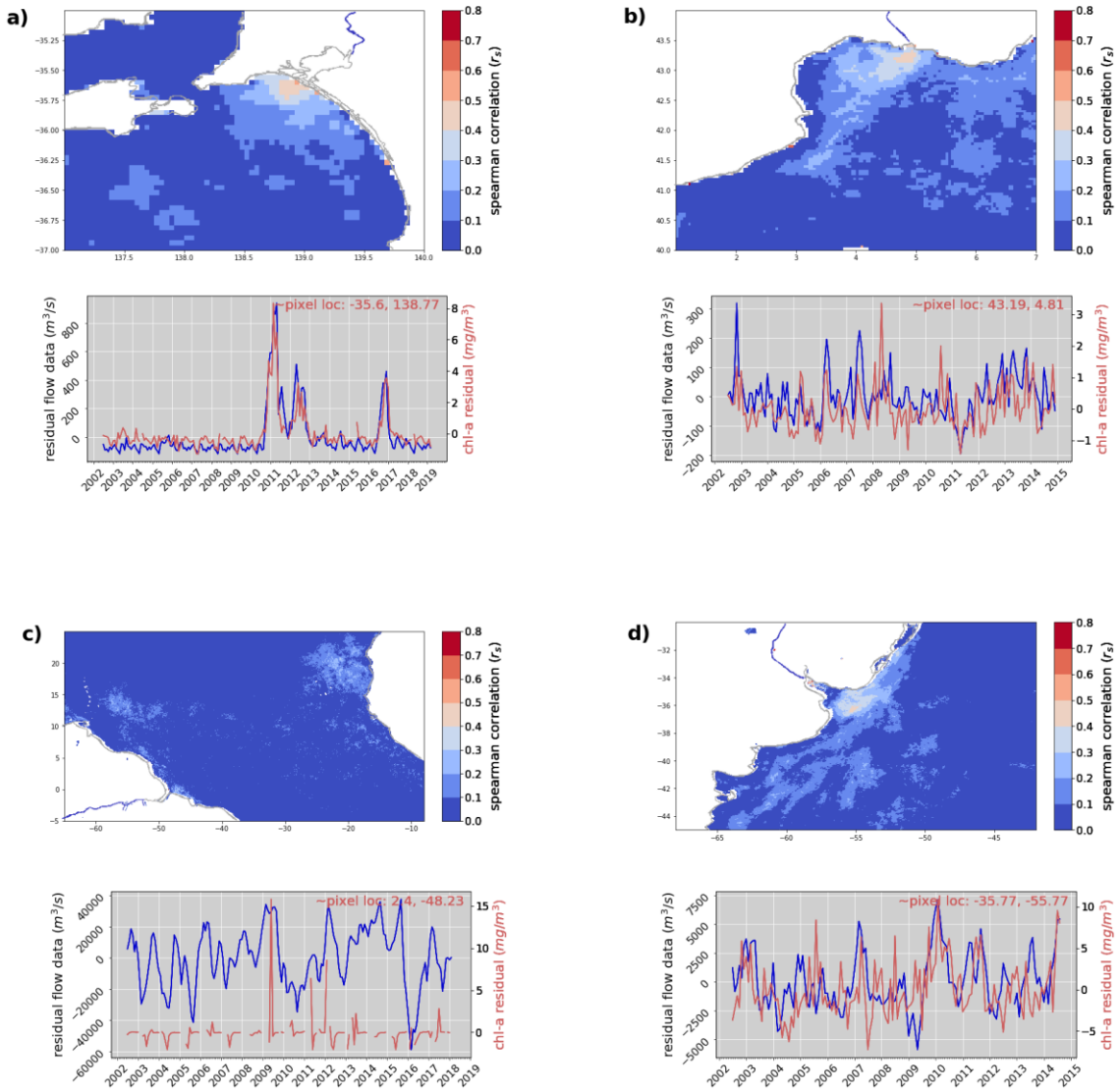

FigureB.2.1: Maps of river discharge influence based on Spearman correlation analysis on remotely sensed MODIS chl-*a* concentrations and corresponding river flow time series and chl-*a* concentrations at pixel (with location on top right of time series plot) for the a) Murray River on the coastal waters in the Southern Ocean of South Australia, b) Rhone River in the Gulf of Lion, France, c) Amazon River on the mid-Atlantic Ocean and along the South American north eastern coast and d) the Parana river on the Southern Atlantic Ocean.

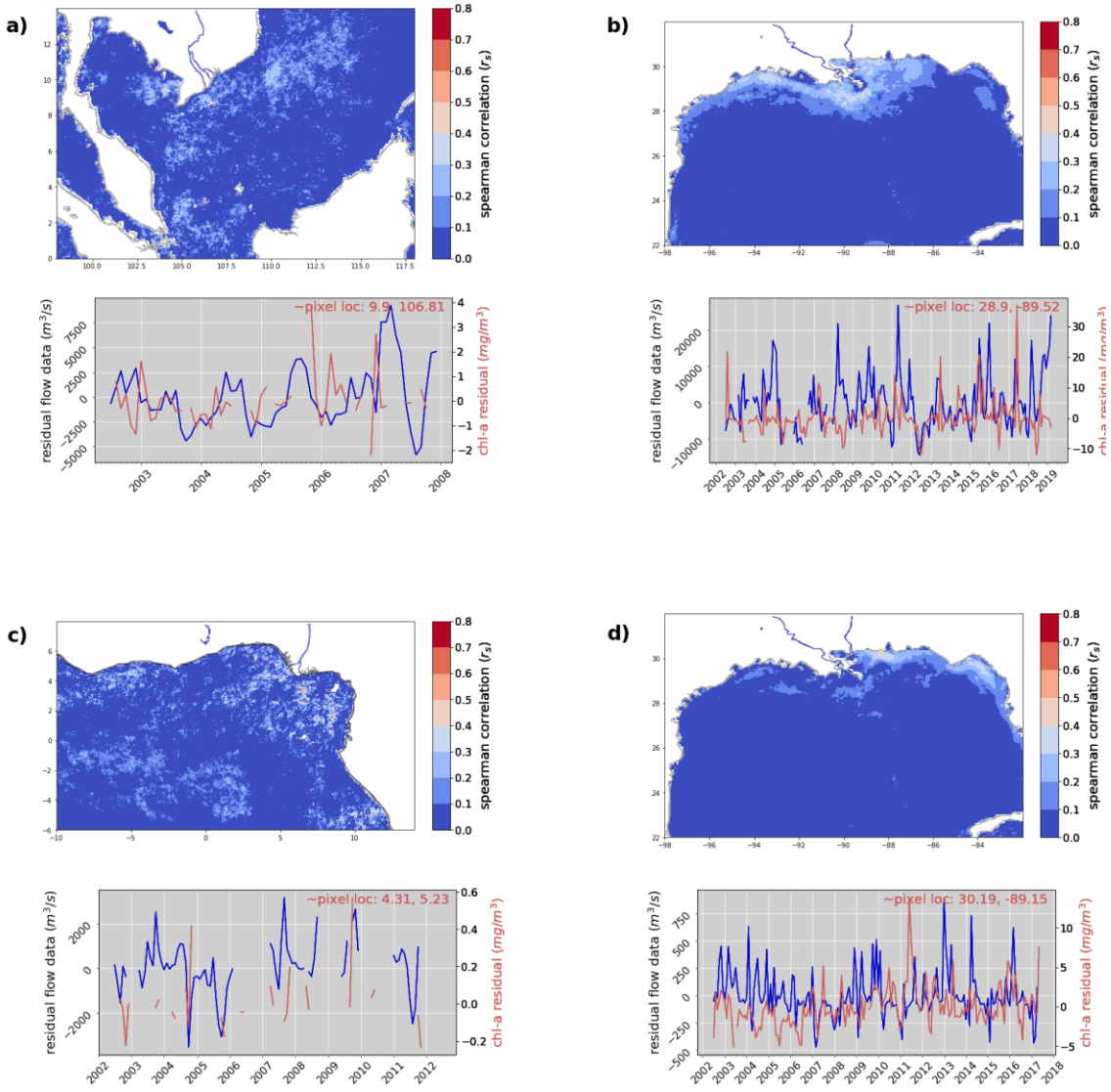

Figure B.2.2: Maps of river discharge influence based on Spearman correlation analysis on remotely sensed MODIS chl-*a* concentrations and corresponding river flow time series and chl-*a* concentrations at pixel (with location on top right of time series plot) for the a) Mekong River on the South China Sea, b) Mississippi River on the northern Gulf of Mexico, c) Niger River on the coastal waters in the Gulf of Guinea and d) Pearl River in the Gulf of Mexico.

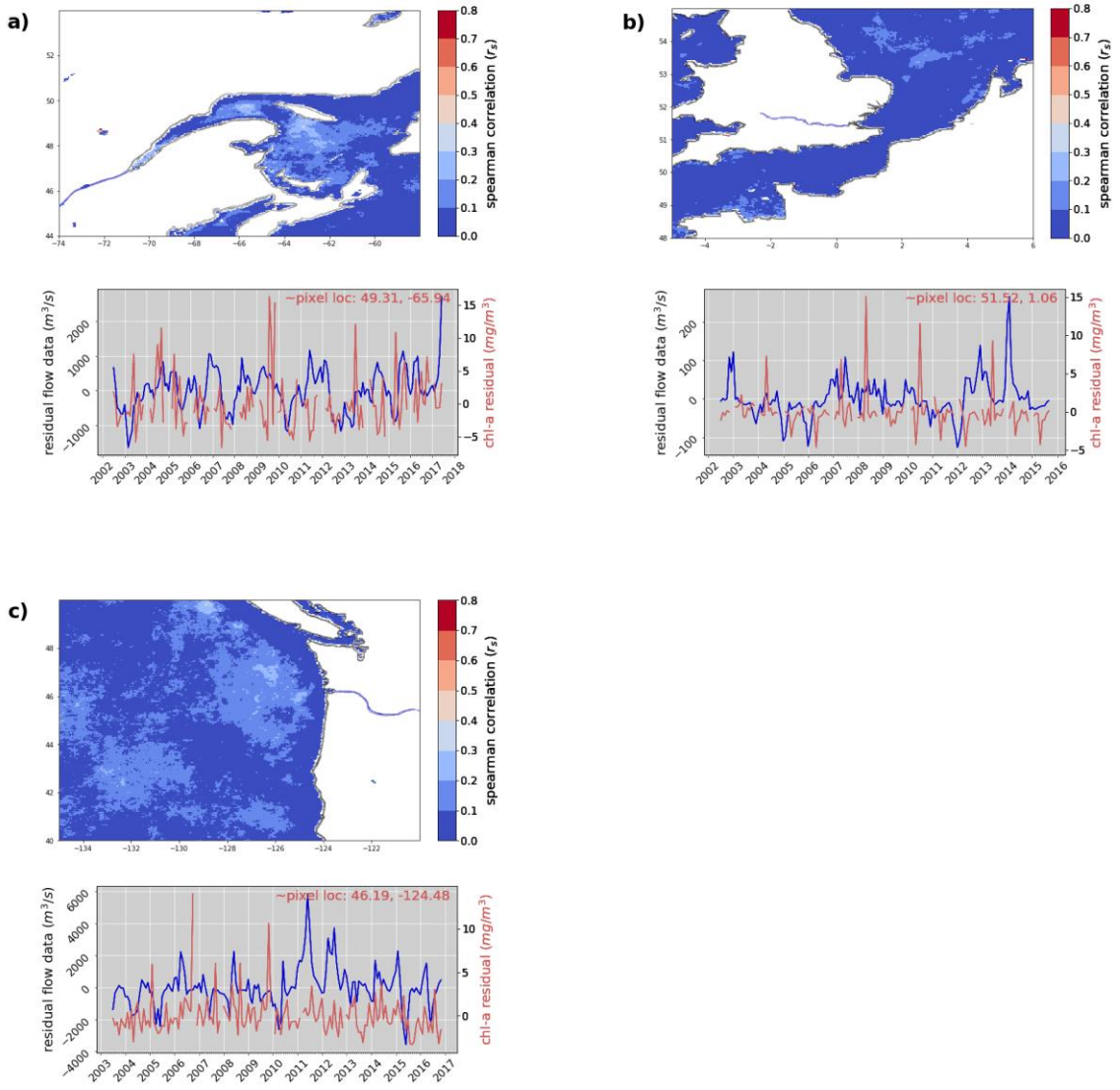

Figure B.2.3: Maps of river discharge influence based on Spearman correlation analysis on remotely sensed MODIS chl-*a* concentrations and corresponding river flow time series and chl-*a* concentrations at pixel (with location on top right of time series plot) for the a) St Lawrence River on the Gulf of St Lawrence, b) Thames River on the English Channel and North Sea and c) Columbia River on the Pacific Ocean.

B.3 Chl-*a* observation maps

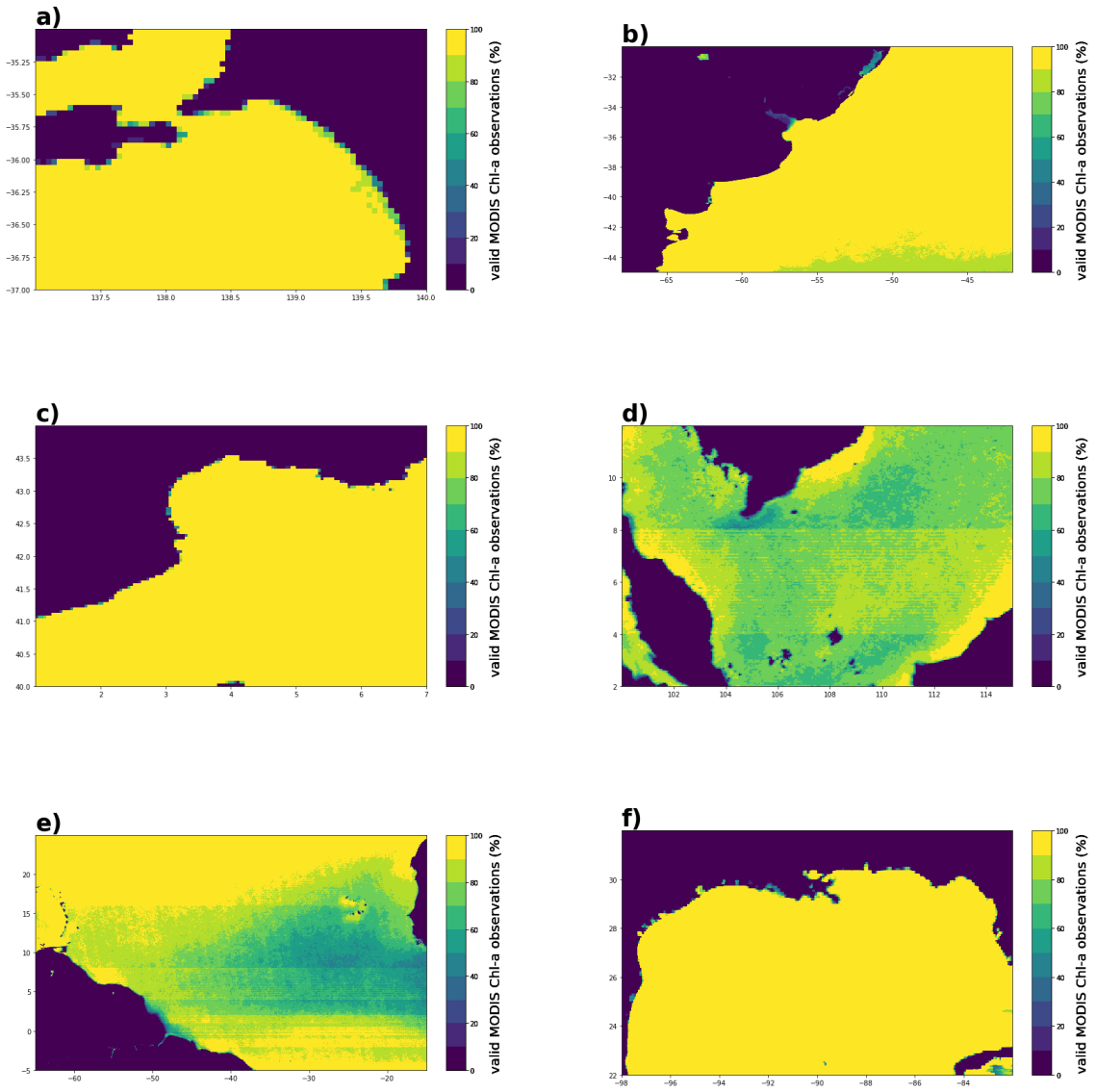

Figure B.3.1: Proportion of chl-*a* observations per pixel used for spatiotemporal correlation analysis between river discharge and chl-*a* for a) Murray River on the coastal waters in the Southern Ocean of South Australia, b) Parana river on the Southern Atlantic Ocean, c) Rhone River in the Gulf of Lion, France, d) Mekong River on the South China Sea, e) Amazon River on the mid-Atlantic Ocean and along the South American north eastern coast, f) Mississippi River on the northern Gulf of Mexico. The maximum number of analysed dates and the record lengths of river flow data available for comparison to chl-*a* can be found in Table 3.1.

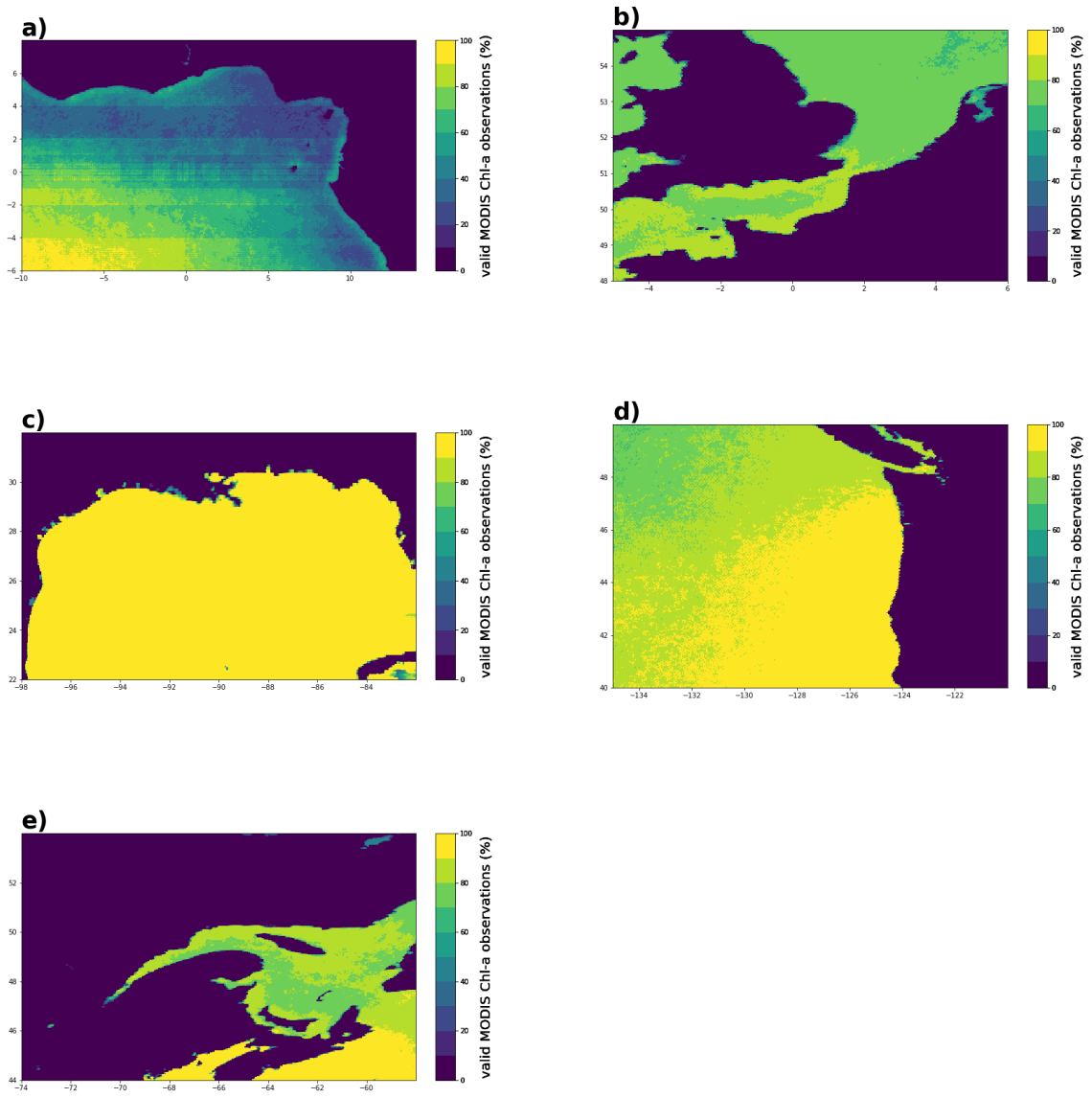

Figure B.3.2: Proportion of chl-*a* observations per pixel used for spatiotemporal correlation analysis between river discharge and chl-*a* for a) Niger River on the coastal waters in the Gulf of Guinea, b) Thames River on the English Channel and North Sea, c) Pearl River in the Gulf of Mexico d), Columbia River on the Pacific Ocean, e) St Lawrence River on the Gulf of St Lawrence. The maximum number of analysed dates and the record lengths of river flow data available for comparison to chl-*a* can be found in Table 3.1.

Chapter 4

Changing influence of river discharge on coastal ocean chlorophyll-*a* and turbidity.

Statement of Authorship

Title of Paper	Changing influence of river discharge on coastal ocean chlorophyll-a and turbidity.	
Publication Status	☐Published ☐Submitted for Publication	☐Accepted for Publication ☒Unpublished and Unsubmitted work written in manuscript style
Publication Details	n/a	

Principal Author

Name of Principal Author (Candidate)	Hannah Auricht	
Contribution to the paper	Conceptualization, methodology, data curation, formal analysis, writing – original draft preparation, writing – review and editing.	
Overall percentage (%)	70%	
Signature		Date: 21/11/2022

Co-author Contributions

By signing the Statement of Authorship, each author certifies that:

i. the candidate's stated contribution to the publication is accurate (as detailed above);

ii. permission is granted for the candidate in include the publication in the thesis; and

iii. the sum of all co-author contributions is equal to 100% less the candidate's stated contribution.

Name of Co-Author	Kenneth Clarke	
Contribution to the Paper	Methodology, formal analysis, writing – review and editing.	
Signature		Date: 28/Nov/2022

Name of Co-Author	Luke Mosley	
Contribution to the Paper	Methodology, formal analysis, writing – review and editing.	
Signature		Date: 2 Dec 2022

Name of Co-Author	Megan Lewis	
Contribution to the Paper	Methodology, formal analysis, writing – review and editing.	
Signature		Date: 30 Nov 2022

Abstract

River systems and coastal ocean systems are often studied as separate entities, but river discharge can have profound influence on coastal water quality and coastal marine systems. While changes in river discharge are known in some cases, it is unclear whether the influence on coastal waters may be changing over time (e.g. due to climate or land use changes and increased river extractions). The aim of this paper is to detect trends in river discharge and coastal water quality parameters, and infer whether the influence of river discharge on coastal waters may be changing. MODIS Aqua chlorophyll-*a* (a proxy for phytoplankton biomass), MODIS Aqua remote sensing reflectance centred at 645 nm (an indicator of turbidity) and up to ~17 years of river flow/discharge time series data for six large global river systems (Murray, Amazon, Rhone, Mississippi, Parana and Mekong) were used to investigate this question. Hamed and Rao's modified Mann Kendall trend test was used to investigate change in river discharge, chl-*a* and turbidity over the study period. This was achieved by querying pre-defined regions of river discharge influence (RoRI) in coastal oceans off the river mouths. The Murray and Mississippi rivers showed increasing trends in coastal ocean chl-*a* concentrations. A decreasing trend in turbidity was apparent within the Amazon RoRI from 2002. Other rivers (Parana, Mekong and Rhone) showed no significant trends in discharge, chl-*a* or turbidity. These findings may be limited by the temporal coverage of MODIS satellite chl-*a* and turbidity products, with records beginning in 2002. As global water scarcity increases, and river flows become more modified by both anthropogenic and climatic factors, monitoring and management will become increasingly important to ensure maintenance of ecosystem function.

4.1 Introduction

Changes in river discharge to the ocean have been described as "comprehensive manifestations of climate change and human activities" (Shi *et al.* 2019). This is due to the effects of global climate change, modification of water courses via damming and extraction of river waters for anthropogenic use, causing significant changes in volume, timing and concentration of discharge to the ocean. Land-use changes and hydrological system alterations (e.g. damming) affect the concentrations of dissolved and undissolved nutrients, sediments, pollutants and other materials reaching the oceans via rivers (Ajani *et al.* 2018; Auricht *et al.* 2018; Axler 2019; Chai *et al.* 2009; Masotti *et al.* 2018; Yunev *et al.* 2007). Therefore, changes in river discharge have consequences for coastal water quality and marine ecosystems. For example, the Mississippi, Nile and Yangtze Rivers have all experienced changes in the concentrations of constituents (e.g. nitrogen, phosphorus and sediments) in freshwater discharge over the last century, causing further changes in water quality and productivity of receiving coastal waters (Ajani *et al.* 2018; Axler 2019). In some cases, these changes have affected the yields of regional fisheries. It is therefore clear that a strong influence and relationship is present between river discharge and coastal water quality, but that it is poorly understood, especially over broad spatial and temporal scales. It is also unclear whether that relationship is changing under these complex stressors.

The body of research which has investigated trends in river flow and trends in volume of river discharge to oceans has usually been focused on local or national scales (e.g. Chalise *et al.* (2021); Germolus *et al.* (2021); Goesch *et al.* (2020); Srinivas *et al.* (2020)). Some global scale studies have also found that the majority of the world's rivers have declining flow trends or decreasing volumes of river discharge reaching the oceans, with the exception of the Arctic, where ice melt and warming increases discharge (Biemans *et al.* 2011; Gill *et al.* 2015; Grill *et al.* 2019; Milly *et al.* 2005; Seitzinger *et al.* 2010; Su *et al.* 2018). This knowledge is critical for global water management due to human reliance on freshwater as a limited resource and transboundary issues.

However, studied far less often and usually at very fine scales, is the more specific influence of river discharges on coastal ocean productivity, turbidity or general water quality. Put simply, there is limited understanding or knowledge of what happens once river discharge reaches ocean waters, and even less in circumstances where it doesn't (i.e. due to drought, damming, water diversion for agriculture, or other effects).

At present and in most regions, it is unclear whether changes in river discharge volume and concentration have also caused changes in coastal water quality. This is in part due to limited data on river flow and discharge rates. In some cases, for remote locations or where transboundary water management is contentious, this data is unavailable to the public. Data on the concentrations of nutrients, sediments or other materials which freshwater carries to the sea, let alone that of coastal ocean waters, is even more scarce. To then determine the relationship between river discharge and coastal water quality is a great challenge. Fortunately, remote sensing technology enables coastal water quality monitoring at a range of spatial and temporal scales, under various flow conditions.

Previous research has taken advantage of optical remote sensing products to estimate the concentration, direction and risk which river plumes may have on marine environments (Constantin *et al.* 2018; Devlin *et al.* 2015; Fabricius *et al.* 2016; Fernandez-Novoa *et al.* 2017; Hopkins *et al.* 2013; Petus *et al.* 2014). However, most river discharge and river plume studies which use remote sensing techniques have aimed to determine the density or direction of river plumes over days or months instead of years. These studies are usually conducted under higher flow conditions rather than under a variety of flow conditions. For example, Fernández-Nóvoa *et al.* (2019) characterised four Cantabrian river plumes between 2003 and 2014, but did not investigate change in relative influence of river discharge on coastal water quality or productivity. Similarly, a study of several Borneo rivers used both *in situ* and remote sensing techniques to determine the direction and concentrations of river plumes off the coast. This research benefited local river and coastal monitoring and management sectors in the region (Cherukuru *et al.* 2021). If conducted at broader spatial and

temporal scales, this information could shed light on the long-term implications of river flow management on coastal water quality and whether influence of river discharge on coastal ocean water quality is changing over time

In this chapter, I aim to apply the new method of Auricht *et al.* (2022) (Chapter 3 herein) to determine whether the influence of river discharge on coastal chl-*a* and turbidity has changed over time in several global river systems. Regions of river discharge influence (RoRI) are defined per river. From each of these RoRI, chl-*a* concentrations and turbidity estimates over the entire MODIS temporal record are extracted. A modified Mann-Kendall trend test is then applied to these data and is used to identify changes in these variables over time. This allows qualitative assessment of whether chl-*a* concentrations and relative turbidity are changing in these coastal waters, relative to river discharge. I hypothesise that a declining trend in river discharge will correspond to declining trends in chl-*a* and turbidity in each river's RoRI. There is a clear need to understand the impact of climate and anthropogenic effects on river and coastal systems and ultimately human populations. Monitoring river discharge and coastal water quality for change across various spatial and temporal scales is therefore required.

4.2 Methods

4.2.1 River discharge data and regions of river discharge influence (RoRIs)

Six rivers and adjacent coastal ocean regions are studied in this chapter. Using the spatiotemporal correlation analysis results from Auricht *et al.* (2022) (Chapter 3 herein), I investigated coastal regions where positive and significant Spearman rank correlations (>= 0.3 r_s, p <= 0.01) were found between river discharge and coastal chl-*a*. These regions of river discharge influence are henceforth referred to as RoRI. The RoRIs studied here are the Murray, Mekong, Rhone, Amazon, Parana and Mississippi as these rivers showed stronger and more defined areas or regions of river discharge influence. These rivers represent a diversity of climates and environments (Chapter 3, Figure 3.1).

The majority of river discharge data was obtained from the Global Runoff Data Centre (access via https://www.bafg.de/GRDC/) at monthly temporal resolution. The record length varied by river and while some river discharge data is distributed at monthly temporal resolution by some sources (e.g. the GRDC), it was calculated from daily flow data for others (e.g. the Amazon). These data should be placed in the context of the locations of the river discharge recording stations (see Chapter 3 Figure 3.1).

4.2.2 MODIS ocean colour products

4.2.2.1 Chlorophyll-a

NASA's Moderate Resolution Imaging Spectroradiometer (MODIS) sensor, on board the sun-synchronous, polar-orbiting satellite Aqua, became operational in 2002 and is still operational today. Monthly composite Level 3 MODIS ocean colour chlorophyll-*a* products (estimates produced by the OC3M algorithm, see Hu *et al.* (2012); O'Reilly *et al.* (1998)) were obtained at 4 km spatial resolution and spanning July 2002 to Dec 2019. These products (access via https://oceancolor.gsfc.nasa.gov/) are produced by the Ocean Biology Processing Group (OBPG) at NASA's Goddard Space Flight Centre and are a proxy for phytoplankton biomass in the water column (mg m^{-3}), widely used to indicate productivity of coastal waters (Davies *et al.* 2018; Dring and Dring 1992).

4.2.2.2 Turbidity

Ocean chlorophyll-*a* estimates can be overestimated in coastal waters, especially those where turbidity and suspended sediment concentrations are high (such as in river plumes, shallow estuaries and coastal regions where sediments can be re-suspended). Therefore, a measure of turbidity or suspended matter in the water column is used in this Chapter to contextualise findings. Remote sensing reflectance centred at 645 nm (Rrs645) is used to indicate relative turbidity due to river discharge and coastal (wave and tidal) energy in each RoRI. Remote sensing reflectance is the at-surface spectral remote-sensing reflectance observed by the satellite instrument after atmospheric correction (OBPG 2022). Atmospheric correction reduces the impact of contamination of readings due to nearby land, atmospheric interferences and other factors. The MODIS Rrs645 product has been described as an "excellent indicator" of turbidity and suspended sediment and has been used in several previous studies with good results (Aurin *et al.* 2013; Babin *et al.* 2012; Dogliotti *et al.* 2015; Kirk 1994; Miller and McKee 2004; Wang *et al.* 2009). Several previous studies (e.g. Fernández-Nóvoa *et al.* (2015); Hamidi *et al.* (2017); McCarthy *et al.* (2018)) have determined linear relationships between this MODIS band and turbidity in coastal waters. Many of these studies have commented that absorption features due to coloured dissolved organic matter (CDOM) and phytoplankton can impact reflectance measurements in this band, leading to underestimations of turbidity (Babin et al. 2012; Dogliotti et al. 2015). This makes this band more reliable in lower turbidity waters (where NTU ranges between 0 and 15 NTU). However, Rrs645 has the benefit of a lower water penetration depth than some other water quality products, which reduces interference from shallow seafloor areas and contribution to signals from upwelling and resuspension (Chen *et al.* 2007; Fernandez-Novoa *et al.* 2017). Furthermore, the scope of this study is focussed on interpreting broad scale temporal patterns in coastal ocean turbidity and relationships between this and chl-*a* and river discharge, rather than highly precise measurements of turbidity. Analysis ready 4 km Rrrs645 products (henceforth referred to as 'turbidity'), enable

understanding of the influence of river discharge on coastal water turbidity over the long term.

4.2.3 Extracting time series for trend analysis

Areas where Spearman rank correlation (rs) >= 0.3 between river discharge and chl-a were used to define each river's region of river influence (RoRI) (for correlation methods, refer Chapter 3). The sum of turbidity per pixel was calculated from each monthly composite satellite image and within each river's RoRI, respectively. This was repeated with monthly composite chl-*a* imagery products. These MODIS product chl-*a* and turbidity time-series (refer Figure 4.1) respectively, were then subject to trend analyses in order. Constraining the extraction of time-series data to RoRIs aimed to reduce noise contributing to trend from other (e.g. seasonal) factors.

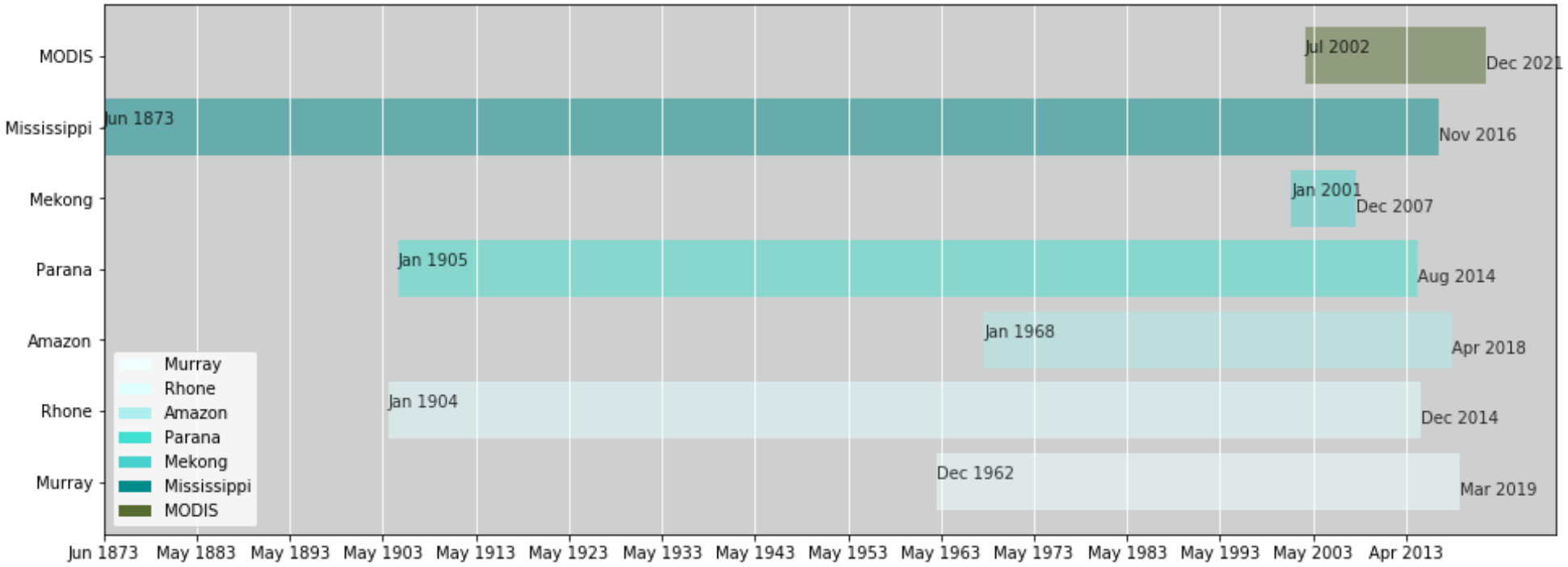

Figure 4.1: Lengths of available historical river discharge data used in this paper compared to MODIS Aqua data product availability.

Table 4.1: Region of river discharge influence (RoRI) for the study rivers where correlation between river discharge and chl-*a* concentration is >= 0.3.

River RoRI	Number of pixels	Approximate area (km^2)
Murray	39	677
Rhone	49	850
Amazon	143,771	2,495,226
Parana	1,078	18,709
Mekong	24,639	427,624
Mississippi	6,085	105,609

4.2.4 Trend tests and overall correlation

The non-parametric Mann-Kendall trend test is one of the most commonly used trend tests used in climate and hydrologic time series analysis (Helsel and Hirsch 1992). However, the Hamed and Ramachandra Rao (1998) modified Mann-Kendall test (henceforth, modified MK test) has demonstrated greater accuracy when tested on auto-correlated data (e.g. time series with strong seasonal auto correlation) than the original Mann-Kendall test, with a greater empirical significance level and whilst retaining power (Hamed and Ramachandra Rao 1998). Here I use the modified MK test to determine presence or absence of an upward or downward monotonic trend in; river discharge, extracted time series of chl-*a* concentrations and Rrs645 (turbidity) in coastal RoRIs.

To understand the strength of the relationship between variables, a nonparametric Spearman rank correlation test was also performed between variables' time series extracted from each RoRI. These findings, alongside results of trend analysis and within the context of each river's management and location, the presence or absence of a changing influence of river discharge on coastal water quality.

4.3 Results

A summary of the trend results is shown in Table 4.2. The coastal waters influenced by the Murray and Mississippi Rivers showed increasing trends in chl-*a*. Interestingly, Murray River discharge showed an increasing trend. The Amazon's coastal RORI showed a decreasing turbidity trend, indicating declining turbidity in the coastal waters influenced by Amazon river discharge between 2002 and 2019. No significant monotonic trends were detected in river discharge data for the Rhone, Parana or Mekong rivers, respectively. This is also true of chl-*a* and turbidity time series for each of the same rivers (Table 4.2).

Table 4.2: Trend directions from Hamed and Rao modified Mann-Kendall trend tests on monthly river discharge data, chl-*a* concentrations in coastal areas where Spearman correlation (between river discharge and chl-*a* time series) >= 0.3. Turbidity data was extracted per month within the region of interest (>= 0.3 rho between river discharge and chl-*a* time series).

	Flow	**chl-a**	**Turbidity**	**Record end**
Murray	increasing	increasing	no trend	March 2019
Rhone	no trend	no trend	no trend	December 2014
Amazon	no trend	no trend	decreasing	April 2018
Parana	no trend	no trend	no trend	August 2014
Mekong	no trend	no trend	no trend	December 2007
Mississippi	no trend	increasing	no trend	November 2016

4.3.1 Murray River

The Murray River showed increasing trends in flow and chl-*a* concentrations in coastal waters between July 2002 and March 2019 (Figure 4.2a and b), but no clear trends in turbidity during this period (Figure 4.2c). Peaks in river flow and chl-*a* concentrations occur at approximately the same time (e.g. peaks in river discharge in late 2010, 2011, mid 2012 and late 2016/early 2017 coincide with peaks in chl-*a*) (Figure 4.2a). In addition, the pattern of turbidity appears somewhat synchronised with both river

discharge and chl-*a*. Most of the tallest peaks across the turbidity time series occur in synchrony with peaks in river discharge (November 2010, April –May 2012, June 2016 – Jan 2017) (Figure 4.2b and c). However, at some times, higher turbidity occurs independently of river discharge (e.g. Feb – March 2003, April – May 2015). A seasonal pattern is also present in time series data for both chl-*a* and turbidity (within the Murray RoRI) which was also observed in results of Auricht *et al.* (2018) (Chapter 2 herein). A moderate, positive relationship exists between river discharge and chl-*a* (r_s =0.45) overall, as well as between river discharge and turbidity (r_s = 0.4) while turbidity and chl-*a* in the Murray RoRI are strongly correlated (r_s = 0.78).

4.3.2 Mississippi River

Mississippi River discharge data from Vicksburg station, Mississippi showed no trend, while chl-*a* within the Mississippi RoRI has an increasing trend (Figure 4.3a and b). The modified Mann-Kendall test did not reveal any significant monotonic trend for turbidity (Figure 4.3c). Similarly to the results for the Murray River and correlated coastal waters, peaks in chl-*a* within the northern Gulf of Mexico RoRI coincided with peaks in Mississippi River discharge. Mississippi discharge and chl-*a* in the Mississippi RoRI are strongly correlated overall (Figure 4.3d, r_s = 0.76). Turbidity in this region appears to peak alternately to chl-*a* and river discharge between October and January, on an annual basis. Mississippi River discharge is comparatively more variable but has an annual signal, with high flow rates usually reaching peak flow once per year above 30,000 m^3/s. This usually occurs between April and July, but sometimes occurs earlier. There is weak correlation between turbidity and river discharge (r_s = 0.14) and between chl-*a* and turbidity (r_s = -0.06) (Figure 4.3e and f).

4.3.3 Amazon River

The Amazon River discharge and RoRI chl-*a* concentrations show no clear trends (Figure 4.4a and b). Turbidity, however, showed an overall decreasing trend in the Amazon RoRI. Peaks and troughs in river discharge time series are synchronised with peaks in chl-*a* at this monthly temporal resolution (Figure 4.4c). The highest values of chl-*a* concentration and river discharge in this region sometimes coincide with highs in

turbidity, but the signal of turbidity over time is largely inverse to the other variables. Amazon River discharge and chl-*a* in the very large Amazon RoRI (Figure 4.4g) have a strong, positive correlation overall (r_s = 0.88) but there is effectively no relationship observed between river discharge and turbidity, and between chl-*a* and turbidity in this region (Figure 4.4e and f).

4.3.4 Mekong, Parana and Rhone rivers

The remaining rivers studied in this chapter showed no definitive trends in river discharge, chl-*a* or turbidity within respective RoRIs. However, in some river RoRIs, sum of chl-*a* and sum of turbidity were correlated. For example, correlation between turbidity and chl-*a* was strong (rs = 0.88) in the Mekong RoRI, yet weak between river discharge and turbidity (rs = 0.13). A strong positive correlation between Rhone RoRI chl-*a* and turbidity in the Gulf of Lion (rs = 0.8) was also present. Correlation results for the Parana River RoRI were also positive between turbidity and chl-*a*.

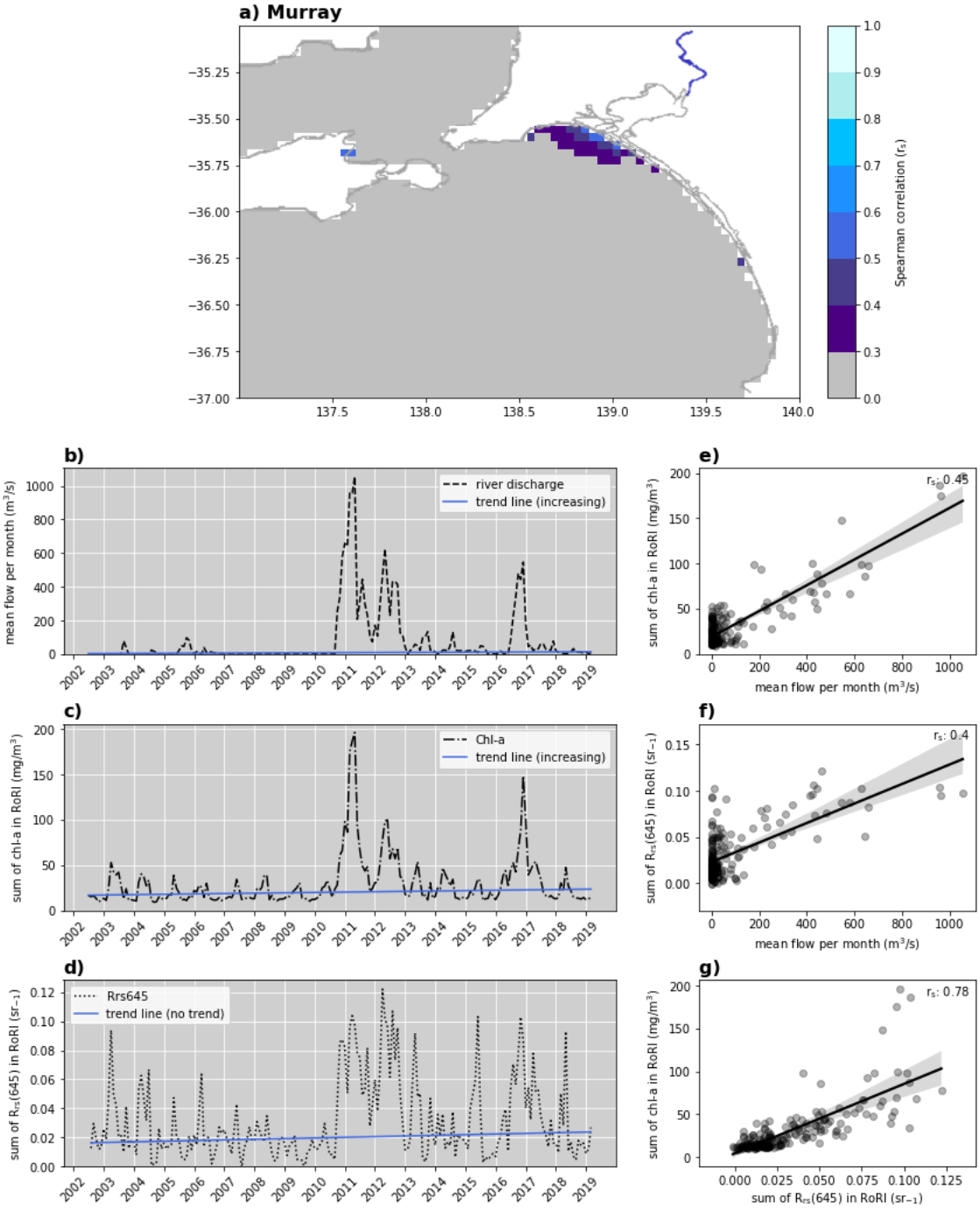

Figure 4.2: The spatial extent of the Murray region of river discharge influence (RoRI), where $r_s > 0.3$ is shown in a). The results of Hamed and Rao modified Mann-Kendall trend tests on b) Murray River discharge, c) sum of chl-*a* concentrations per month within Murray RoRI d) sum of Rrs645 (turbidity) concentrations per month within the Murray RoRI, and Spearman rank correlation (r_s) between e) river discharge and chl-*a*

concentration, f) river discharge and turbidity, and g) turbidity and chl-*a* over the MODIS time period.

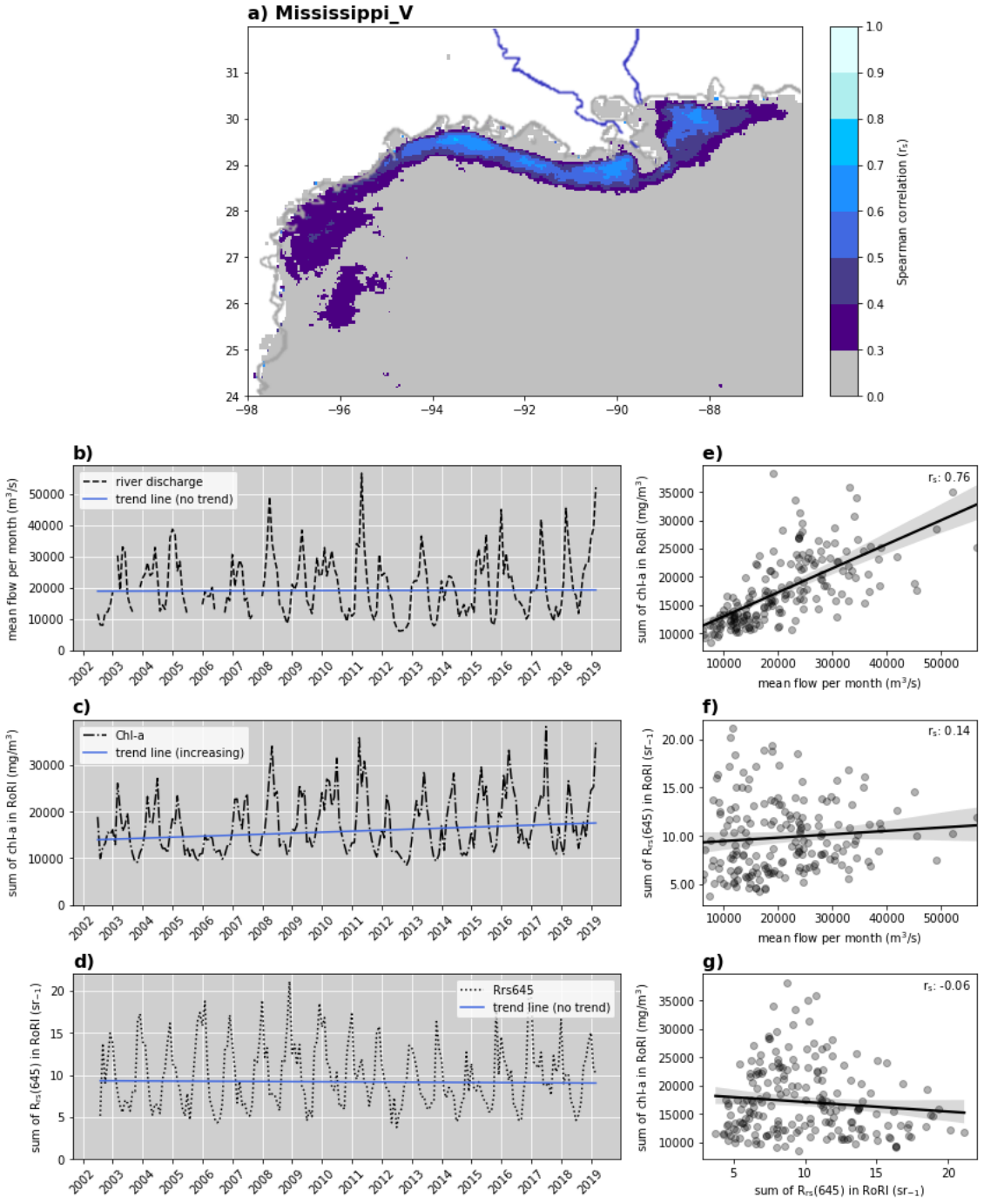

Figure 4.3: The spatial extent of the Mississippi region of river discharge influence (RoRI), where $r_s > 0.3$ is shown in a). The results of Hamed and Rao modified Mann-Kendall trend tests on b) Mississippi River discharge, c) sum of chl-*a* concentrations per month within Mississippi RoRI d) sum of Rrs645 (turbidity) concentrations per month within the Mississippi RoRI, and Spearman rank correlation (r_s) between e) river

discharge and chl-*a* concentration, f) river discharge and turbidity, and g) turbidity and chl-*a* over the MODIS time period.

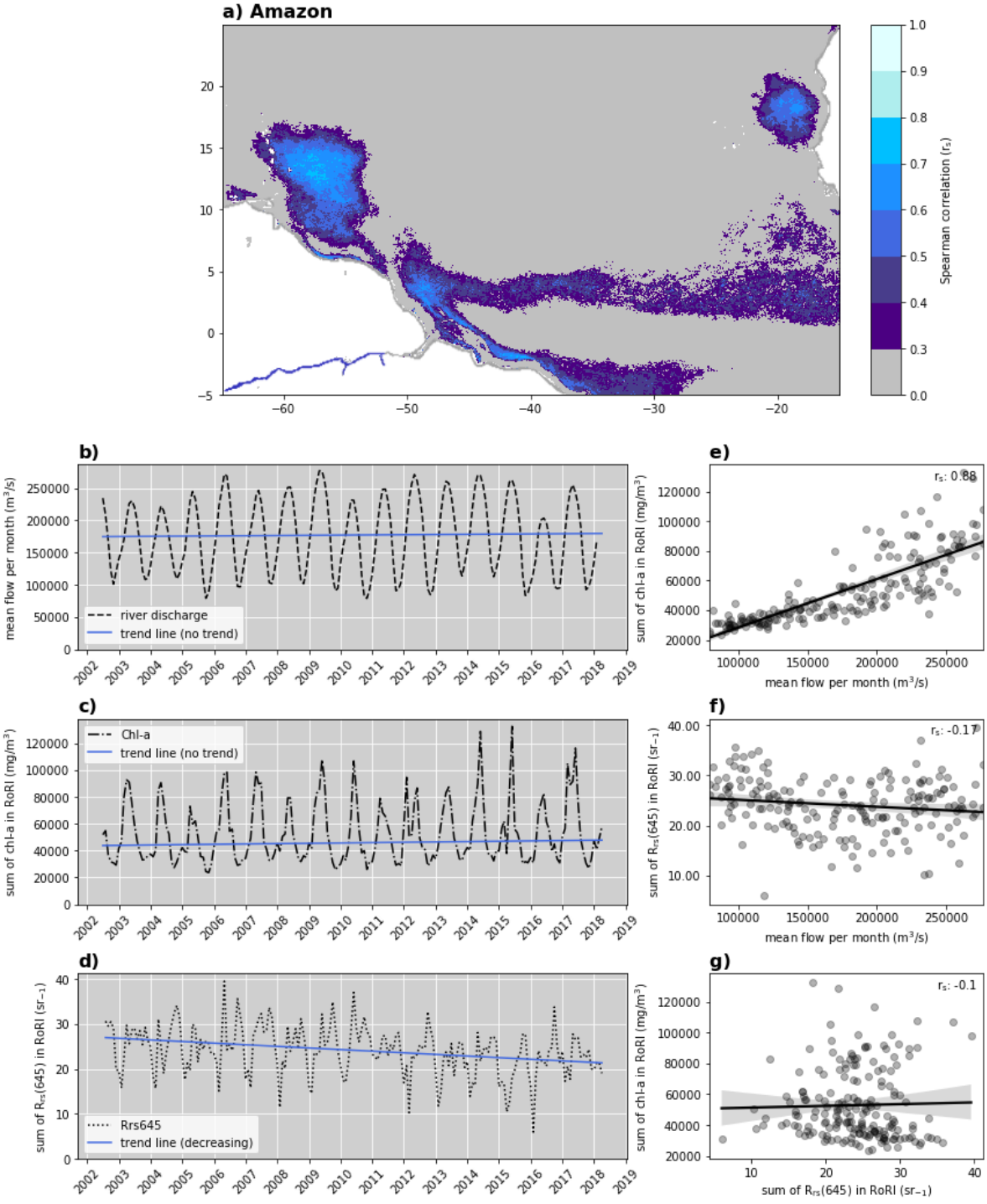

Figure 4.4: The spatial extent of the Amazon region of river discharge influence (RoRI), where $r_s > 0.3$ is shown in a). The results of Hamed and Rao modified Mann-Kendall trend tests on b) Amazon River discharge, c) sum of chl-*a* concentrations per month within Amazon RoRI d) sum of Rrs645 (turbidity) concentrations per month within the Amazon RoRI, and Spearman rank correlation (r_s) between e) river discharge and chl-*a*

concentration, f) river discharge and turbidity, and g) turbidity and chl-*a* over the MODIS time period.

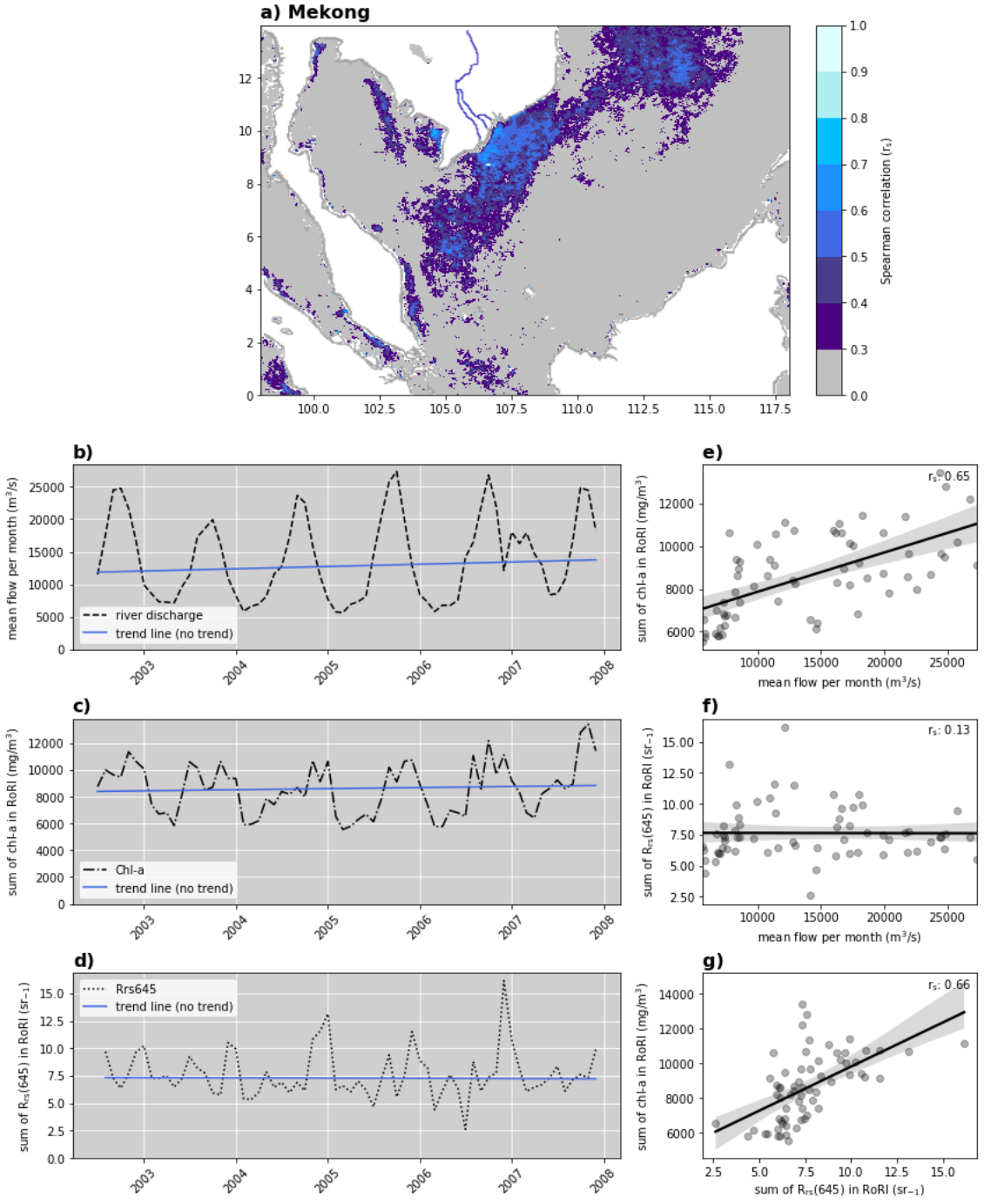

Figure 4.5: The spatial extent of the Mekong region of river discharge influence (RoRI), where r_s > 0.3 is shown in a). The results of Hamed and Rao modified Mann-Kendall trend tests on b) Mekong River discharge, c) sum of chl-*a* concentrations per month within Mekong RoRI d) sum of Rrs645 (turbidity) concentrations per month within the Mekong RoRI, and Spearman rank correlation (r_s) between e) river discharge and chl-*a*

concentration, f) river discharge and turbidity, and g) turbidity and chl-*a* over the MODIS time period.

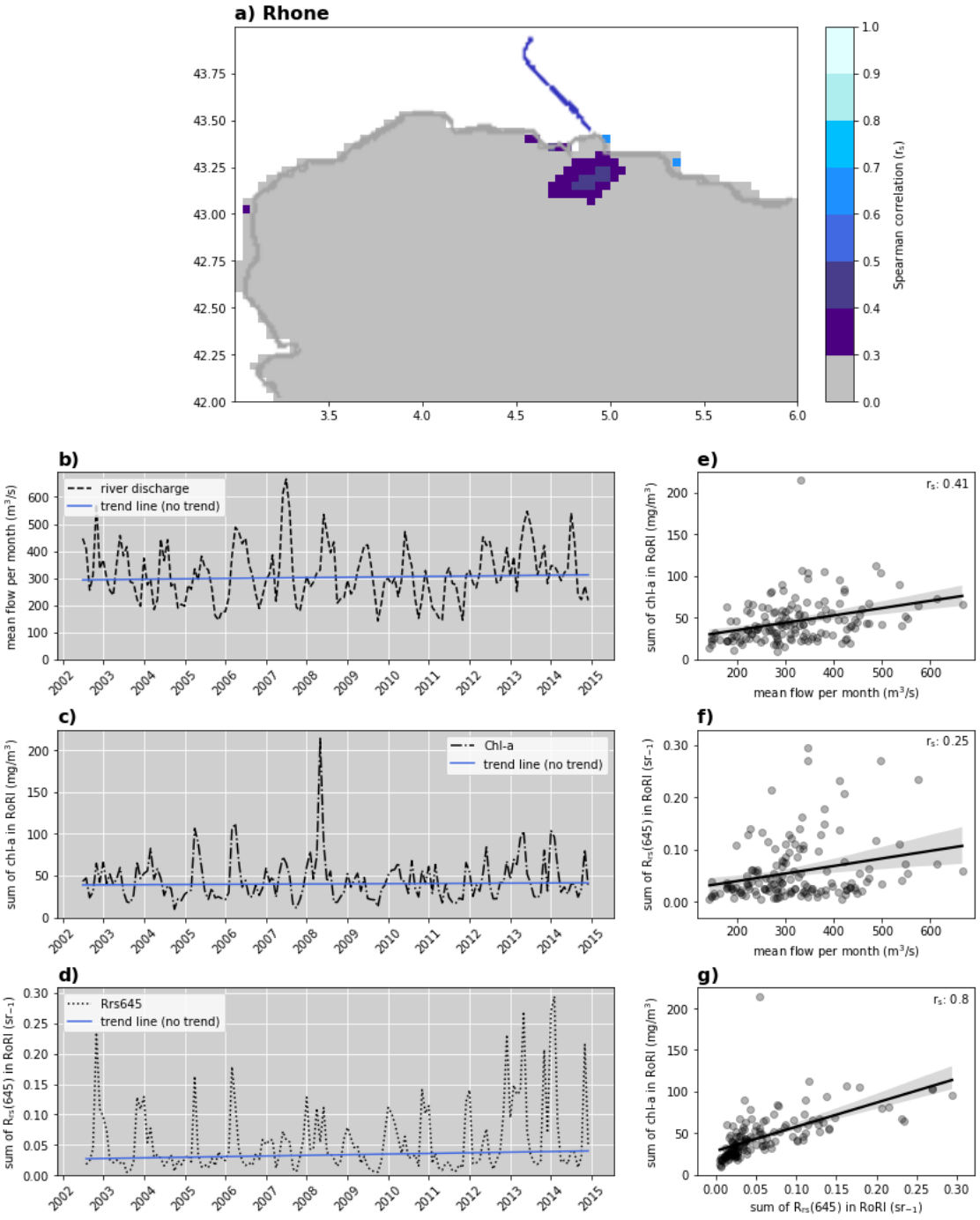

Figure 4.6: The spatial extent of the Rhone region of river discharge influence (RoRI), where $r_s > 0.3$ is shown in a). The results of Hamed and Rao modified Mann-Kendall trend tests on b) Rhone River discharge, c) sum of chl-*a* concentrations per month within Rhone RoRI d) sum of Rrs645 (turbidity) concentrations per month within the Rhone RoRI, and Spearman rank correlation (r_s) between e) river discharge and chl-*a*

concentration, f) river discharge and turbidity, and g) turbidity and chl-*a* over the MODIS time period.

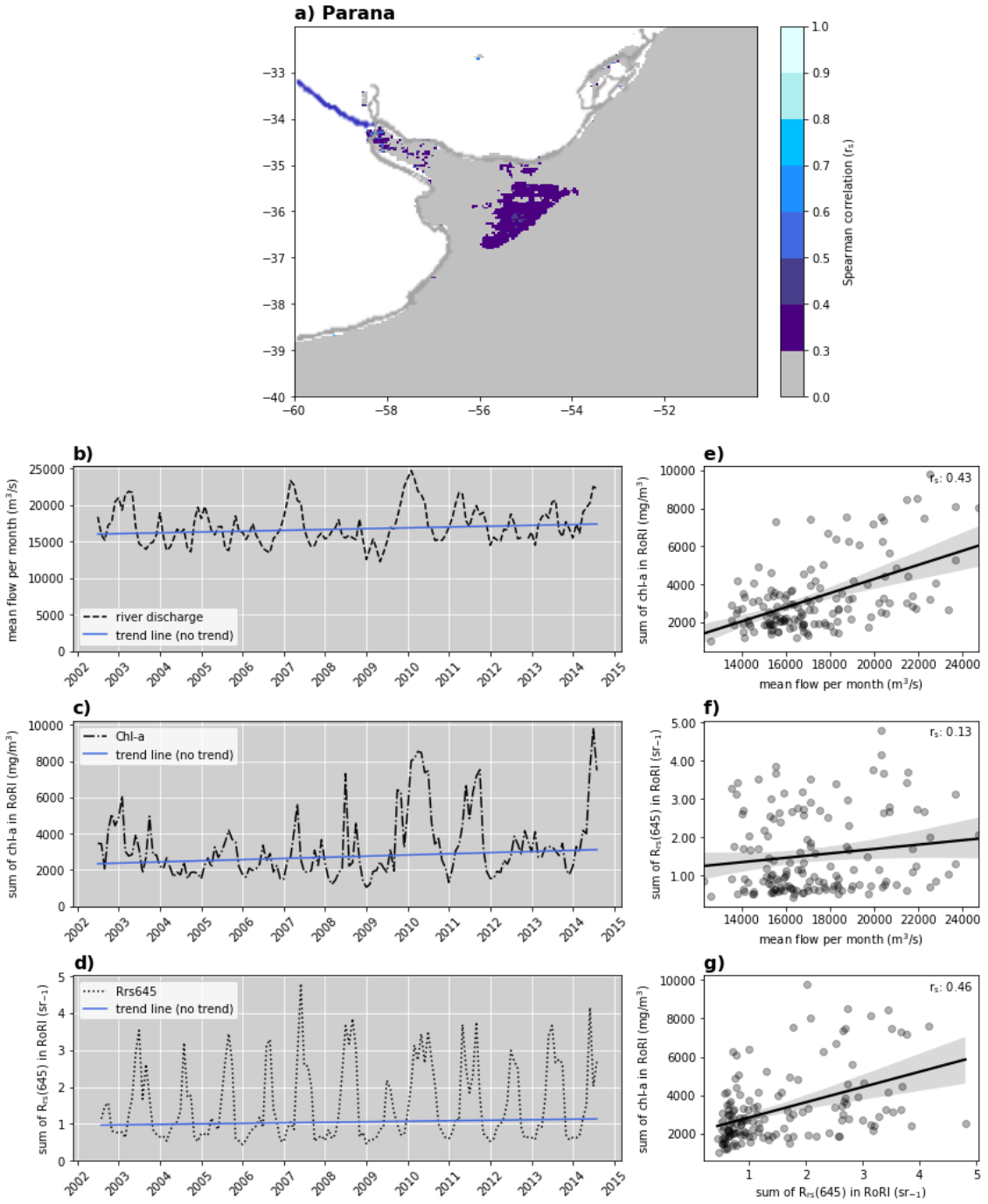

Figure 4.7: The spatial extent of the Parana region of river discharge influence (RoRI), where $r_s > 0.3$ is shown in a). The results of Hamed and Rao modified Mann-Kendall trend tests on b) Parana River discharge, c) sum of chl-*a* concentrations per month within Parana RoRI d) sum of Rrs645 (turbidity) concentrations per month within the Parana RoRI. Spearman rank correlation (r_s) between e) river discharge and chl-*a*

concentration, f) river discharge and turbidity, and g) turbidity and chl-*a* over the MODIS time period.

4.4 Discussion

River discharge has a profound influence on coastal productivity and coastal marine ecosystems (Gomes *et al.* 2018; Jickells *et al.* 2017; Sharples *et al.* 2017). However, the spatial scale of this influence is often not well understood, nor is how the influence may change over time. This knowledge is critical, as river flow is increasingly modified due to both anthropogenic and climatic factors. The findings of this chapter indicate that for some river systems (Murray, Mississippi and Amazon), in coastal regions where there is a known influence on water quality due to river discharge, water quality has also changed over time. However, the results of analysis on all rivers studied here showed largely unexpected trends and some which are contrary to previous studies (e.g. Murray river discharge), while others show no trend (e.g. Amazon, Mekong and Rhone river discharge and chl*a,* respectively). These findings do not support the initial hypothesis that declining or increasing trends in river discharge will be parallel to trends in chl-*a* and turbidity in RoRI of the same direction. This demonstrates that more research is required on this frontier.

The modified Mann-Kendall test indicates increasing trends in chl-*a* concentrations within RoRI of two of the six rivers studied: the Murray and Mississippi rivers. Interestingly, while there is no trend detected in Amazon River discharge or chl-*a* within the Amazon RoRI, trend in turbidity is decreasing in this region (Figure 4.4c). For the remaining rivers and their corresponding coastal regions investigated in this chapter, there were no strong increasing or decreasing trends in river flow, chl-*a* concentrations or turbidity in respective RoRI.

The Murray River discharge showed an increasing trend across the study period (Figure 4.2a). This result was unexpected as several previous studies of the river have indicated the opposite, although many of these spanned longer or different study periods. The Murray River experienced the “millennium drought” from early 2000’s until roughly 2011, with no flow from the river mouth to the sea in 2007. Then widespread heavy rainfall broke the drought in late 2010 (Aldridge *et al.* 2018; Gibbs *et al.* 2018), with high

flows from 2011-2013 and in late 2016 (Figure 4.2a). The Murray Darling Basin Plan, which recovered water for the environment from irrigators, also began to be implemented from 2012. The sequence of the events and changes captured in the time series explain the unexpected increasing trend seen here, contrary to longer term study periods which reveal different overall trends (e.g. CSIRO (2008); Goesch *et al.* (2020); BoM (2020)). The Millennium Drought event in the time series may also have biased the results of the modified MK trend test which has underlying assumptions of monotonic trends.

Increased severity and length of droughts and reduced flow are likely to occur in the future (and indeed, the millennium drought may have been a sign of these). Thus, these flooding events cause large distinctive peaks in the time series and suggest an increasing river discharge trend (Figure 4.2a). Our previous research, Auricht *et al.* (2018), presented in Chapter 2, shows that chl-*a* concentrations remained consistently low during the drought period beyond the Murray Mouth, and this region of the coast exhibited no characteristics of the stimulation effect that river discharge would usually promote in nearby coastal waters.

Some peaks in Murray RoRI turbidity occur at opposite times of year to river discharge but coincide with peaks in chl-*a* (e.g. between 2007 and 2009, Figure 4.2b and c). This suggests that turbidity and chl-*a* are more closely related to one another than each are to river discharge. This is reflected in the Spearman correlation results, where chl-*a* and turbidity have an r_s of 0.78 (Figure 4.2f). For example, peaks in both turbidity and chl-*a* occur sometime between April and June, annually. At these times of year, this region experiences lower mean wind speeds but higher maximum wind gust speeds with greater variability in wind direction (BoM 2022a; BoM 2022b). These conditions influence mixing of the water column, likely affecting mixed layer depth and thus are likely the primary drivers in change in turbidity and phytoplankton productivity here, in the absence of river discharge (Hopkins *et al.* 2021). However, the dynamics of wind-driven mixing require further investigation in this specific location. Although chl-*a* estimations

can be affected by concurrent increases in turbidity, *in situ* measurements in Auricht *et al.* (2018), Chapter 2, showed that turbidity is removed (e.g. via sedimentation) within 10 km of the river mouth during high flow events. They therefore do not likely affect chl-*a* estimations here.

Amazon River flow and chl-*a* within the Amazon RoRI showed no trends, while turbidity showed a decreasing trend between July 2002 and April 2018 (Figure 4.4c). This suggests that while concentrations of phytoplankton have not changed over this period, turbidity has decreased. Spearman correlation overall between Amazon River discharge and the sum of chl-*a* within the Amazon RoRI is very strong with r_s = 0.88. However, correlation is weak between turbidity and chl-*a*, and river discharge and turbidity (Figure 4.4d and e). The signal of turbidity over time is largely inverse to the other variables, but is occasionally synchronised to increases in river discharge. The true cause of the turbidity trend is difficult to determine with certainty, as the Amazon RoRI covers a vast area of both coastal and open ocean. However, correlation between Amazon River discharge and turbidity in the Amazon RoRI is very weak (r_s = -0.17), perhaps indicating that the trend in turbidity is not strongly linked to river discharge. The reasons for this observation are unclear but it is possible a declining trend in turbidity in coastal waters beyond the mouth could be attributed to reduction of deforestation in the Amazon basin. Official deforestation rates in the Brazilian Amazon reached a historical peak in 2004 during which 22,772 km² of rainforest were clear-cut (Assis *et al.* 2019; Silva Junior *et al.* 2021). The rate was reduced by 84% of this value by 2012, but has been increasing again since 2013 with more than > 10,000 km² of forest cleared in 2019 (Silva Junior *et al.* 2021). The MODIS Rrs645 dataset used to indicate turbidity in this study begins in 2002 and extends to April 2018, capturing the period of these changes in the basin. Although there is no trend in river discharge, this study does not explore river discharge concentrations (e.g. N and P concentrations) for the Amazon. It is possible that while river discharge volume has remained relatively steady from 2002 to 2019, concentrations of nutrients and sediments in river discharge have changed, possibly declining as deforestation rates have reduced. This could explain a declining trend in turbidity in the

Amazon RoRI, in the absence of a trend in chl-*a* or river discharge. However, it still does not explain a weak correlation between river discharge and turbidity, and further study would be required to determine whether turbidity in the coastal waters beyond the Amazon River mouth has truly been affected by changes in deforestation rates and land-use changes within the Amazon basin.

Based on the modified Mann-Kendall trend test results, the Mississippi had no strong trend in river discharge. While this finding is not consistent with the results of Pinter *et al.* (2008) who assessed 66 stations along the Mississippi river system and confirmed a pattern of overall increasing flows, the significant tends were only detected on the upper reaches of the Mississippi, upstream of most of the reservoir storages of the system. The data used in the present study to analyse Mississippi river discharge came from Vicksburg, Mississippi, below the Missouri and Ohio River confluences. In contrast, Liu *et al.* (2013) developed a dynamic land ecosystem model integrating evapotranspiration and runoff data estimations, and examined a century of modelled annual Mississippi River discharge data (between 1901 and 2008). They detected no significant trends in runoff, precipitation or river discharge across the full study period. However, climate change and land use change had similar magnitudes of impact on runoff and precipitation ratio and water fluxes in the Mississippi-Atchafalaya River basin. It appears that reductions in peak flows due to dam retention have been offset by increases in runoff due to climate change and changes in land-use (Pinter *et al.* 2008; Yasarer *et al.* 2020). Despite the presence of these factors, no clear trend was detected for monthly river discharge data between 2002 and 2019. It is possible that the records from 2002 (when MODIS became operational) are insufficient to capture a strong monotonic trend, if there is one. In addition, the increasing trends of chl-*a* in the Mississippi RoRI are consistent with increasing nutrient loading. The northern coast of the Gulf of Mexico is a known and predictable “dead zone” where river discharge from the Mississippi and Atchafalaya rivers have annually increased productivity to the point that coastal waters become anoxic (Rabalais *et al.* 2002; Syvitski *et al.* 2005). It therefore makes sense to see an increasing chl-*a* trend in this RoRI.

Although most results here do not necessarily suggest distinct trends in river discharge since 2002, or consequent trends in chl-*a* concentration or turbidity (Rrs645), examination of longer or different periods of data, where they exist, would reveal different patterns to further enhance our understanding of global scale river influence on coastal waters. The duration of MODIS Aqua's operation is a limitation of this paper, as a longer temporal record would provide more information from which to determine a monotonic trend against river flow records. Despite that Landsat has been used in previous studies for similar studies (e.g. Han and Jordan (2005); Hu (2009), sometimes in combination with MODIS data (e.g. Fu *et al.* (2018)) the temporal frequency of Landsat imagery is not as fine as MODIS and the sensor was not designed for ocean applications. There is still no globally-accepted Landsat chl-*a* method for water quality analysis applications (Bierman 2010). Further development of sensors to monitor coastal and inland waters is required.

Results in this chapter, derived from the modified Man-Kendall trend testing of MODIS time series, do not always result in monotonic trend detection. In future research, it will be beneficial to explore other statistical approaches to trend testing and correlation between river discharge, chl-*a* concentrations and turbidity of receiving coastal waters.

The global scale influence of river discharge on coastal phytoplankton biomass and turbidity has not been estimated as of yet. While some rivers studied in this chapter have arguably some of the world's greatest discharge volumes (e.g. the Mississippi and Amazon), more global rivers require investigation. This would not only enable development of more globally representative estimates but also increase local to global scale understanding of the influence of river discharge on coastal water quality. As our freshwater resources are increasingly under demand and river flow is continually modified, with climate change further reducing rainfall and catchment runoff in many regions of the world, the response of coastal waters to these changes is critical to monitor.

4.5 Conclusion

Coastal ecosystems are some of the most productive and important in the world, and a part of the ocean's hydrological and carbon cycle. Findings of this chapter provide an indication on whether the anthropogenic changes (including climate change) affecting river discharge for six target rivers, are also affecting the coastal productivity and water quality of coastal marine systems. Three rivers investigated in this paper have significant temporal trends in coastal water quality within regions of river discharge influence, indicating changes in river influence over time. However, for the other three rivers, a monotonic trend spanning multiple decades may be present but cannot be revealed from the shorter time-spans examined here. Future research may further develop the methods used herein, to contribute further knowledge and understanding of the spatial and temporal scale of influence of river discharge on coastal water chl-*a* and turbidity, and how this may change over time.

4.6 References

Aldridge, K.T., Mosley, L.M., and Oliver, R.L.f. (2018) Water quality in the Coorong Lower Lakes and Murray Mouth. . In Natural History of the Coorong, Lower Lakes and Murray Mouth (Yarluwar-Ruwe). (Eds. LM Mosley, S Shepherd, Q Ye, S Hemming and RW Fitzpatrick). (University of Adelaide Press: Adelaide)

Ajani, P.A., Larsson, M.E., Woodcock, S., Rubio, A., Farrell, H., Brett, S., and Murray, S.A. (2018) Bloom drivers of the potentially harmful dinoflagellate Prorocentrum minimum (Pavillard) Schiller in a south temperate Australian estuary. *Estuarine Coastal and Shelf Science* **215**, 161-171.

Assis, L.F.F.G., Ferreira, K.R., Vinhas, L., Maurano, L., Almeida, C., Carvalho, A., Rodrigues, J., Maciel, A., and Camargo, C. (2019) TerraBrasilis: A Spatial Data Analytics Infrastructure for Large-Scale Thematic Mapping. *ISPRS International Journal of Geo-Information* **8**(11).

Auricht, H., Mosley, L., Lewis, M., and Clarke, K. (2022) Mapping the long-term influence of river discharge on coastal ocean chlorophyll-a. *Remote Sensing in Ecology and Conservation* **8**(5), 629-643.

Auricht, H.C.C., Clarke, K.D., Lewis, M.M., and Mosley, L.M. (2018) Have droughts and increased water extraction from the Murray River (Australia) reduced coastal ocean productivity? *Marine and Freshwater Research* **69**(3), 343-356.

Aurin, D., Mannino, A., and Franz, B. (2013) Spatially resolving ocean color and sediment dispersion in river plumes, coastal systems, and continental shelf waters. *Remote Sensing of Environment* **137**, 212-225.

Axler, K.E. (2019) Influence of river plumes on larval fish distributions, predator-prey relationships and fitness in the northern Gulf of Mexico. Oregon State University,

Babin, M., Doxaran, D., Ehn, J., Matsuoka, A., Belanger, S., and Hooker, S. (2012) Optical Characterisation of Suspended Particles in the Mackenzie River Plume (Canadian Arctic Ocean) and Implications for Ocean Colour Remote Sensing. Vol. 9. pp. 3213-3229.

Biemans, H., Haddeland, I., Kabat, P., Ludwig, F., Hutjes, R.W.A., Heinke, J., von Bloh, W., and Gerten, D. (2011) Impact of reservoirs on river discharge and irrigation water supply during the 20th century. *Water Resources Research* **47**(3), n/a-n/a.

Bierman, P.E. (2010) Remote sensing to montior interactions between aquaculture and the environment of Spencer Gulf, South Australia. PhD Thesis, The University of Adelaide, Adelaide.

BoM (2020) Trends in historical conditions in the Murray-Darling Basin. Bureau of Meteorology, Melbourne.

BoM (2022a) Climate statistics for Australian locations. In Summary statistics Victor Habour Comparison. (Bureau of Meteorology)

BoM (2022b) Climate statistics for Australian locations: 023751 Victor Harbour comparison. In Monthly climate statistics. Vol. 2020.

Chai, C., Yu, Z., Shen, Z., Song, X., Cao, X., and Yao, Y. (2009) Nutrient characteristics in the Yangtze River Estuary and the adjacent East China Sea before and after impoundment of the Three Gorges Dam. *Science of The Total Environment* **407**(16), 4687-4695.

Chalise, D.R., Sankarasubramanian, A., and Ruhi, A. (2021) Dams and Climate Interact to Alter River Flow Regimes Across the United States. *Earth's Future* **9**(4), e2020EF001816.

Chen, Z., Hu, C., and Muller-Karger, F. (2007) Monitoring turbidity in Tampa Bay using MODIS/Aqua 250-m imagery. *Remote Sensing of Environment* **109**(2), 207-220.

Cherukuru, N., Martin, P., Sanwlani, N., Mujahid, A., and Müller, M. (2021) A Semi-Analytical Optical Remote Sensing Model to Estimate Suspended Sediment and Dissolved Organic Carbon in Tropical Coastal Waters Influenced by Peatland-Draining River Discharges off Sarawak, Borneo. *Remote Sensing* **13**(1).

Constantin, S., Doxaran, D., Derkacheva, A., Novoa, S., and Lavigne, H. (2018) Multi-temporal dynamics of suspended particulate matter in a macro tidal river Plume (the Gironde) as observed by satellite data. *Estuarine Coastal and Shelf Science* **202**, 172-184.

CSIRO (2008) Water availability in the Murray-Darling Basin. CSIRO, Australia.

Davies, C.H., Ajani, P., Armbrecht, L., Atkins, N., Baird, M.E., Beard, J., Bonham, P., Burford, M., Clementson, L., Coad, P., Crawford, C., Dela-Cruz, J., Doblin, M.A., Edgar, S., Eriksen, R., Everett, J.D., Furnas, M., Harrison, D.P., Hassler, C., Henschke, N., Hoenner, X., Ingleton, T., Jameson, I., Keesing, J., Leterme, S.C., James McLaughlin, M., Miller, M., Moffatt, D., Moss, A., Nayar, S., Patten, N.L., Patten, R., Pausina, S.A., Proctor, R., Raes, E., Robb, M., Rothlisberg, P., Saeck, E.A., Scanes, P., Suthers, I.M., Swadling, K.M., Talbot, S., Thompson, P., Thomson, P.G., Uribe-Palomino, J., van Ruth, P., Waite, A.M., Wright, S., and Richardson, A.J. (2018) A database of chlorophyll a in Australian waters. *Scientific Data* **5**(1), 180018.

Devlin, M.J., Petus, C., da Silva, E., Tracey, D., Wolff, N.H., Waterhouse, J., and Brodie, J. (2015) Water Quality and River Plume Monitoring in the Great Barrier Reef: An Overview of Methods Based on Ocean Colour Satellite Data. *Remote Sensing* **7**(10), 12909-12941.

Dogliotti, A.I., Ruddick, K.G., Nechad, B., Doxaran, D., and Knaeps, E. (2015) A single algorithm to retrieve turbidity from remotely-sensed data in all coastal and estuarine waters. *Remote Sensing of Environment* **156**, 157-168.

Dring, M.J., and Dring, M. (1992) 'The biology of marine plants.' (Cambridge University Press)

Fabricius, K.E., Logan, M., Weeks, S.J., Lewis, S.E., and Brodie, J. (2016) Changes in water clarity in response to river discharges on the Great Barrier Reef continental shelf: 2002-2013. *Estuarine Coastal and Shelf Science* **173**, A1-A15.

Fernández-Nóvoa, D., Costoya, X., deCastro, M., and Gómez-Gesteira, M. (2019) Dynamic characterization of the main Cantabrian river plumes by means of MODIS. *Continental Shelf Research* **183**, 14-27.

Fernandez-Novoa, D., Gomez-Gesteira, M., Mendes, R., deCastro, M., Vaz, N., and Dias, J.M. (2017) Influence of main forcing affecting the Tagus turbid plume under high river discharges using MODIS imagery. *Plos One* **12**(10).

Fernández-Nóvoa, D., Mendes, R., deCastro, M., Dias, J.M., Sánchez-Arcilla, A., and Gómez-Gesteira, M. (2015) Analysis of the influence of river discharge and wind on the Ebro turbid plume using MODIS-Aqua and MODIS-Terra data. *Journal of Marine Systems* **142**, 40-46.

Fu, Y., Xu, S., Zhang, C., and Sun, Y. (2018) Spatial downscaling of MODIS Clorophyll-a using Landsat 8 images for complex coastal water monitoring. *Estuarine Coastal and Shelf Science* **209**, 149-159.

Germolus, N.P., Brezonik, P.L., Hozalski, R.M., and Finlay, J.C. (2021) Long-term water color and flow trends in the Mississippi River Headwaters, 1944–2010. *Limnology and Oceanography* **66**(9), 3552-3567.

Gibbs, M., Joehnk, K., Webster, I., and Heneker, T.M. (2018) Hydrology and Hydridynamics of the Lower Lakes, Coorong and Murray Mouth. In Natural History of the Coorong, Lower Lakes and Murray Mouth Region (Yarluwar-Ruwe). (Eds. LM Mosley, Q Ye, S Shepherd, S Hemming and RW Fitzpatrick). (University of Adelaide Press: Adelaide)

Gill, G., Lehner, B., Lumsdon, A.E., MacDonald, G.K., Zarfl, C., and Reidy Lierman, C. (2015) An index based framework for assessing patterns and trends in river fragmentation and flow regulation by global dams at multiple scales. *Environmental Research Letters* **10**.

Goesch, T., Legg, P., and Donoghoe, M. (2020) Murray-Darling Basin water markets: trends and drivers 2002-03 to 2018-19. Australian Bureau of Agricultural and Resource Economics and Sciences, No. 20.5, Canberra.

Gomes, H.d.R., Xu, Q., Ishizaka, J., Carpenter, E.J., Yager, P.L., and Goes, J.I. (2018) The Influence of Riverine Nutrients in Niche Partitioning of Phytoplankton Communities–A Contrast Between the Amazon River Plume and the Changjiang (Yangtze) River Diluted Water of the East China Sea. *Frontiers in Marine Science* **5**(343). [In English]

Grill, G., Lehner, B., Thieme, M., Geenen, B., Tickner, D., Antonelli, F., Babu, S., Borrelli, P., Cheng, L., Crochetiere, H., Ehalt Macedo, H., Filgueiras, R., Goichot, M., Higgins, J., Hogan, Z., Lip, B., McClain, M.E., Meng, J., Mulligan, M., Nilsson, C., Olden, J.D., Opperman, J.J., Petry, P., Reidy Liermann, C., Sáenz, L., Salinas-Rodríguez, S., Schelle,

P., Schmitt, R.J.P., Snider, J., Tan, F., Tockner, K., Valdujo, P.H., van Soesbergen, A., and Zarfl, C. (2019) Mapping the world's free-flowing rivers. *Nature* **569**(7755), 215-221.

Hamed, K.H., and Ramachandra Rao, A. (1998) A modified Mann-Kendall trend test for autocorrelated data. *Journal of Hydrology* **204**(1), 182-196.

Hamidi, S.A., Hosseiny, H., Ekhtari, N., and Khazaei, B. (2017) Using MODIS remote sensing data for mapping the spatio-temporal variability of water quality and river turbid plume. *Journal of Coastal Conservation* **21**(6), 939-950.

Han, L., and Jordan, K.J. (2005) Estimating and mapping chlorophyll-a concentration in Pensacola Bay, Florida using Landsat ETM+ data. *International Journal of Remote Sensing* **26**(23), 5245-5254.

Helsel, D.R., and Hirsch, R.M. (1992) 'Statistical methods in water resources.' (Elsevier)

Hopkins, J., Lucas, M., Dufau, C., Sutton, M., Stum, J., Lauret, O., and Channelliere, C. (2013) Detection and variability of the Congo River plume from satellite derived sea surface temperature, salinity, ocean colour and sea level. *Remote Sensing of Environment* **139**, 365-385.

Hu, C. (2009) A novel ocean color index to detect floating algae in the global oceans. *Remote Sensing of Environment* **113**(10), 2118-2129.

Hu, C., Lee, Z., and Franz, B. (2012) Chlorophyll aalgorithms for oligotrophic oceans: A novel approach based on three-band reflectance difference. *Journal of Geophysical Research: Oceans* **117**(C1).

Jickells, T.D., Buitenhuis, E., Altieri, K., Baker, A.R., Capone, D., Duce, R.A., Dentener, F., Fennel, K., Kanakidou, M., LaRoche, J., Lee, K., Liss, P., Middelburg, J.J., Moore, J.K., Okin, G., Oschlies, A., Sarin, M., Seitzinger, S., Sharples, J., Singh, A., Suntharalingam, P., Uematsu, M., and Zamora, L.M. (2017) A reevaluation of the magnitude and impacts of anthropogenic atmospheric nitrogen inputs on the ocean. *Global Biogeochemical Cycles* **31**(2), 289-305.

Kirk, J.T. (1994) 'Light and photosynthesis in aquatic ecosystems.' (Cambridge university press)

Liu, M., Tian, H., Yang, Q., Yang, J., Song, X., Lohrenz, S.E., and Cai, W.-J. (2013) Long-term trends in evapotranspiration and runoff over the drainage basins of the Gulf of Mexico during 1901–2008. *Water Resources Research* **49**(4), 1988-2012.

Masotti, I., Aparicio-Rizzo, P., Yevenes, M.A., Garreaud, R., Belmar, L., and Farías, L. (2018) The Influence of River Discharge on Nutrient Export and Phytoplankton Biomass Off the Central Chile Coast (33°–37°S): Seasonal Cycle and Interannual Variability. *Frontiers in Marine Science* **5**(423). [In English]

McCarthy, M.J., Otis, D.B., Mendez-Lazaro, P., and Muller-Karger, F.E. (2018) Water Quality Drivers in 11 Gulf of Mexico Estuaries. *Remote Sensing* **10**(2).

Miller, R.L., and McKee, B.A. (2004) Using MODIS Terra 250 m imagery to map concentrations of total suspended matter in coastal waters. *Remote Sensing of Environment* **93**(1), 259-266.

Milly, P.C.D., Dunne, K.A., and Vecchia, A.V. (2005) Global pattern of trends in streamflow and water availability in a changing climate. *Nature* **438**(7066), 347-350.

O'Reilly, J.E., Maritorena, S., Mitchell, B.G., Siegel, D.A., Carder, K.L., Garver, S.A., Kahru, M., and McClain, C. (1998) Ocean color chlorophyll algorithms for SeaWiFS. *Journal of Geophysical Research: Oceans* **103**(C11), 24937-24953.

OBPG (2022) Remote Sensing Reflectance (Rrs). Vol. 2022. (Ed. S Bailey). (NASA Ocean Colour, Ocean Biology Processing Group)

Petus, C., da Silva, E.T., Devlin, M., Wenger, A.S., and Álvarez-Romero, J.G. (2014) Using MODIS data for mapping of water types within river plumes in the Great Barrier Reef, Australia: Towards the production of river plume risk maps for reef and seagrass ecosystems. *Journal of Environmental Management* **137**, 163-177.

Pinter, N., Jemberie, A.A., Remo, J.W.F., Heine, R.A., and Ickes, B.S. (2008) Flood trends and river engineering on the Mississippi River system. *Geophysical Research Letters* **35**(23).

Rabalais, N.N., Turner, R.E., Dortch, Q., Justic, D., Bierman, V.J., and Wiseman, W.J. (2002) Nutrient-enhanced productivity in the northern Gulf of Mexico: past, present and future. In Nutrients and Eutrophication in Estuaries and Coastal Waters: Proceedings of the 31st Symposium of the Estuarine and Coastal Sciences Association (ECSA), held in Bilbao, Spain, 3–7 July 2000. (Eds. E Orive, M Elliott and VN de Jonge) pp. 39-63. (Springer Netherlands: Dordrecht)

Seitzinger, S.P., Mayorga, E., Bouwman, A.F., Kroeze, C., Beusen, A.H.W., Billen, G., Van Drecht, G., Dumont, E., Fekete, B.M., Garnier, J., and Harrison, J.A. (2010) Global river nutrient export: A scenario analysis of past and future trends. *Global Biogeochemical Cycles* **24**(4).

Sharples, J., Middelburg, J.J., Fennel, K., and Jickells, T.D. (2017) What proportion of riverine nutrients reaches the open ocean? *Global Biogeochemical Cycles* **31**(1), 39-58.

Shi, X., Qin, T., Nie, H., Weng, B., and He, S. (2019) Changes in Major Global River Discharges Directed into the Ocean. *International Journal of Environmental Research and Public Health* **16**(8).

Silva Junior, C.H.L., Pessôa, A.C.M., Carvalho, N.S., Reis, J.B.C., Anderson, L.O., and Aragão, L.E.O.C. (2021) The Brazilian Amazon deforestation rate in 2020 is the greatest of the decade. *Nature Ecology & Evolution* **5**(2), 144-145.

Srinivas, R., Singh, A.P., Dhadse, K., and Magner, J. (2020) Hydroclimatic river discharge and seasonal trends assessment model using an advanced spatio-temporal model. *Stochastic Environmental Research and Risk Assessment* **34**(2), 381-396.

Su, L., Miao, C., Kong, D., Duan, Q., Lei, X., Hou, Q., and Li, H. (2018) Long-term trends in global river flow and the causal relationships between river flow and ocean signals. *Journal of Hydrology* **563**, 818-833.

Syvitski, J.P.M., Vorosmarty, C.J., Kettner, A.J., and Green, P. (2005) Impact of Humans on the Flux of Terrestrial Sediment to the Global Coastal Ocean. *Science* **308**(5720), 376-380.

Wang, M., Son, S., and Harding, L.W. (2009) Retrieval of diffuse attenuation coefficient in the Chesapeake Bay and turbid ocean regions for satellite ocean color applications. *Journal of Geophysical Research* **114**.

Yasarer, L.M.W., Taylor, J.M., Rigby, J.R., and Locke, M.A. (2020) Trends in Land Use, Irrigation, and Streamflow Alteration in the Mississippi River Alluvial Plain. *Frontiers in Environmental Science* **8**(66). [In English]

Yunev, O.A., Carstensen, J., Moncheva, S., Khaliulin, A., Ærtebjerg, G., and Nixon, S. (2007) Nutrient and phytoplankton trends on the western Black Sea shelf in response to cultural eutrophication and climate changes. *Estuarine, Coastal and Shelf Science* **74**(1), 63-76.

Appendix C

C.1 Additional statistical information and results from Mann-Kendall trend test on river discharge, chl-*a*, and turbidity.

Table C.1.: Hamed and Rao modified Mann-Kendall trend test results of river discharge data.

	trend in flow	p-val	z	Tau	s	var_S	slope	intercept
Murray	increasing	0.02	2.27	0.29	5842	6628704.87	0.05	3.43
Rhone	no trend	0.71	0.38	0.03	381	1022567.55	0.13	293.83
Amazon	no trend	0.70	0.38	0.01	248	415505.94	26.08	174767.93
Parana	no trend	0.16	1.40	0.11	1146	670021.89	9.46	16044.12
Mekong	no trend	0.35	0.93	0.07	159	28735.02	28.88	11876.48
Mississippi	no trend	0.81	0.24	0.01	185	580334.08	1.98	18908.96

Table C.2: Hamed and Rao modified Mann-Kendall trend test results on chl-*a* concentrations over time for each river's region of river influence (RoRI).

RoRI	trend in chl-*a*	p-val	z	Tau	s	var_S	slope	intercept
Murray	increasing	0.04	2.01	0.17	3358	2791111.91	0.03	16.73
Rhone	no trend	0.50	0.67	0.03	301	198757.43	0.02	38.93
Amazon	no trend	0.15	1.43	0.04	791	305631.25	21.10	43812.24
Parana	no trend	0.19	1.30	0.12	1295	994579.02	5.33	2338.42
Mekong	no trend	0.68	0.41	0.05	99	55960.82	6.83	8405.84
Mississippi	increasing	0.00	7.67	0.14	2720	125569.64	17.95	13945.76

Table C.3: Hamed and Rao modified Mann-Kendall trend test results on turbidity (Rrs645) concentrations over time for each river's region of river influence (RoRI).

RoRI	trend in Rrs645	p-val	z	Tau	s	var_S	slope	intercept
Murray	no trend	0.27	1.10	0.08	1646.00	2232388.95	0.00	0.02
Rhone	no trend	0.15	1.43	0.09	1012.00	503132.68	0.00	0.03
Amazon	decreasing	0.00	-4.66	-0.22	-3824.00	672439.28	-0.03	27.00
Parana	no trend	0.11	1.58	0.06	664.00	175621.97	0.00	0.97
Mekong	no trend	0.92	-0.10	-0.01	-22.00	46596.18	0.00	7.34
Mississippi	no trend	0.72	-0.37	-0.01	-278.00	575880.34	0.00	9.30

Chapter 5

Conclusion

There is a paucity of knowledge of the influence of river discharge on coastal ocean waters in many regions of the world. There are no standard, conventional methods or broadly applicable approaches for estimating the spatial scale of influence or the strength of the relationship between river discharge and coastal ocean productivity and water quality. However, such a method could enable investigation into the influence of river discharge on marine systems around the world and be incorporated into broader scale modelling and predictions. How this relationship may change under declining river flow, due to anthropogenic intervention and climate change is crucial to decision-makers, managers and environmental policy makers from local to global scales. In this thesis I demonstrate the development and use of remote sensing methods for investigating and understanding the broad scale relationships between river discharge and coastal water quality and productivity for a number of globally significant rivers. This has led to several important findings.

5.1 Key findings

5.1.1 Local to regional scale stimulative effects of river discharge on coastal water quality.

The research presented in Chapter 2 investigated the influence of the Murray River (Australia) on coastal waters using remotely sensed ocean colour data over the millennium drought (low and no flow periods) and following high flow years. The study demonstrated local to regional scale influence of river discharge on chlorophyll-*a* (chl-*a*) concentration, a proxy for phytoplankton biomass, and particulate organic carbon (POC) in the Southern Ocean. The research revealed that this influence and stimulative effect was not present during the Millennium drought, likely due to lack of river discharge. Key findings of this Chapter included:

- A strong linear relationship between Murray River discharge and coastal ocean chl-*a* (R^2 = ~0.8) and particulate organic carbon (R^2 = ~0.6) in an 8 km radial buffer zone from the Murray Mouth.
- The stimulative effect of river discharge on chl-*a* in the Southern Ocean coastal waters was lost during the millennium drought. There was no additional coastal

ocean productivity above background levels between 2007 and 2010, when river discharge ceased.

- Under high flow conditions (post-drought flood in 2012), chl-*a* concentration was elevated up to 60 km from the Murray River mouth.
- The observed zone of Murray River influence was at least three times greater than the measured maximum extent of salinity dilution caused by the freshwater river plume and turbidity was not substantially elevated beyond 10 km from the mouth (indicated by *in situ* salinity transect data). This suggested a causal link between the observed increased coastal-ocean productivity and the river discharge.

5.1.2 Image based ocean colour analysis can be used to effectively identify regions of river discharge influence.

Satellite remote sensing imagery has been used successfully in all research chapters of this thesis (Chapters 2, 3 and 4) to identify regions where coastal chl-a and other water quality parameters are influenced by river discharge.

The methodology of Chapter 2 depended on local knowledge of the plume direction under high flow. However, river plume extent and direction is not known for many systems and can change under various conditions. Chapter 3 used an objective method, less reliant on local knowledge than some other approaches, in an attempt to identify region(s) of river discharge influence (RoRIs). Identifying RoRIs enables monitoring of these regions for change into the future and helps to focus future research. Determining RoRI was done by performing a spatiotemporal correlation analysis between the time series of chl-*a* (for each pixel in several years of satellite imagery) and a corresponding time series of river discharge data. The research presented in Chapters 2, 3 and 4 showed that for many regions, river discharge may have a great influence on coastal ocean productivity and water quality. More specifically, these findings include:

- Analysis of several years of MODIS ocean chl-*a* imagery showed that Murray River discharge has a large influence, elevating chl-*a* concentrations up to 60 km from the river mouth under high flow conditions (refer Chapter 2).
- When Murray River flows ceased, the stimulation effect of river discharge on coastal waters is lost and reduced to background (seasonal) levels. This illustrates that the Murray River may have a greater stimulative effect on the marine environment than has been previously acknowledged. Prior to this study, there was no published, empirical evidence of this specific link between Murray River discharge and coastal ocean productivity.
- Based on MODIS ocean chl-*a* products, the method developed in Chapter 3 identified the spatial extent of long-term river discharge influence on chl-*a* concentrations in coastal oceans, indicating strong links between variables for six out of eleven globally significant rivers. These included the Rhone (France), Amazon (South America), Parana (South America), Murray (Australia), Mekong (Asia) and Mississippi (USA) rivers.
- Spatiotemporal analysis of MODIS satellite imagery products in Chapter 3 identified a large area where Amazon river discharge influences not only coastal ocean chl-*a*, but also chl-*a* concentrations of the open ocean, in areas consistent with previous studies as well as areas beyond. These are indicated by correlations greater than 0.5 r_s.
- Chapter 4 applied the methodology of Chapter 3 to investigate the relationships between river discharge and regions of river discharge influence and how these relationships may change over time. The study indicated strong relationships in some areas and highlighted the complexities of river influence on coastal productivity and turbidity.

5.1.3 Development of a more objective, repeatable method of identifying coastal waters influenced by river discharge.

The spatiotemporal analysis used in Chapter 3 was more objective than some other image-based methods used in previous research because it does not require local knowledge of the system, or supervised classification of ocean colour products.

- The spatiotemporal method of Chapter 3 was found to be more effective for larger river systems discharging to ocean waters with less complex nutrient dynamics and weaker seasonal productivity patterns, most notably in temperate regions (e.g. the Mediterranean Sea, to which the Rhone River discharges). For rivers with irregular flow time series, identification of the long-term spatial influence of chl-*a* concentration could be determined more effectively.

5.2 Significance and broader implications

Findings from my thesis highlight the capacity of Earth observation techniques and analysis for monitoring changes in coastal ocean water quality. The MODIS chl-*a* ocean colour product used in this thesis is based on the OC3M algorithm and is designed for application in Case 1 waters where colour is predominantly influenced by phytoplankton. Generally, use of these Case 1 products is discouraged in Case 2 waters (Bierman *et al.* 2011). However, the findings of this thesis demonstrate that these products can be used effectively to identify regions influenced by changing volumes of river discharge, including broad application in coastal Case 2 waters. Further consideration and potential review of Case 1 and Case 2 waters may therefore be necessary. It could also be beneficial to attempt further classification of Case 2 waters. This could break down a range of water types from those where reflectance is dominated by chl-*a* alongside CDOM and other reflective matter in the water column, to those where the majority of optical reflectance is derived from non-algal turbidity and CDOM. This would help to identify more appropriate ocean colour algorithms for analysing a range of global coastal environments.

To the best of my knowledge, the research of Chapter 2 was the first study to investigate the relative effects of Murray River discharge on the coastal waters beyond the Murray River mouth, and the first to do so with remote sensing techniques. It is therefore a ground breaking study, and has increased interest in the potential effects of river flow on marine species which have so far gone largely unmonitored in this region, as well as the potential effects this may have had, or will have as flows have been or are reduced in the future.

In addition, the method developed in Chapter 3 contributes a more objective and broadly applicable remote sensing based method for detection and monitoring of regions influenced by river discharge. There is currently no standardised or conventional method, based on objective image based analysis, to identify regions of coastal waters which are influenced or affected by river discharge of varying volume across space and time. A rapid method is required which can aid decision makers to determine whether these land-sea connections should be included in the scope of management and warrant further resources for investigation (Fredston-Hermann *et al.* 2016). However, river plume extent and direction is not known for many systems in data-poor regions, and can change under various conditions. The methods of Chapter 2 depended on local and regional scale knowledge of the system and is repeatable. However, it is not necessarily transferable across systems, due to its reliance on local knowledge or data. The spatiotemporal analysis used in Chapter 3 does not rely on local or regional knowledge, meaning it is more applicable to data-poor regions. Without this knowledge, it is difficult to effectively conserve natural systems. The techniques of this thesis can inform how the linked systems could be managed, including those in data-poor regions, as it is based on freely available satellite imagery products with global coverage and river discharge data (which can also be obtained for free in many instances). In regions where local knowledge on the extent of river plumes is understood, the methodology of Chapter 2 may be useful. While in locations where it is not known, or studies comparing a number of discharging systems, the methods of Chapter 3 may prove more useful. The methods of this thesis could be further developed for monitoring purposes in the future.

Although river discharge patterns and river plumes have been studied in some coastal regions, it remains to be seen if and how the influence of river discharge on coastal productivity and water quality has changed over the long term. This is a pertinent question, as river discharge has been altered at global scales and, in many locations, has reduced due to extraction, modification and management. Chapter 4 explored the long term trends in river discharge, alongside trends in coastal chl-*a* concentrations and turbidity (via time series extracted from RoRIs identified in Chapter 3). The findings of this Chapter did not support the initial hypothesis that declining or increasing trends in river discharge will be parallel to trends in chl-*a* and turbidity, but suggested the relationship between river discharge, coastal chl-*a* and turbidity are likely very complex for these systems. It is likely the relationships between these variables may be changing over time. The lack of clear trends for three of the six rivers investigated, highlights the need continued and further development of spatiotemporal research methods based on satellite imagery. It is crucial that as river discharge volumes are altered in the future due to anthropogenic pressures (including climate change) there is continued research into the numerous ways this may affect coastal water quality, productivity and ecosystems.

Overall, the research of this thesis lays a groundwork from which future research can build in order to more closely monitor river plume waters and river plume influence on coastal ocean waters and marine environments. This can be achieved by using remote sensing or Earth observations techniques.

5.3 Limitations and recommendations

While a number of important and useful advancements in knowledge and methodology are presented in this thesis, it is important to consider the limitations of the research herein.

5.3.1 Awareness of general limitations in monitoring change in natural environments

In some regions, river flow has been managed since ancient times and indeed, many ancient and present-day civilisations could not exist without careful management of

freshwater systems (Mithen 2010). In the more recent past, prior to modification at the scales we see today, many river systems delivered larger volumes of water to the coast than they have in the last century. Historical data and information prior to intensive river flow regulation and management is often limited or in some cases, non-existent. Therefore, it is unclear how river discharge influenced coastal ocean waters and ecosystems prior to exhaustive anthropogenic pressure and anthropogenic climate change. There is therefore limited data available to 1) establish a baseline of coastal ocean productivity or river discharge, and 2) to compare to current day estimates of river discharge influence or the impact of river flow management on coastal water quality and productivity. However, current research and data available suggests that the influence of river discharge was greater in the past than in more recent decades, at least in some regions. For example, the findings of Chapter 2 show that the Millennium drought reduced coastal ocean productivity of the Southern Ocean to background levels as Murray River flows ceased. Hind-cast time series data also revealed that it is likely that productivity was higher in this region with greater flow in the past. Similarly, chapter 3 determined large regions of river discharge influence for many global rivers, including the Amazon River, extending beyond the estimates of other research. However, river discharge data and the record length of operational remote sensors limits the ability of researchers to determine the true scale of change. This is also true of the methods used and developed in this thesis. Because of these limitations, the need to monitor river-discharge affected or influenced regions is crucial in the future. Although the ability to compare present day river discharge influence to that of rivers before intensive anthropogenic pressure and intervention is limited, there are a number of areas where we can further improve our understanding of river influence on coastal ecosystems into the future.

5.3.2 Refining methodology and testing alternative approaches

I have several suggestions for possible refinements to the methodology used in this thesis for future research. These include incorporation of temporal and spatial 'decay' in the

spatiotemporal analysis method presented in Chapter 3 and potential ways of increasing satellite imagery record lengths.

5.3.2.1 Incorporating temporal and spatial 'decay'

A limitation of the method developed in Chapter 3 was the lack of a method to integrate temporal and spatial decay. Therefore, future method development to incorporate temporal lag between river discharge and chl-*a*, POC and turbidity may reveal stronger relationships between variables than was detected in this research. The research herein is based on monthly composite satellite imagery. Use of composite data was a deliberate choice, to minimise data-loss due to cloud cover and to capture effects at a moderate temporal resolution. The current, presented methodology assumes that ocean water quality at a point (pixel) close to the river mouth would respond during the same period (month) and would have the same sensitivity as a point several kilometres away. It is also possible that temporal autocorrelation within this data allows a relationship to be detected even if there is a one-month lag. Lagged relationships are typical in natural systems, therefore it is possible there are lagged temporal and spatial relationships between river discharge and coastal water quality, as well as river discharge and open ocean water quality and productivity, beyond one month. Therefore, incorporating finer temporal resolution, and the development of temporal and spatial decay analysis methodology may create a more accurate and reliable picture of the true influence of river discharge on coastal water productivity.

5.3.2.2 Combining and comparing imagery from different satellite-based sensors

Combining imagery from multiple sensors may help to lengthen remote sensing time series and therefore improve detection of long-term trends in river discharge and coastal ocean productivity and water quality. The length of river discharge records in these chapters were necessarily restricted to those of the MODIS ocean colour product record. This meant record starts were limited to July of 2002 (when MODIS Aqua became operational), even though for some rivers much longer temporal flow records were available. This influenced some of the findings of Chapters 3 and 4. For example, use of

the Hamed and Ramachandra Rao (1998) modified Mann-Kendall (MK) trend test implemented on Murray river discharge data in Chapter 4, suggested an overall increasing trend in river discharge. This is an artefact of the restricted temporal extent, and not consistent with studies covering longer temporal records (e.g. Meteorology (2020) studied more than 50 years of daily river flow data and determined an overall declining trend in the Southern regions of the Murray River system). While the modified MK trend test results are accurate for the studied periods, they may not be representative of the broader scale temporal trends, including that of the Murray River. For rivers which have long pre-2002 records, remote sensing image products from other sensors could potentially be used to investigate longer-term relationships between variables. However, this would need to be done with caution. For example, NASA's Thematic Mapper TM sensor has delivered Earth observation data for almost 27 years, aboard Landsat 5 and operational between 1984 and 2011. This has several years of overlap with MODIS Aqua data which could be compared and used to buffer estimations. Landsat 5 TM data have shortcomings when compared to MODIS Aqua in that Landsat's sensors were not designed for ocean colour applications. Despite this, Landsat data may help to extend the record length of imagery for analysis for investigating long-term trends. However, users would need to be careful when comparing between Landsat and MODIS products.

Alternatively, or in addition to these changes, the use of the spatiotemporal correlation method should be tested on ocean colour products with greater spatial resolution. It is possible to process MODIS Aqua imagery at ~250 m resolution, rather than ~4 km which was used in Chapters 2, 3 and 4. While this resolution was sufficient for investigating broad scale and long-term influence of river discharge, the spatiotemporal correlation analysis developed in Chapter 3 was less effective at identifying regions of river discharge influence for those rivers with lower flow volumes, or where flow was highly seasonal in nature. The use of finer scale spatial imagery products may increase the effectiveness of this approach in identifying RoRI for smaller rivers and to delineate seasonal patterns of productivity from those due solely to river discharge.

5.4 Recommendations for future research

The research in this thesis has led to the identification of several important potential and promising avenues of research, pertinent and essential to monitoring open and coastal ocean water quality and productivity with satellite imagery and remote sensing techniques in the future. These include the use of the spatiotemporal method used in Chapter 3 to explore the relationships between productivity and other naturally occurring phenomena in the context of anthropogenic climate change, the importance and need for continued *in situ* monitoring and satellite based sensor and algorithm development.

5.4.1 Using spatiotemporal analysis to explore effects of other broad scale phenomena

The spatiotemporal correlation method presented in Chapter 3 has potential for monitoring a range of other broad scale phenomena which influence open ocean phytoplankton, beyond the scope of this thesis. For example, the spatiotemporal method could be refined or adjusted to estimate the strength of the relationship between aerosol emissions or iron-dust deposition and phytoplankton biomass. Aerosol emissions, such as those derived from wildfires, can carry macro-nutrients and trace metals such as iron, nitrogen and phosphorus (Barkley *et al.* 2019; Schlosser *et al.* 2017), stimulating phytoplankton blooms in open ocean regions, far from land (Tang *et al.* 2021). Wildfires in many areas of the world are also predicted to increase in frequency and severity in the future (Bowman *et al.* 2020). Therefore, climate change is predicted to affect the magnitude of phosphorus provided to the worlds' ocean basins by aerosol deposition (Mahowald 2011; Okin *et al.* 2004). Indeed, some continents have seen an increase in catastrophic wildfires in very recent years. Widespread, unprecedented wildfires occurred in the Amazon rainforest and across several states of Australia, respectively, in 2019 and 2020. Tang *et al.* (2021) determined a strong link between chl-*a* of the open ocean and optical aerosol thickness with MODIS products. Using the spatiotemporal analysis method could enable detection and monitoring of these relationships at broad scales.

The spatiotemporal method could also be adjusted and used to detect phytoplankton blooms due to iron dust deposition. Wind speed and soil erosion is also predicted to increase due to extreme winds in the future (Mahowald *et al.* 2011). Therefore, there may be greater amounts of limiting nutrients supplied to oceans in the future, compared to earlier years. However, how this will affect the productivity of oceans in the future is uncertain. It will therefore be necessary to further develop monitoring detection methods and applications to determine how these events may affect global or even regional scale productivity and water quality in future years.

5.4.2 A necessity for further in situ coastal water quality monitoring alongside remote sensing methodologies

There is an undeniable need to explore coastal regions of river discharge influence both *in situ* and remotely. In some locations, the ability of river plumes to alter pH, sedimentation, salinity and light penetration of the coastal water column had led to the assumption that these conditions would suppress aquatic and marine life in these locations (Moura *et al.* 2016). However, there is cumulative evidence of species dependencies on river discharge to coastal regions. Some research suggests preferential foraging of species in coastal river plume regions (Broadley *et al.* 2022; Burla *et al.* 2010; Drinkwater and Frank 1994; Gillanders and Kingsford 2002). For example, it was suggested that little penguin populations off the coast of South Australia may depend on river discharge to stimulate productivity in the region or provide a queue for spawning or aggregation of prey fishes (Colombelli-Négrel 2015). Further emphasising the need for continued *in situ* exploration and sampling is the discovery of a large and extensive carbonate reef system off the Amazon River mouth, beneath the river plume (Moura *et al.* 2016). Now known as the Great Amazon Reef System, more recent research suggests this mesophotic reef, appearing to be mostly consisting of sponges and other calcareous filter-feeding organisms, could span up to ~56,000 km^2 (Francini-Filho *et al.* 2018). Discoveries like these, which have only occurred in the last decade, demonstrate the lack of knowledge and understanding regarding the influence of river discharge and river plumes on coastal waters and marine species. This highlights the need for continued

research in river plumes regions of influence. These discoveries were only made due to exploration of and attempts to monitor these environments. In earlier times, exploration, observation and sampling of river plume regions and below benthic communities *in situ* was limited by technical specifications of equipment (e.g. depth limitations). In more recent years, technology has advanced and exploration and sampling is easier to conduct in turbid plume waters both *in situ* and remotely. In addition, sampling of water in river plumes will enable further validation, refinement and development of ocean colour algorithms. Some of this data could be used specifically to target, identify and classify river plume waters and regions of river discharge influence.

5.4.3 Sensor development, increased sampling and advancement of optical algorithms

5.4.3.1 Current initiatives

Several developed ocean colour satellite imagery products currently exist for water quality monitoring of open ocean waters, but fewer have been developed specifically for coastal and inland water applications. There is a clear gap in applications of remote sensing in these regions which is largely due to the limitations of current ocean colour products. However, there is now an increasing number of projects, including Australian Government funded projects, to investigate and develop solutions for the purpose of monitoring conditions in coastal and inland waters. For example, AquaWatch Australia is a mission with collaborators across industry, research and Australian Government bodies to establish a comprehensive "ground-to-space" national water quality monitoring system of both coastal and inland water bodies and waterways (see https://www.csiro.au/en/about/challenges-missions/aquawatch). Projects such as these are promising and necessary for improving our understanding of land-sea interactions and change in water quality and productivity in optically complex waters. However, assessing water quality at times prior to the launch and operation of these new projects (at time of writing, the sensor for the AquaWatch project was still under development), still requires older sources of data.

5.4.3.2 Measuring salinity from space

Another line of research that could further develop our knowledge of riverine influence on marine systems as well as inland waters, is the development of algorithms specifically designed to estimate salinity. At present, satellite imagery based salinity estimates are available at somewhat coarse spatial resolution because of three satellite based missions. NASA's Aquarius instrument and mission as well as the European Space Agency's Soil Moisture and Ocean Salinity (SMOS) mission all aim to estimate sea surface salinity at very coarse spatial resolution (150 km and 200 km, respectively). Aquarius has a seven day return period and was operational between 2011 and 2015. The SMOS satellite was launched in 2009 and is still operational with a temporal resolution of approximately 28 days and sun-synchronous orbit. These products are likely too coarse to detect the plumes of the majority of the world's rivers. Development of sensors that can map salinity at finer spatial resolution would enhance the ability of researchers to track and identify river plume and river influenced waters in coastal regions, particularly those with more moderate flow volumes and rates.

There remains to this day a lack of knowledge about ocean systems in general. More funds are currently applied towards research focussed on the mysteries and exploration of outer space than the depths of our own oceans on Earth (Etzioni 2014). However, the research herein relies on some technologies (remote sensing via satellite platforms) which were in part, developed for space exploration as well as a deep understanding and desire to understand natural systems on Earth. This thesis is a small demonstration of the capabilities possible by combining both Earth observation, spatial and marine sciences. The research within and following this thesis may aid in better articulating to funding bodies the importance of research at the land-sea interface, and that this can be done in parallel and in combination with investment in space technologies such as orbiting satellites and remote sensing algorithm refinement. There are many more discoveries to be made from Earth observation and from researching land-sea interactions.

The influence of river discharge on coastal ocean productivity is often viewed as an "impact" which has negative effects on marine environments and species. However, this view is derived from a generalised belief that freshwater discharge to the coast is harmful, stemming from a lack of knowledge and understanding of the potential positive role of freshwater discharge in marine systems. The relationship between coastal water quality and productivity is very complex and sensitive to change. Whether the effects of discharge are positive or negative or at a mid-point for marine environments and species, depends on volume, timing, location, concentration and consistency of river discharge into the coastal environment as well as the biophysical drivers at play in the coastal environment and finally, the communities and stakeholders which depend on them. Ways of measuring the influence of river discharge on coastal environments such as those developed in this thesis, continue to be needed to improve the understanding on where, when and under what conditions river flows have "negative" or "positive" impacts on marine environments. It is these views and beliefs that ultimately inform future anthropogenic management of both terrestrial, freshwater and marine systems.

5.5 References

Barkley, A.E., Prospero, J.M., Mahowald, N., Hamilton, D.S., Popendorf, K.J., Oehlert, A.M., Pourmand, A., Gatineau, A., Panechou-Pulcherie, K., Blackwelder, P., and Gaston, C.J. (2019) African biomass burning is a substantial source of phosphorus deposition to the Amazon, Tropical Atlantic Ocean, and Southern Ocean. *Proceedings of the National Academy of Sciences* **116**(33), 16216-16221.

Bierman, P., Lewis, M., Ostendorf, B., and Tanner, J. (2011) A review of methods for analysing spatial and temporal patterns in coastal water quality. *Ecological Indicators* **11**(1), 103-114.

Bowman, D.M.J.S., Kolden, C.A., Abatzoglou, J.T., Johnston, F.H., van der Werf, G.R., and Flannigan, M. (2020) Vegetation fires in the Anthropocene. *Nature Reviews Earth & Environment* **1**(10), 500-515.

Broadley, A., Stewart-Koster, B., Burford, M.A., and Brown, C.J. (2022) A global review of the critical link between river flows and productivity in marine fisheries. *Reviews in Fish Biology and Fisheries* **32**(3), 805-825.

Burla, M., Baptista, A.M., Casillas, E., Williams, J.G., and Marsh, D.M. (2010) The influence of the Columbia River plume on the survival of steelhead (*Oncorhynchus mykiss*) and Chinook salmon (*Oncorhynchus tshawytscha*): a numerical exploration. *Canadian Journal of Fisheries and Aquatic Sciences* **67**, 1671-1684.

Colombelli-Négrel, D. (2015) Low survival rather than breeding success explains little penguin population decline on Granite Island. *Marine and Freshwater Research* **66**(11), 1057-1065.

Drinkwater, K.F., and Frank, K.T. (1994) Effects of river regulation and diversion on marine fish and invertebrates. *Aquatic Conservation: Marine and Freshwater Ecosystems* **4**, 134-151.

Etzioni, A. (2014) Final Frontier vs. Fruitful Frontier: The Case for Increasing Ocean Exploration. *Issues in Science and Technology* **30**(4).

Francini-Filho, R.B., Asp, N.E., Siegle, E., Hocevar, J., Lowyck, K., D'Avila, N., Vasconcelos, A.A., Baitelo, R., Rezende, C.E., Omachi, C.Y., Thompson, C.C., and Thompson, F.L. (2018) Perspectives on the Great Amazon Reef: Extension, Biodiversity, and Threats. *Frontiers in Marine Science* **5**. [In English]

Fredston-Hermann, A., Brown, C.J., Albert, S., Klein, C.J., Mangubhai, S., Nelson, J.L., Teneva, L., Wenger, A., Gaines, S.D., and Halpern, B.S. (2016) Where Does River Runoff Matter for Coastal Marine Conservation? *Frontiers in Marine Science* **3**, 273.

Gillanders, B.M., and Kingsford, M.J. (2002) Impact of changes in flow of freshwater on estuarine and open coastal habitats and the associated organisms. *Oceanography and Marine Biology* **40**, 233-309.

Hamed, K.H., and Ramachandra Rao, A. (1998) A modified Mann-Kendall trend test for autocorrelated data. *Journal of Hydrology* **204**(1), 182-196.

Mahowald, N. (2011) Aerosol Indirect Effect on Biogeochemical Cycles and Climate. *Science* **334**(6057), 794-796.

Mahowald, N., Ward, D.S., Kloster, S., Flanner, M.G., Heald, C.L., Heavens, N.G., Hess, P.G., Lamarque, J.-F., and Chuang, P.Y. (2011) Aerosol impacts on climate and biogeochemistry. *Annual review of environment and resources* **36**, 45-74.

Meteorology, B.o. (2020) Trends and historical conditions in the Murray-Darling Basin, A report prepared for the Murray-Darling Basin Authority by the Bureau of Meteorology. Bureau of Meteorology, Melbourne, Vic.

Mithen, S. (2010) The domestication of water: water management in the ancient world and its prehistoric origins in the Jordan Valley. *Philosophical Transactions of the Royal Society A: Mathematical, Physical and Engineering Sciences* **368**(1931), 5249-5274.

Moura, R.L., Amado-Filho, G.M., Moraes, F.C., Brasileiro, P.S., Salomon, P.S., Mahiques, M.M., Bastos, A.C., Almeida, M.G., Silva, J.M., Araujo, B.F., Brito, F.P., Rangel, T.P., Oliveira, B.C.V., Bahia, R.G., Paranhos, R.P., Dias, R.J.S., Siegle, E., Figueiredo, A.G., Pereira, R.C., Leal, C.V., Hajdu, E., Asp, N.E., Gregoracci, G.B., Neumann-Leitão, S., Yager, P.L., Francini-Filho, R.B., Fróes, A., Campeão, M., Silva, B.S., Moreira, A.P.B., Oliveira, L., Soares, A.C., Araujo, L., Oliveira, N.L., Teixeira, J.B., Valle, R.A.B., Thompson, C.C., Rezende, C.E., and Thompson, F.L. (2016) An extensive reef system at the Amazon River mouth. *Science Advances* **2**(4), e1501252.

Okin, G.S., Mahowald, N., Chadwick, O.A., and Artaxo, P. (2004) Impact of desert dust on the biogeochemistry of phosphorus in terrestrial ecosystems. *Global Biogeochemical Cycles* **18**(2).

Schlosser, J.S., Braun, R.A., Bradley, T., Dadashazar, H., MacDonald, A.B., Aldhaif, A.A., Aghdam, M.A., Mardi, A.H., Xian, P., and Sorooshian, A. (2017) Analysis of aerosol composition data for western United States wildfires between 2005 and 2015: Dust emissions, chloride depletion, and most enhanced aerosol constituents. *Journal of Geophysical Research: Atmospheres* **122**(16), 8951-8966.

Tang, W., Llort, J., Weis, J., Perron, M.M.G., Basart, S., Li, Z., Sathyendranath, S., Jackson, T., Sanz Rodriguez, E., Proemse, B.C., Bowie, A.R., Schallenberg, C., Strutton, P.G., Matear, R., and Cassar, N. (2021) Widespread phytoplankton blooms triggered by 2019–2020 Australian wildfires. *Nature* **597**(7876), 370-375.